QUANTIFYING THE IMPACTS OF VEHICLE TECHNOLOGIES AND OPERATIONAL IMPROVEMENTS ON AIR TRANSPORTATION SYSTEM PERFORMANCE

A Thesis
Presented to
The Academic Faculty

by

Mohammed Hassan

In Partial Fulfillment
of the Requirements for the Degree
Doctor of Philosophy in the
School of Aerospace Engineering

Georgia Institute of Technology
August 2017

QUANTIFYING THE IMPACTS OF VEHICLE TECHNOLOGIES AND OPERATIONAL IMPROVEMENTS ON AIR TRANSPORTATION SYSTEM PERFORMANCE

Approved by:

Professor Dimitri N. Mavris, Advisor
School of Aerospace Engineering
Georgia Institute of Technology

Professor Brian J. German
School of Aerospace Engineering
Georgia Institute of Technology

Professor Daniel P. Schrage
School of Aerospace Engineering
Georgia Institute of Technology

Dr. Jens Holger Pfaender
School of Aerospace Engineering
Georgia Institute of Technology

Mr. David R. Maroney
The MITRE Corporation

Date Approved: 04 May 2017

To my parents and sisters

ACKNOWLEDGEMENTS

This thesis is the culmination of extensive academic research conducted during my Ph.D. studies. The successes of my endeavor could not have been realized without the guidance and assistance of many. I am grateful to the people who believed in me from the beginning and who have supported me along the way.

First, I would like to thank my advisor, Prof. Dimitri Mavris, for allowing me to be part of the Aerospace Systems Design Laboratory (ASDL) and giving me the opportunity to pursue this achievement under his supervision. I would also like to thank my committee members, Prof. Brian German, Prof. Daniel Schrage, Dr. Holger Pfaender, and Mr. David Maroney, for their valuable feedback and guidance.

Second, I would like to acknowledge all my colleagues and friends at ASDL with whom I shared the graduate school experience and who provided me with many great memories to cherish. I would like to especially thank my good friend Gregory Busch, Imon Chakraborty, Gökçin Çınar, and Burak Bağdatlı.

Last, but certainly not least, I would like to thank my family for their continuous love and encouragement; their support is the bedrock of my academic success.

TABLE OF CONTENTS

LIST OF TABLES

LIST OF FIGURES

LIST OF ACRONYMS

ABF	Available Biofuel
ANN	Artificial Neural Networks
ASM	Available Seat Miles
ASP	Airspace Systems Program
BTS	Bureau of Transportation Statistics
BWB	Blended-Wing-Body
CAB	Civil Aeronautics Board
CAEP	Committee on Aviation Environmental Protection
CLEEN	Continuous Lower Emissions, Energy, and Noise
EDS	Environmental Design Space
EO	Executive Order
EPA	Environmental Protection Agency
ERA	Environmental Responsible Aviation
FAA	Federal Aviation Administration
FC	Fuel Cost
FLOPS	Flight Optimization System
FP	Fuel Price
FW	Fixed Wing
IATA	International Air Transport Association
ICAO	International Civil Aviation Organization
IPPD	Integrated Product and Process Development
JPDO	Joint Planning and Development Office
LC	Labor Cost
LSA	Large Single Aisle
LTA	Large Twin Aisle

MDO	Multidisciplinary Design Optimization
MOO	Multi-Objective Optimization
NAS	National Airspace System
NASA	National Aeronautics and Space Administration
NPSS	Numerical Propulsion System Simulation
NRC	National Research Council
OD	Origin-Destination
OEC	Overall Evaluation Criterion
R&D	Research and Development
RJ	Regional Jet
RMSE	Root Mean Square Error
RPM	Revenue Passenger Miles
RSM	Response Surface Methodology
SSA	Small Single Aisle
STA	Small Twin Aisle
TOC	Total Operating Cost
TP	Turboprop
TRL	Technology Readiness Level
VLA	Very Large Aircraft
WATE	Weight Analysis of Turbine Engines

SUMMARY

Over the past decades, passenger demand for air transportation has grown steadily. Aviation forecasts predict a continued growth into the future at possibly higher rates. The consequent rise in number of flights would undoubtedly lead to an increase in fuel consumption, emissions, and airport noise levels; environmental effects that regulatory bodies have been striving to limit.

Among the solutions considered by the aviation industry to mitigate the adverse environmental impacts of demand growth are vehicle technologies and operational improvements. The former aims to enhance aircraft vehicle-level performance, while the latter seeks both vehicle-level and system-level enhancements. The primary research objective of this thesis is to provide a methodological framework that incorporates both vehicle technologies and operational improvements in order to evaluate their projected impacts on air transportation system performance.

Both technological and operational solutions have been investigated in the past; however, independently. The existing inter-dependencies between both solutions have been largely considered insignificant and thus, disregarded. Consequently, to compute the total impact on system performance resulting from implementing both solutions, current assessments analyze them independently and simply sum the individual contributions. This thesis focuses on the inter-dependencies between vehicle technologies and operational improvements and argues that: 1) they should not be generally disregarded in performance evaluations of the aviation system, and 2) they can be exploited to further enhance system performance. Those two arguments are posed as a single hypothesis, which is tested using the methodological framework.

There are two main contributions for this thesis. First, the development of an all-encompassing capability that evaluates system-level performance at reasonable accuracy and manageable uncertainty. Stakeholders and policy makers are better informed about the potential system-level impacts of various technological and operational solutions. As a consequence, future investment and resource allocation decisions could be impacted. The second major contribution of this thesis is testing the commonly accepted assumption regarding the independence of technologies and operations. The thesis indeed argues that independence should not be generally assumed. Therefore, technologies and operations need to be considered simultaneously in order to account for their inter-dependencies.

CHAPTER I

INTRODUCTION

The prospects of the US commercial aviation sector remain positive with a long-term outlook of growth, driven by US and world economies. According to the International Civil Aviation Organization (ICAO), the aviation industry has been reporting strong growth performance as it continues to recover from the recent economic recession [1]. Worldwide passenger air traffic reached a record 3.53 billion in 2015, up 7% from 2014 and 30% from 2010 [1]. This current trend of aviation growth is expected to continue in the future. In order to accommodate the increase in air travel demand, the worldwide passenger fleet is projected to double in size by 2035 [2, 3]. In the US, air carrier operations are expected to increase from an average of 37 000 flights per day in 2015 to 65 000 by 2035 [4]. Without intervention, this huge number of additional flights will increase pressure on the US National Airspace System (NAS). The NAS is anticipated to become congested and delays are likely to propagate throughout. Environmental consequences include an immense escalation in harmful nitrogen oxide (NOx) and carbon dioxide (CO_2) emissions, and a significant increase in noise near airports [5]. Aviation fuel consumption in the US is forecast to rise approximately 40% by 2035 relative to 2010 levels [4].

In order to mitigate the adverse environmental impacts of operational growth, and to enhance the overall efficiency and safety of the NAS, the US —through its Federal Aviation Administration (FAA)— has invested heavily in the Next Generation Air Transportation System (NextGen). From 2010 to 2016, total expenditures on NextGen programs amounted to 6.31 billion dollars [6]. The various programs seek to transform the current NAS by improving its operational capacity, efficiency,

and resilience [7]. Alongside the FAA efforts, the National Aeronautics and Space Administration (NASA) has been investing in the development of technologies that will either enable the implementation of NextGen or enhance the environmental performance of commercial aircraft [8]. From 2010 to 2016, total expenditures on NASA aeronautics research totaled 3.98 billion dollars [9]. NASA has set forth an implementation plan to guide its aeronautics research along six strategic thrusts that will enable a sustainable, efficient, safe, and autonomous future for aviation [10].

Globally, the International Air Transport Association (IATA) has defined high-level targets to address the projected increase in aviation-related CO_2 emissions. Those targets include a cap on carbon growth starting 2020 and a reduction of 50% in net carbon emissions by 2050 relative to 2005 levels (Figure 1) [11]. In September 2009, IATA targets were endorsed by the aviation industry including aircraft manufacturers, airlines, airports, and air navigation service providers. At the 37th ICAO assembly in October 2010, governments resolved to adopt the targets as well [12]. Additionally, IATA has laid out a strategy that relies on new technology, efficient operations, effective infrastructure, and sustainable biofuels to enable its environmental vision [13]. The whole aviation community, including ICAO member states, adopted the four-pillar strategy as a guiding framework to achieve the aggressive targets.

Since the US is an ICAO member state, the 2010 resolution imposed additional requirements on domestic aviation investments to meet the global targets. While the US has invested billions of dollars in transforming its aviation sector, and future research commitments are expected to be of comparable figures, it still remains unclear whether the aviation environmental targets will be met. In fact, the near term target of achieving an average fuel efficiency improvement of 1.5% per year from 2009 to 2020, has not been met yet. Data reported by the Bureau of Transportation Statistics (BTS) show that the average US fuel efficiency improvement from 2009 to 2015 was approximately 0.7% per year (the fuel efficiency metric being available seat miles

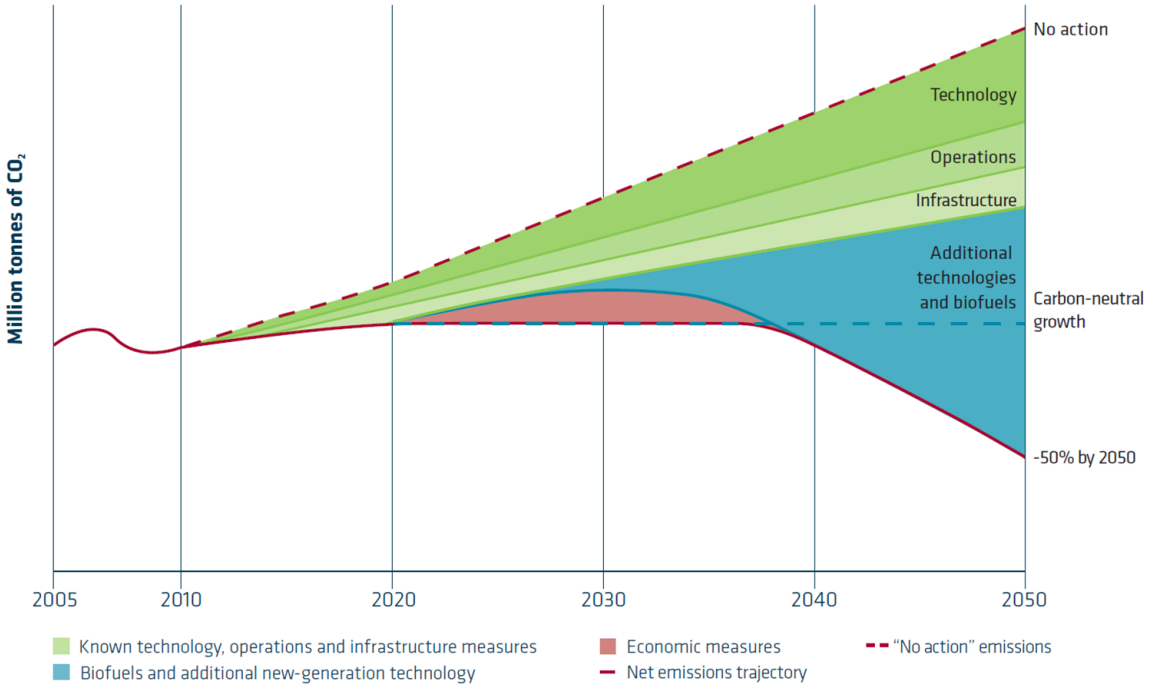

Figure 1: IATA schematic CO_2 emissions reduction roadmap [11]

per gallon) [14]. Furthermore, the mid term target of carbon neutrality starting 2020 continues to be challenging given current improvement trends. In 2015, an FAA study concluded that carbon neutral growth will not be achieved with moderate system improvements [15]. The slow progress towards the targets has raised many concerns regarding the current US aviation investment strategy.

At the request of the US Congress, the National Research Council (NRC) formed a committee to report on the status of NextGen and examine the technical activities related to its implementation. The report severely criticized the FAA for its management of NextGen, and emphasized that the current implementation strategy seeks an evolutionary upgrade of the NAS rather than the originally promised revolutionary transformation [16]. The NRC report echoed previous warnings by the Inspector General of the US Department of Transportation who has been following the progress of NextGen closely [17, 18]. Even more alarming is the 2015 study conducted by the FAA itself, which showed that NextGen improvements would contribute very little

towards achieving the environmental targets, and that almost all savings in CO_2 emissions would come from vehicle technologies and sustainable biofuels [15]. Despite the previous research findings, the allocation of investment resources over the past years has been skewed in favor of operational improvements. The aforementioned constitutes a basis to at least consider alternative investment strategies.

While the NRC report called on the FAA, US Congress, and all NAS stakeholders to "reset expectations" for NextGen, this thesis investigates resetting the US aviation investment strategy altogether. The research aims at formulating a methodology that can be used to quantify expected contributions from vehicle technologies and operational improvements, in order to guide stakeholder decision making and investment resource allocation. Such methodological framework is to address questions regarding the feasibility of the IATA targets, and the extent to which the emissions gap can be closed by utilizing those two 'enablers'. The temporal aspect associated with implementing those enablers, as to when changes need to be introduced and at what rate, is also addressed. Before formally stating the research objective of this thesis along with the guiding research questions, pertinent background information is reviewed to emphasize ongoing efforts, and highlight the relevance of the present work.

1.1 Background

Over the past four decades, demand for air transportation has grown steadily in the US (Figure 2). BTS data indicate that 804 million passengers were transported on US carriers in 2015, an increase of 11% from 2010 and 19% from 2000 [19]. FAA forecasts suggest that passenger demand will continue to grow in the future at even higher rates [4]. This growth, and its consequent rise in flight operations, will undoubtedly lead to an increase in aviation fuel consumption, aviation CO_2 and NOx emissions, noise in the vicinity of airports, and the congestion of the air transportation network. To guarantee the sustainability of the NAS, the intervention of the US government

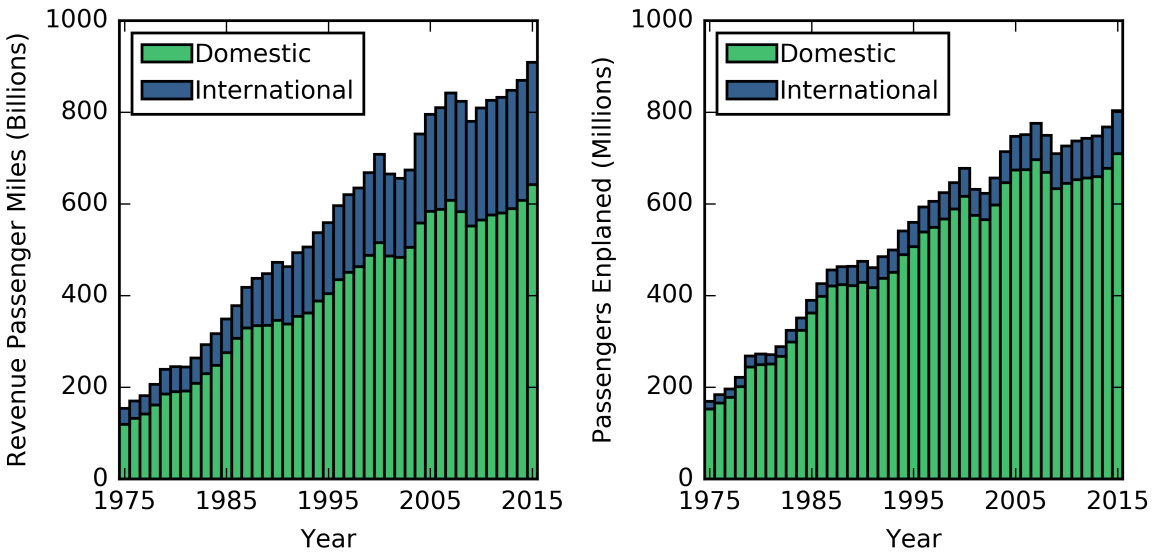

Figure 2: US air transportation demand growth (1975–2015) [19]

was deemed necessary to incentivize change through a series of policies and research initiatives.

In 2003, the Vision 100 – Century of Aviation Reauthorization Act was signed in order to "strengthen America's aviation sector, provide needed authority to the [FAA], and enhance the safety of the traveling public" [20]. The act led to the establishment of the Joint Planning and Development Office (JPDO) to manage NextGen, which "represents a substantial and long-term change in the management and operation of the national air transportation system" [20, 21]. It is considered "the largest aviation infrastructure project in history" and a comprehensive initiative that leverages current and new technology to improve capacity, efficiency and safety while reducing the overall environmental impact [22, 23]. Satellite navigation, advanced digital communications, and enhanced connectivity between components of the air transportation system are features to be realized through NextGen technologies. Passengers, air carriers, general aviation pilots, and air traffic controllers will benefit from NextGen [22].

In 2006, Executive Order (EO) 13419 initiated the National Aeronautics Research and Development Policy to guide "federal aeronautics research and development

(R&D) through 2020," and outline key principles regarding energy, environment, safety, and air mobility [24]. Those principles were the framework for the National Plan for Aeronautics Research and Development and Related Infrastructure, first published in 2007, which led to a number of research initiatives involving various government agencies, industry affiliates and academic institutions [25]. Until it was decommissioned in 2014, the JPDO acted as the umbrella under which many of these initiatives fell with the main goal of bringing NextGen online. The JPDO managed partnerships across multiple departments and agencies including the Departments of Transportation, Commerce, Defense, and Homeland Security, along with the White House Office of Science and Technology Policy, NASA, and the FAA [26].

To track the progress of NextGen implementation, all initiatives and/or programs that fell under the JPDO utilized metrics that directly mapped to NextGen requirements. For example, Table 1 shows the operational improvement metrics that NASA defined and utilized for its Airspace Systems Program (ASP) [27]. Similarly, Table 2 shows the vehicle technology metrics and goals that were employed by the FAA for its Continuous Lower Emissions, Energy, and Noise (CLEEN) program, and by NASA for its Environmentally Responsible Aviation (ERA) and Fixed Wing (FW) projects [8]. While each program only focused on a subset of NextGen requirements and/or goals, the purpose of having traceable metrics was for the programs to collectively enable the full realization of NextGen.

In addition to the aforementioned, the US, along with other ICAO state members, adopted three high-level environmental targets at the 37th ICAO assembly in 2010:

1. An average improvement in fuel efficiency of 2% per year up to 2020[1]
2. A cap on net aviation CO_2 emissions starting 2020
3. A reduction in net aviation CO_2 emissions of 50% by 2050 relative to 2005 levels

[1]IATA originally proposed a 1.5% per year improvement target in 2009, but ICAO states adopted a 2% per year improvement target instead [11].

Table 1: NASA operational improvement metrics [27]

Capacity	C1	number of flights that can be operated on a good-weather day within specified delay limits
	C2	number of passenger origin-to-destination trips that can be operated on a good-weather day within specified delay limits
	C3	freight tonnage that can be transported on a good-weather day within specified delay limits
Efficiency	E1	aircraft transit time
	E2	passenger origin-to-destination trip time
	E3	fuel usage of the aircraft fleet in terms of fuel consumed per aircraft nautical mile
	E4	fuel usage of the aircraft fleet in terms of fuel consumed per passenger nautical mile
	E5	fuel usage of the aircraft fleet in terms of fuel consumed per passenger origin-to-destination great-circle nautical mile
	E6	fuel usage of the aircraft fleet in terms of fuel consumed per freight ton nautical mile
Robustness	R1	ratio of capacity metrics for poor weather or system failure compared with good weather nominal operating conditions
	R2	mean of flight delays for poor weather or system failure compared with good weather nominal operating conditions
	R3	variance of flight delays for poor weather or system failure compared with good weather nominal operating conditions
Safety	S1	number of losses of separation due to traffic or weather
	S2	time to predicted loss of separation from time of conflict detection
	S3	variance of closest point of approach for resolved conflicts
	S4	consequence of hazardous event
	S5	likelihood of hazardous event

Table 2: NASA vehicle improvement metrics and goals [8]

Technology Benefits	Near Term	Mid Term	Far Term
	2015–2025	2025–2035	beyond 2035
Noise*	22–32 dB	32–42 dB	42–52 dB
LTO NOx emissions†	70–75%	80%	>80%
Cruise NOx emissions‡	65–70%	80%	>80%
Aircraft fuel consumption‡	40–50%	50–60%	60–80%

* reduction in cumulative margin below FAA Stage 4 noise limit
† reduction relative to ICAO CAEP/6 standard
‡ reduction relative to 2005 best in class

Those aspirational targets were first introduced a year earlier by IATA and endorsed by the aviation industry. By adopting them, the US imposed additional requirements on the domestic efforts geared towards NextGen implementation.

Since 2010, despite immense investments in the previously discussed efforts, there has been little progress in the US towards achieving the IATA environmental targets. Data published by the Environmental Protection Agency (EPA) indicate that from 2010 to 2014, aviation's share of total greenhouse gas emissions remained a constant 2.2% (Figure 3) [28]. Furthermore, BTS data suggest that aviation fuel efficiency, in terms of available seat miles per gallon, improved from 2010 to 2015 at a gradual rate of <1% per year (Figure 4) [19]. Those figures clearly show that the aviation system is under-performing and not meeting the near term IATA target.

In 2012, the US Congress ordered an expert review of NextGen enterprise architecture and all related technical activities. Section 212 of the FAA Modernization and Reform Act requested the NRC to conduct such review and to submit a comprehensive report of findings. In 2015, the NRC completed its report and its overarching conclusions were as follows [16]:

> "The original vision for NextGen is not what is being implemented today. Instead, NextGen today primarily emphasizes replacing and modernizing

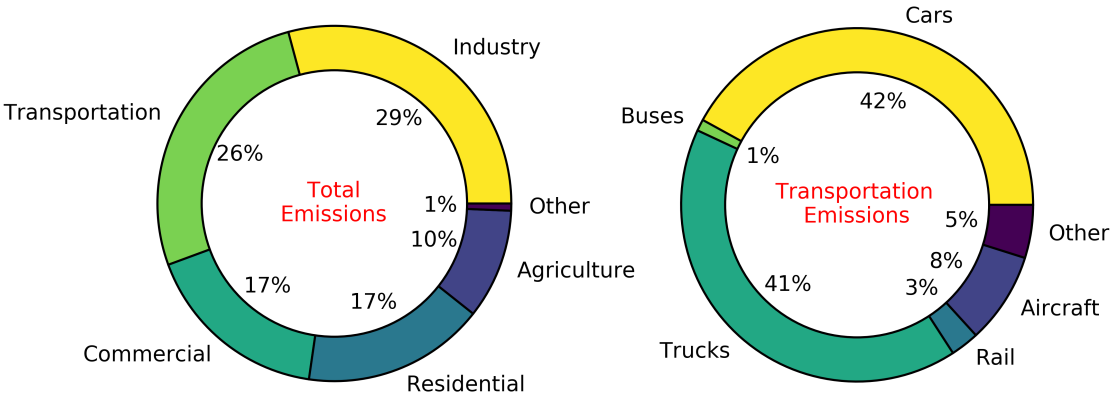

Figure 3: US greenhouse gas emissions by economic sector in 2014 [28]

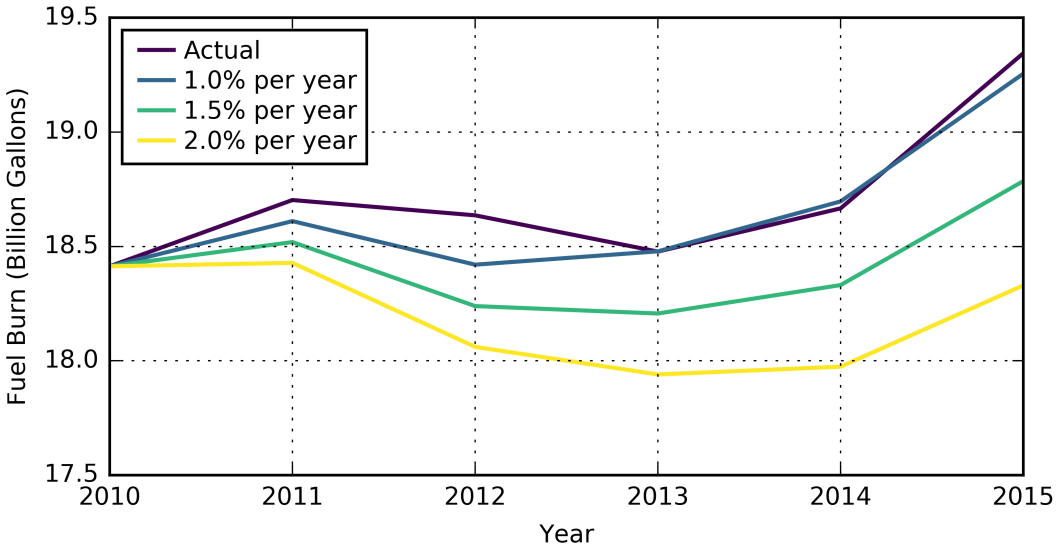

Figure 4: US aviation fuel burn compared to target trends (2010–2015) [19]

aging equipment and systems. This shift in focus has not been clear to all stakeholders."

The report went on to signify the importance of systems engineering in managing this "modernization project," and the need for specialists in probability and statistics to manage uncertainties and mitigate risks.

In a recent 2015 submission to ICAO, the US government provided an update on its aviation emissions reduction plan given current progress trends [15]. It included

a system performance analysis conducted by the FAA in which two scenarios were considered. The first assumed moderate system improvements and failed to meet both the mid term and far term targets, while the second assumed aggressive improvements and still failed to meet the far term target.

1.2 Observations

Almost one and a half decades after the US called for a transformation of its aviation system, it still remains unclear what the net performance impact of all R&D efforts would be. Near term environmental targets have not been met yet, and there is little progress towards achieving the mid term and/or far term targets. The 'pigeonholing' of NextGen objectives across multiple programs and initiatives has not accomplished its intended purpose. Instead, there has been a depletion of resources over the years with an unsatisfactory return on investment.

To examine why the aviation system is underperforming, a number of observations are pointed out based on the discussion of section 1.1:

1. The US R&D efforts, along with their research objectives and performance metrics, were initiated years before the IATA environmental targets were proposed and/or endorsed. Whether these efforts can collectively close the emissions gap (Figure 1) remains an open question, although recent findings suggest not [15].

2. IATA envisioned closing the emissions gap using technologies, operations, biofuels and economic measures (Figure 1); however, it did not specify the required contributions from each. Whether the recent shift in focus regarding NextGen implementation affects the feasibility of the targets is not known.

3. Different US R&D efforts aim to enhance the same system metrics. For example, ASP tackles fuel consumption (metrics E1–E6 of Table 1), which is also tackled by CLEEN, ERA and FW (Table 2). Whether the impacts of these efforts affect

one another remains to be investigated.

4. Unlike the target CO_2 emissions trend of IATA which is clearly defined based on 2005 levels, the 'no action' trend is derived from aerospace forecasts. Forecasts constantly change based on varying socioeconomic factors. Thus, the emissions gap is not well defined and needs to be dealt with as such.

Although these observations do not identify the reasons behind the system's slow progress, they do highlight the need for a comprehensive system evaluation capability to be used for strategic decision making and future resource allocation. The capability should quantify the impacts of the different enablers on select system metrics, while accounting for inter-dependencies (if any). In addition, the capability should evaluate system performance in a non-deterministic manner in order to account for inherent sources of uncertainty.

1.3 Research Objective

To summarize, air travel demand is expected to continue to increase at high rates in the future; the US government initiated the JPDO to manage research efforts aimed at transforming the current aviation system and alleviating the adverse effects of demand growth; the FAA and NASA are leading numerous efforts to develop technologies for that purpose; however, despite these ongoing efforts, there are major concerns regarding the current performance progress of the NAS. It was shown, through a number of observations, that there is a need for an all-encompassing capability to evaluate system performance at reasonable accuracy and manageable uncertainty. The **research objective** of this thesis is to provide a framework that incorporates vehicle technologies and operational improvements in order to evaluate their projected system-level impacts. Specifically, the framework would analyze the impacts of these enablers on two distinct, but related system metrics: fuel consumption and CO_2 emissions. Those metrics were chosen since they are the ones targeted by IATA and ICAO.

In order to achieve the above-mentioned research objective, the following research questions need to be addressed. These questions aim to define the research problem and establish value objectives necessary for conventional decision making processes used in top down engineering design. Collectively, the answers to the questions would lead to the formulation of a repeatable methodology for the concurrent assessment of vehicle technologies and operational improvements. The methodology would then be utilized to evaluate the environmental performance of the aviation system.

1. What are the available capabilities used to model vehicle technologies?
2. What are the available capabilities used to model operational improvements?
3. What are the available capabilities used to model their system-level impacts?
4. How can technologies and operations be accounted for simultaneously?
5. How is uncertainty in enabler impact accounted for?
6. How is uncertainty in socioeconomic factors accounted for?

Several decision making processes have been constructed and published to guide engineering design [29, 30]. They are very similar and tend to stem from a common fundamental approach. For the purposes of this thesis, the differences are not critical. The decision support process within the Integrated Product and Process Development (IPPD) methodology was chosen to guide this research (Figure 5) [29]. The IPPD was developed at Georgia Institute of Technology and includes a decision support process that consists of six steps: establishing the need, defining the problem, establishing value objectives, generating feasible alternatives, evaluating alternatives, and finally making decisions. Sections 1.1 and 1.2 were focused on the first two steps. Likewise, this section presented the research objective and the overarching research questions in order to establish the overall value objectives (third step). The upcoming chapters of this document will implicitly follow the remaining steps of the process in order to achieve the research objective.

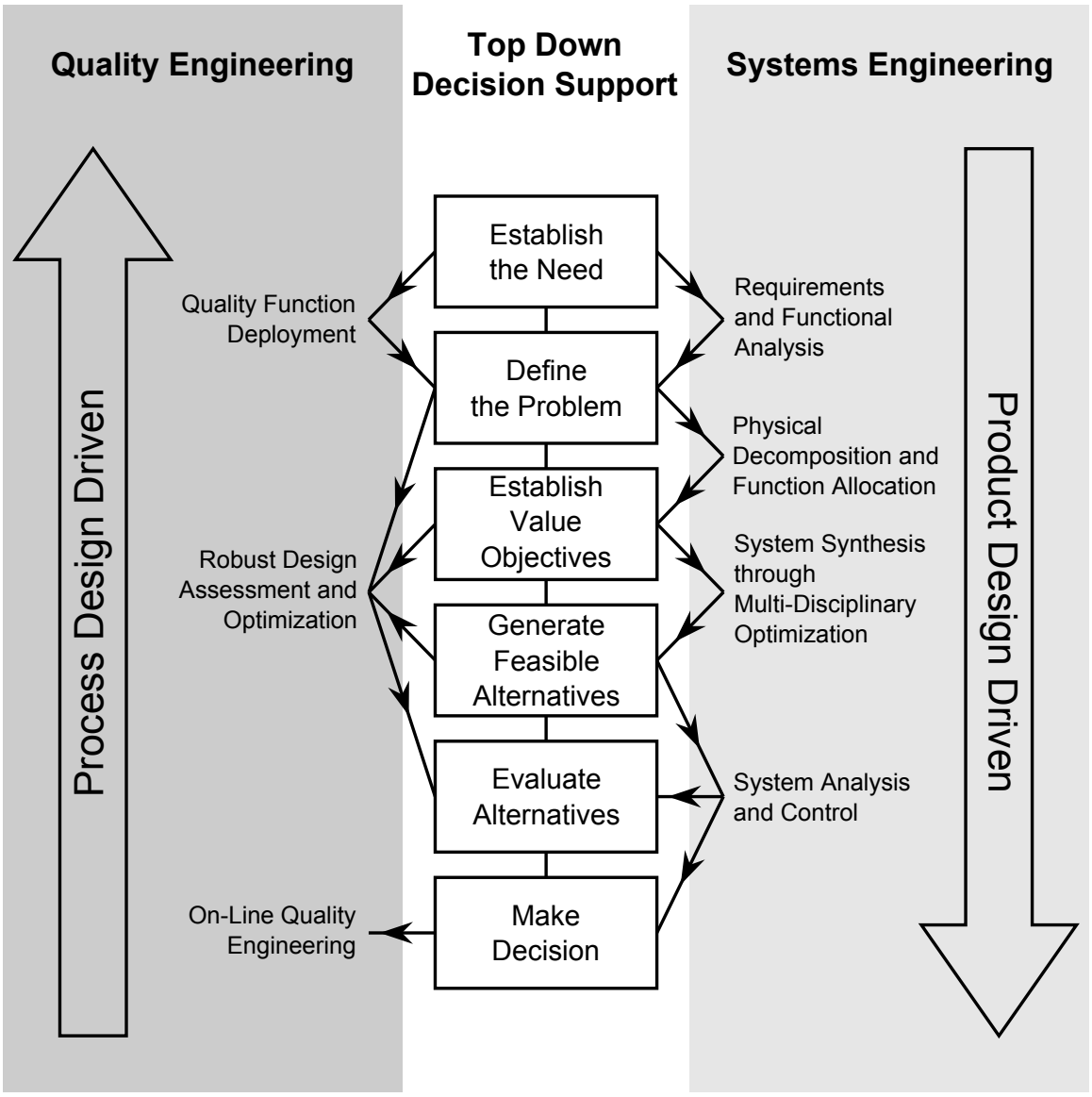

Figure 5: Georgia Tech Integrated Product and Process Development methodology [29]

1.4 Outline

The remainder of this document is organized as follows:

- Chapter II presents the thesis arguments and associated experimental plans.
- Chapter III introduces the methodological framework employed in this thesis.
- Chapter IV surveys the literature for existing modeling approaches and discusses the methods utilized in this thesis.

- Chapter V includes results derived using the methodology of Chapter III.
- Chapter VI focuses on testing the hypotheses of Chapter II.
- Chapter VII presents the conclusions and directions for future work.

CHAPTER II

THESIS ARGUMENTS

Current system performance analyses assume the impacts of vehicle technologies and operational improvements to be independent [15, 31–38]. As mentioned in section 1.2, the significance of inter-dependencies remains to be investigated. Mathematically, this could be represented by the chain rule. Given that fuel burn is a metric for system performance function of time, technologies and operations, $FB = FB(t, T, O)$, and that both technologies and operations are functions of time, $T = T(t)$ and $O = O(t)$, independence implies that:

$$\frac{\mathrm{d}FB}{\mathrm{d}t} = \frac{\partial FB}{\partial t} + \frac{\partial FB}{\partial T}\frac{\mathrm{d}T}{\mathrm{d}t} + \frac{\partial FB}{\partial O}\frac{\mathrm{d}O}{\mathrm{d}t} \tag{1}$$

where $\partial FB/\partial T$ and $\partial FB/\partial O$ represent the change in performance due to changes in technologies and operations, respectively, and $\mathrm{d}T/\mathrm{d}t$ and $\mathrm{d}O/\mathrm{d}t$ represent the rates at which those changes are introduced to the system. For no operational improvements, Eq. 1 reduces to:

$$\frac{\mathrm{d}FB}{\mathrm{d}t} - \frac{\partial FB}{\partial t} = \frac{\partial FB}{\partial T}\frac{\mathrm{d}T}{\mathrm{d}t} \quad \Rightarrow \quad \delta_{\text{Tech}} = \int_a^b \left(\frac{\partial FB}{\partial T}\frac{\mathrm{d}T}{\mathrm{d}t}\right)\mathrm{d}t \tag{2}$$

Similarly, for fixed aircraft technology levels, Eq. 1 reduces to:

$$\frac{\mathrm{d}FB}{\mathrm{d}t} - \frac{\partial FB}{\partial t} = \frac{\partial FB}{\partial O}\frac{\mathrm{d}O}{\mathrm{d}t} \quad \Rightarrow \quad \delta_{\text{Ops}} = \int_a^b \left(\frac{\partial FB}{\partial O}\frac{\mathrm{d}O}{\mathrm{d}t}\right)\mathrm{d}t \tag{3}$$

Finally, integrating Eq. 1 with respect to time yields:

$$\begin{gathered}\int_a^b \left(\frac{\mathrm{d}FB}{\mathrm{d}t} - \frac{\partial FB}{\partial t}\right)\mathrm{d}t = \int_a^b \left(\frac{\partial FB}{\partial T}\frac{\mathrm{d}T}{\mathrm{d}t} + \frac{\partial FB}{\partial O}\frac{\mathrm{d}O}{\mathrm{d}t}\right)\mathrm{d}t \\ \Delta = \delta_{\text{Tech}} + \delta_{\text{Ops}}\end{gathered} \tag{4}$$

Figure 6 graphically shows the implications of such formulation. Assuming independence, fuel burn reductions due to technological improvements (δ_{Tech}) are summed to reductions due to operational improvements (δ_{Ops}) to obtain total system reductions.

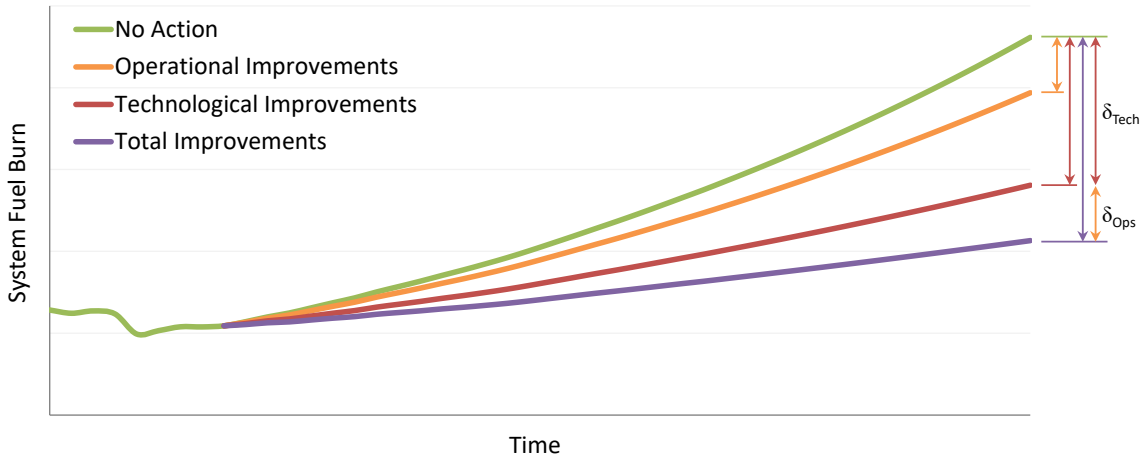

Figure 6: Schematic plot showing the impacts of vehicle technologies and operational improvements to be independent

In this thesis, it is argued that such independence should not be generally assumed, and that inter-dependencies between technological and operational improvements can be exploited to enhance the overall system performance. The following sections illustrate the significance of inter-dependencies, and hypothesize that opportunities exist to exploit them at the system-level.

2.1 Significance of Inter-Dependencies

In this section, the significance of inter-dependencies between vehicle technologies and operational improvements is highlighted at both the vehicle-level and the system-level. The discussion establishes a basis for the hypothesis presented in the next section.

2.1.1 Vehicle-Level Inter-Dependencies

Aircraft performance is a function of both design and operation. This can be demonstrated by deriving the thrust required for an aircraft in steady, level flight. Assuming that the thrust vector is aligned with the free-stream velocity, the four forces of flight balance such that $L = W$ and $T = D$ (Figure 7):

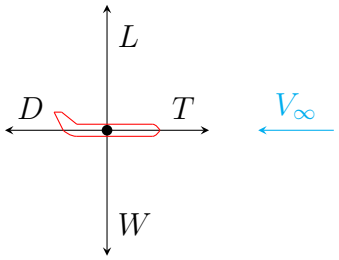

Figure 7: Force diagram

$$L = W = \tfrac{1}{2}\rho_\infty V_\infty^2 S C_L$$
$$T = D = \tfrac{1}{2}\rho_\infty V_\infty^2 S C_D \tag{5}$$

where L is lift, W is weight, T is thrust, D is drag, ρ_∞ is air density, V_∞ is velocity, S is wing area, and $[C_L; C_D]$ are the lift and drag coefficients, respectively. Assuming a parabolic drag polar ($C_D = C_{D,0} + KC_L^2$), the thrust required is thus expressed as:

$$T_R = \frac{W}{L/D} = \tfrac{1}{2}\rho_\infty V_\infty^2 S C_{D,0} + \frac{KS}{\frac{1}{2}\rho_\infty V_\infty^2}\left(\frac{W}{S}\right)^2 \tag{6}$$

Eq. 6 shows that the thrust required T_R depends on fixed structural and aerodynamic design characteristics such as $[S; C_{D,0}; K]$, and variable operational parameters such as $[\rho_\infty; V_\infty]$. Figure 8 shows the effects of velocity, altitude and weight on T_R and L/D.

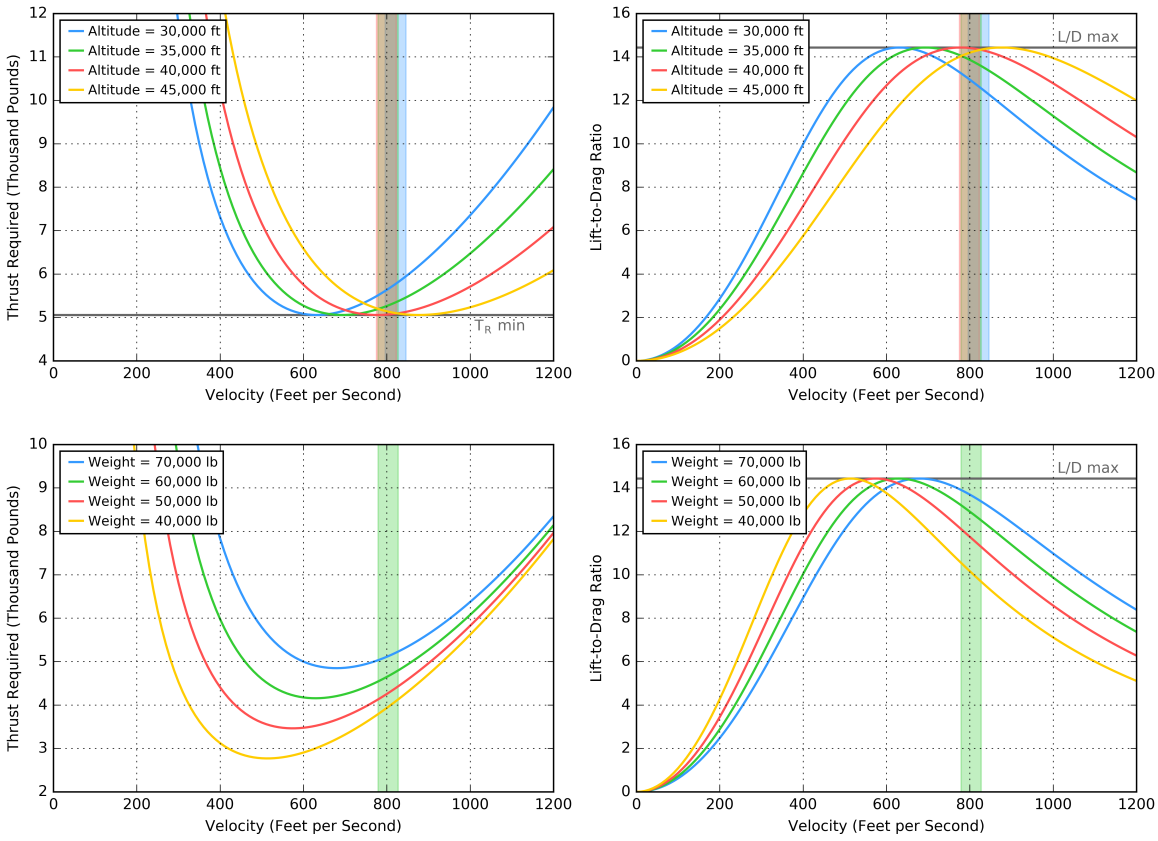

Figure 8: Variation of thrust required and lift-to-drag ratio with velocity, altitude and weight for the Gulfstream IV aircraft (top: constant weight of 73 000 lb; bottom: constant altitude of 35 000 ft; cruise speeds overlaid for different altitudes based on a cruise Mach range of 0.80–0.85)

Both T_R and L/D directly influence aircraft fuel consumption. This is emphasized by the range and endurance equations for propeller-driven and jet-propelled aircraft:

$$R = \begin{cases} \dfrac{\eta_{\text{pr}}}{c}\dfrac{C_L}{C_D}\ln\dfrac{W_0}{W_1}, & \text{if propeller-driven} \\ \dfrac{2}{c_t}\sqrt{\dfrac{2}{\rho_\infty S}}\dfrac{C_L^{1/2}}{C_D}\left(W_0^{1/2} - W_1^{1/2}\right), & \text{if jet-propelled} \end{cases}$$
$$E = \begin{cases} \dfrac{\eta_{\text{pr}}}{c}\sqrt{2\rho_\infty S}\dfrac{C_L^{3/2}}{C_D}\left(W_1^{-1/2} - W_0^{-1/2}\right), & \text{if propeller-driven} \\ \dfrac{1}{c_t}\dfrac{C_L}{C_D}\ln\dfrac{W_0}{W_1}, & \text{if jet-propelled} \end{cases} \tag{7}$$

where R is range, E is endurance, η_{pr} is propeller efficiency, c is specific fuel consumption, c_t is thrust specific fuel consumption, and $[W_0; W_1]$ are the initial and final weights of the cruise segment, respectively. The difference between W_0 and W_1 is the weight of fuel consumed during cruise W_f, from which c and c_t are defined as:

$$c \equiv -\frac{\mathrm{d}W_f/\mathrm{d}t}{P} \qquad \text{and} \qquad c_t \equiv -\frac{\mathrm{d}W_f/\mathrm{d}t}{T} \tag{8}$$

where P is shaft power ($P = TV_\infty/\eta_{\text{pr}}$) [39].

Eqs. 5–8 clearly highlight the inter-dependencies existing between aircraft design and operation, and their significance in evaluating vehicle-level fuel burn performance. Figure 8 illustrates one example in which a cruising aircraft needs to continuously decrease velocity or alternatively increase altitude, to maintain maximum aerodynamic efficiency ($L/D_{\max}$) as it burns fuel and loses weight. Inter-dependencies also impact other flight segments not just cruise. For instance, the rate of climb of an aircraft is highly dependent on velocity and generally decreases with altitude:

$$R/C = V_\infty\frac{T-D}{W} = V_\infty\left[\frac{T}{W} - \left(\frac{\frac{1}{2}\rho_\infty V_\infty^2 S C_{D,0}}{W} + \frac{KW\cos^2\theta}{\frac{1}{2}\rho_\infty V_\infty^2 S}\right)\right] \tag{9}$$

where R/C is rate of climb and θ is climb angle (in climb, the force balance is such that $L = W\cos\theta$ and $T = D + W\sin\theta$) [39].

Current regulations prevent aircraft from operating at optimal fuel burn settings throughout the entire mission. For safety concerns, cruising vehicles are required to

fly at fixed altitudes separated by 2 000 or 4 000 feet, instead of seamlessly increasing altitude to maintain aerodynamic efficiency. Similarly, for noise and safety concerns, the speeds and rates of climbs and descents are regulated near terminal areas. Further, in order to meet tight flight schedules and decrease labor costs, many airlines choose to cruise at speeds greater than the optimum. All the previous deficiencies signify the impact of inter-dependencies on vehicle-level fuel burn performance. The magnitude of such impact varies based on aircraft type (design) and mission flown (operation).

2.1.2 System-Level Inter-Dependencies

As depicted in Figure 9, technologies and operations also impact one another at the system-level. Technologies directly impact fuel burn, which is a major contributor to airline operating costs. Since airline route planning is primarily driven by economics, changes in operating costs could instigate operational changes. Alternatively, airline decisions dictate the mission ranges flown by all vehicles of a fleet, which consequently influence fleet composition. Depending on the vehicle types existing and/or required, certain technology packages may be more beneficial than others and thus, favored for earlier introduction to enhance fleet performance.

Inter-dependencies can also be illustrated using vehicle payload-range diagrams (a notional example is shown in blue in Figure 10). BTS data has consistently shown that commercial aircraft are being operated away from their design ranges [14]. Figure 11 shows that for four Boeing aircraft types in 2015, most missions were of ranges shorter

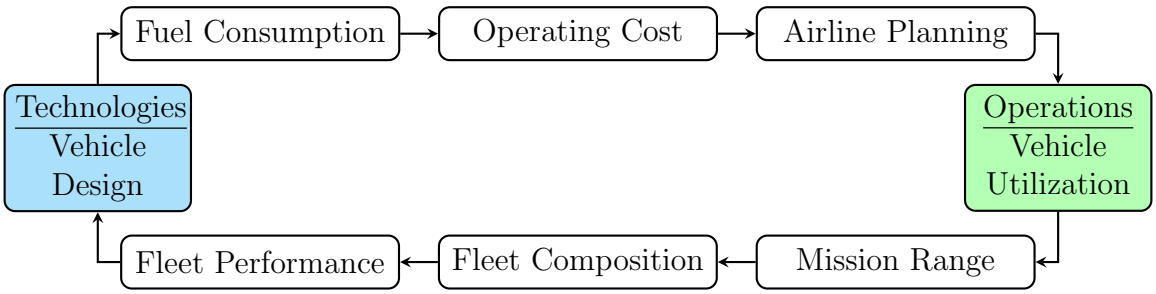

Figure 9: System-level inter-dependencies between vehicle technologies and operational improvements

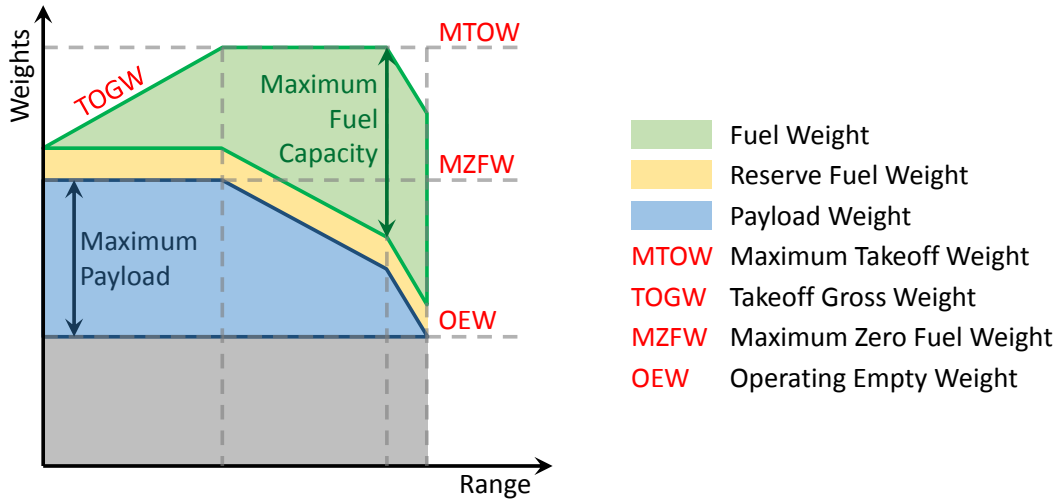

Figure 10: Notional payload-range characteristics

than the design ranges. The data suggests that for current airline utilization, vehicles are oversized and not operating near their optimum performance levels (resulting in excess fuel consumption). This inefficiency was previously identified in a 2010 research study, which called for a CO_2 standard to enforce the "rightsizing" of future aircraft designs according to current utilization strategies [40].

The use of regulatory policy and/or positive economic measures to enhance system fuel burn performance has always been considered (Figure 1) [41]. This is because airlines do not necessarily operate vehicles in the most fuel efficient way. Airlines seek to maximize profit, and although fuel cost is a primary driver of total operating costs, it is not the only factor considered in airline planning. In order to meet the system-level environmental targets, policies and economic measures can provide an incentive for airlines to fully consider the inter-dependencies between vehicle design and operation such that fuel efficiency is increased.

Based on the above-mentioned, ongoing research efforts are seeking to either influence future designs based on current vehicle utilization, or force airlines to prioritize fuel efficiency through regulations. In either case, the goal is to overcome the existing deficiency by exploiting the inter-dependencies between vehicle design and operation.

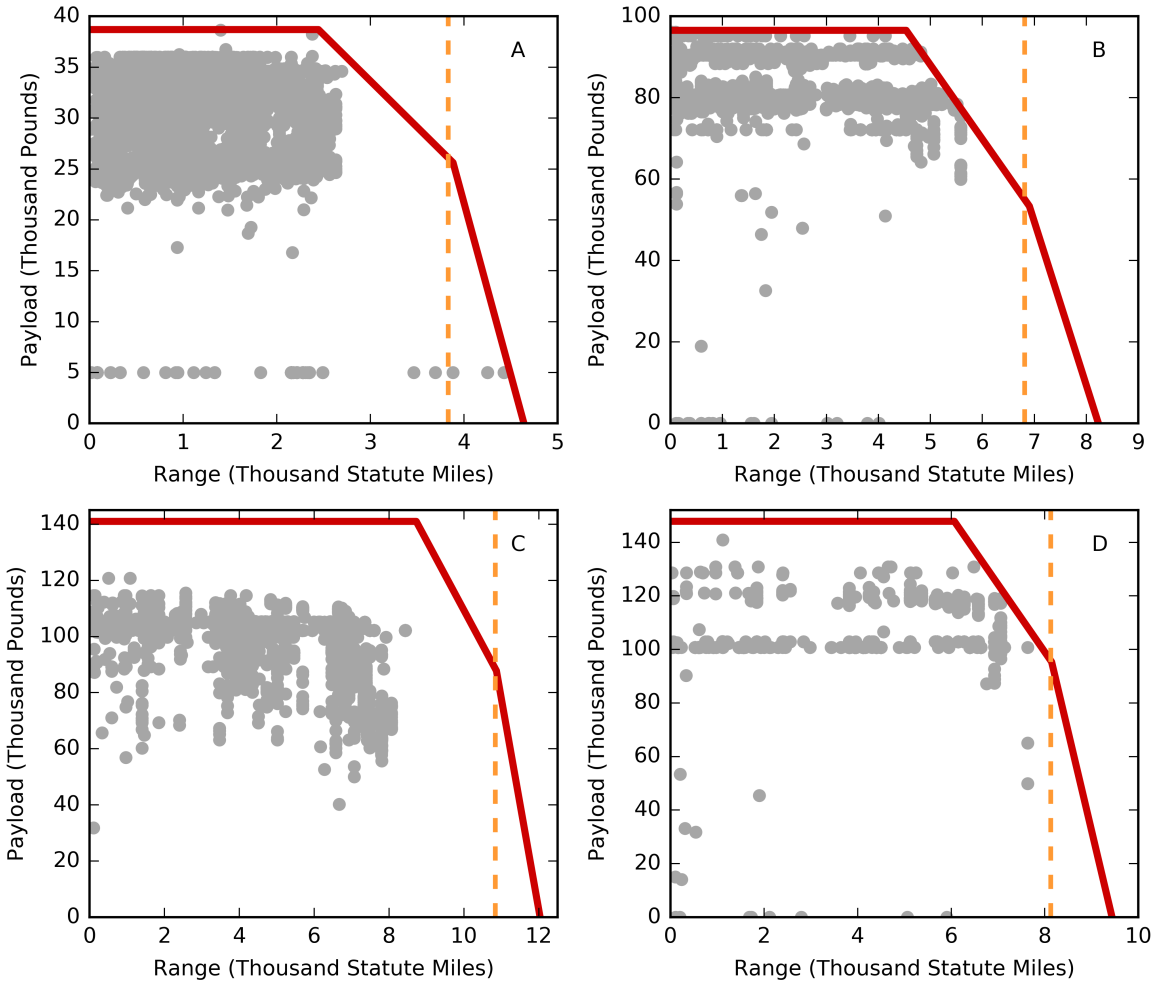

Figure 11: Payload-range diagrams for four Boeing aircraft types in 2015 (A: 737-700; B: 767-300/300ER; C: 777-200ER/200LR/233LR; D: 747-400; design limits overlaid in red; design ranges indicated by dotted lines) [14]

2.2 Hypothesis

By assuming the impacts of vehicle technologies and operational improvements to be independent (Eqs. 1–4), the inter-dependencies are disregarded and not accounted for even though, as illustrated in the previous section, they do exist and are significant. In order to capture their impact on system-level fuel burn, technologies and operations need to be considered simultaneously and not independently. If the impacts of vehicle technologies and operational improvements are not assumed to be independent and are evaluated simultaneously, it is argued that opportunities can be identified at the

system-level to exploit the inter-dependencies such that the net performance impact is augmented. This claim is stated in the form of a hypothesis:

H: Inter-dependencies between vehicle technologies and operational improvements can be exploited to further enhance the performance of aviation systems.

The following subsection details an experimental plan that attempts to increase confidence in this hypothesis.

2.2.1 Experimental Plan

Testing **H** is equivalent to testing the validity of Eq. 4. If the hypothesis fails, then Eq. 4 appropriately describes the system and can be used to evaluate its performance. Conversely, if the hypothesis holds, then Eq. 4 should not be generally assumed to be valid. To test the hypothesis, the following experimental plan is employed:

1. Given a technology implementation scenario (TS_i), compute the impact of technologies on system performance assuming no operational changes
2. Given an operational improvement scenario (OS_i), compute the impact of operations on system performance assuming no technological changes
3. Given TS_i and OS_i, compute the total impact on system performance
4. Compare the results of step 3 with the sum of the results of steps 1 and 2
5. Repeat steps 1–4 for different technological and operational scenarios
6. Repeat steps 1–5 for different socioeconomic scenarios

The hypothesis is accepted if for all scenarios, step 4 consistently shows that combinations of TS_i and OS_i would result in:

$$\Delta \geq \delta_{\mathrm{Tech}} + \delta_{\mathrm{Ops}} \quad \Longleftrightarrow \quad \frac{\mathrm{d}FB}{\mathrm{d}t} \leq \frac{\partial FB}{\partial T}\frac{\mathrm{d}T}{\mathrm{d}t} + \frac{\partial FB}{\partial O}\frac{\mathrm{d}O}{\mathrm{d}t} + \frac{\partial FB}{\partial t} \tag{10}$$

Eq. 10 asserts that simultaneous contributions from vehicle technologies and operational improvements reinforce one another such that the net impact is enhanced.

Steps 1–3 of the experimental plan to test **H** assume that a modeling capability is available to analyze the system-level impacts of vehicle technologies and operational improvements. While steps 1 and 2 require the analysis of technologies and operations independently, step 3 requires simultaneous consideration of both enablers. However, as previously discussed, a framework that provides the required capability to conduct step 3 is lacking in the literature. In the next chapter, the methodological framework developed to achieve the research objective of this thesis and utilized to test **H** is presented.

2.2.2 Implications of Hypothesis

If the previous experiment successfully increases confidence in **H**, then the dependence of technologies and operations implies that $T = T(t, O)$ or alternatively, $O = O(t, T)$. Given that $FB = FB(t, T, O)$, $\mathrm{d}FB/\mathrm{d}t$ is therefore expressed as:

$$\begin{aligned} \frac{\mathrm{d}FB}{\mathrm{d}t} &= \frac{\partial FB}{\partial t} + \left[\frac{\partial FB}{\partial T}\frac{\partial T}{\partial t}\right] + \left[\frac{\partial FB}{\partial O} + \frac{\partial FB}{\partial T}\frac{\partial T}{\partial O}\right]\frac{\mathrm{d}O}{\mathrm{d}t} \\ \frac{\mathrm{d}FB}{\mathrm{d}t} &= \frac{\partial FB}{\partial t} + \left[\frac{\partial FB}{\partial T} + \frac{\partial FB}{\partial O}\frac{\partial O}{\partial T}\right]\frac{\mathrm{d}T}{\mathrm{d}t} + \left[\frac{\partial FB}{\partial O}\frac{\partial O}{\partial t}\right] \end{aligned} \tag{11}$$

where the first expression assumes $T = T(t, O)$ and the second assumes $O = O(t, T)$. Both expressions include terms that relate technologies and operations (shown in red). Integrating the first expression of Eq. 11 yields:

$$\int_a^b \left(\frac{\mathrm{d}FB}{\mathrm{d}t} - \frac{\partial FB}{\partial t}\right)\mathrm{d}t = \int_a^b \left(\frac{\partial FB}{\partial T}\frac{\partial T}{\partial t} + \frac{\partial FB}{\partial O}\frac{\mathrm{d}O}{\mathrm{d}t} + \frac{\partial FB}{\partial T}\frac{\partial T}{\partial O}\frac{\mathrm{d}O}{\mathrm{d}t}\right)\mathrm{d}t \tag{12}$$

$$\Delta = \delta_{\text{Tech}} + \delta_{\text{Ops}} + \delta_{\text{Inter}}$$

where δ_{Inter} represents system performance improvements due to inter-dependencies. The same equality would result from integrating the second expression of Eq. 11. From Eqs. 10 and 12, the hypothesis implies that for a given socioeconomic scenario, there exists a combination of technological and operational scenarios such that:

$$\delta_{\text{Inter}} \geq 0 \tag{13}$$

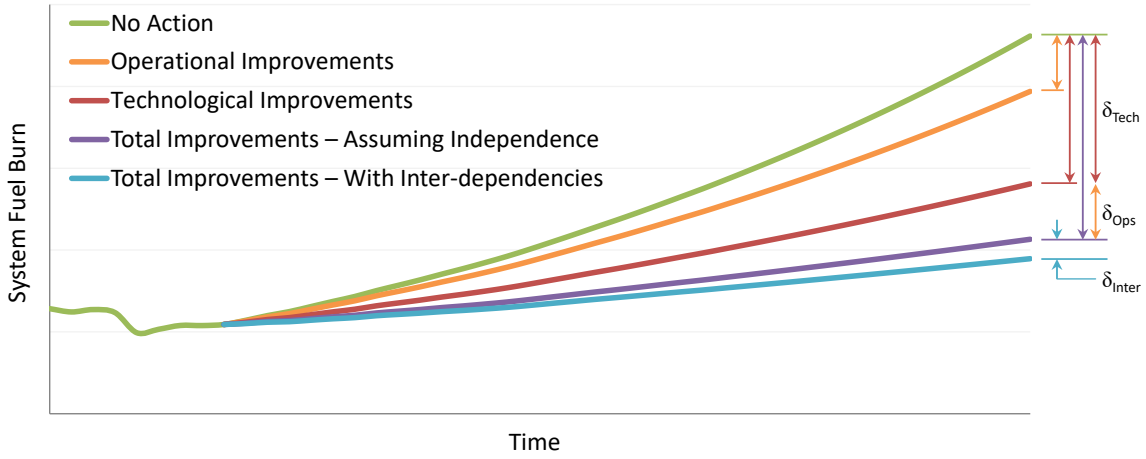

Figure 12: Schematic plot showing the impacts of vehicle technologies and operational improvements to be reinforcing

Figure 12 graphically shows the inter-dependencies between vehicle technologies and operational improvements to contribute positively towards the reduction of system fuel consumption.

Inter-dependencies between technologies and operations provide an opportunity to enhance overall system performance. Technological and operational upgrades could be introduced to the system such that the dependency terms $\partial T/\partial O$ and/or $\partial O/\partial T$ are exploited, and further reductions in system fuel burn are achieved. This is especially significant considering that next generation technologies are of low maturity. In the near future, those technologies will have slow introduction rates and thus, would not affect $\mathrm{d}FB/\mathrm{d}t$ considerably. However, simultaneous operational changes could exploit the minimal technological benefits through inter-dependencies. Conversely, in the far future when technology rates are indeed higher, minor operational upgrades could be exploited as well.

Technologies and operations are considered means and ways to achieve the system performance and environmental targets. Proper modeling of the system's response to improvements provides guidance for strategic decision making and resource allocation. The quantification of both technological and operational impacts, while accounting

for inter-dependencies, would be used to assess the feasibility of future environmental targets set by the aviation industry. As a result, policy makers and stakeholders would be able to identify appropriate actions for the enhancement of system performance.

CHAPTER III

METHODOLOGY

To achieve the research objective of this thesis, the methodological framework should enable the evaluation of system-level performance for various technology introduction and operational improvement scenarios. Furthermore, uncertainties in socioeconomic factors such as demand growth and fuel price need to be accounted for and managed effectively. This chapter discusses the development of such framework and describes in detail its different building blocks.

3.1 Framework Development

As mentioned in section 1.3, there are two metrics of interest for this methodological framework: fuel consumption and CO_2 emissions. While those two metrics need to be evaluated at the system-level (since environmental targets set by IATA and/or ICAO apply to the aviation system as a whole), all vehicle technologies and most operational improvements primarily impact vehicle-level performance. Therefore, this framework should provide a link between vehicle-level impacts and system-level impacts. Further, the link should be a two-way one so that vehicle-level improvements can be evaluated at the system-level (exploratory forecasting) or alternatively, system-level targets can be used to set requirements for vehicle-level performance (normative forecasting)[1].

Figure 13 presents an overview of the methodological framework and its function. Given performance improvements at the vehicle-level, the framework is to compute

[1]Exploratory forecasting attempts to predict the impact of technological advancements in a given time frame (*present* $\Longrightarrow$ *future*). Normative forecasting attempts to provide technology development guidance in order to achieve certain performance levels in a given time frame (*present* $\Longleftarrow$ *future*) [42]. Both forecasting techniques were investigated by Jantsch in 1967 concluding that "the full potential of technological forecasting is realized only where exploratory and normative components are joined in an iterative, or ultimately, in a feedback cycle" [43].

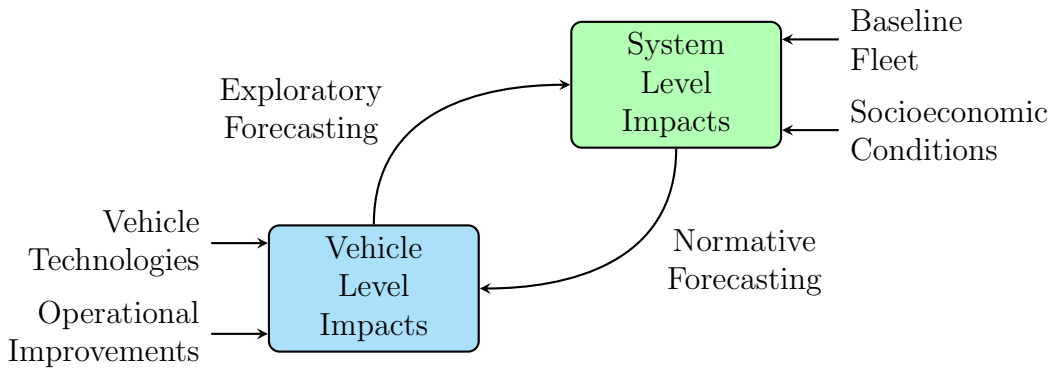

Figure 13: Overview of the methodological framework

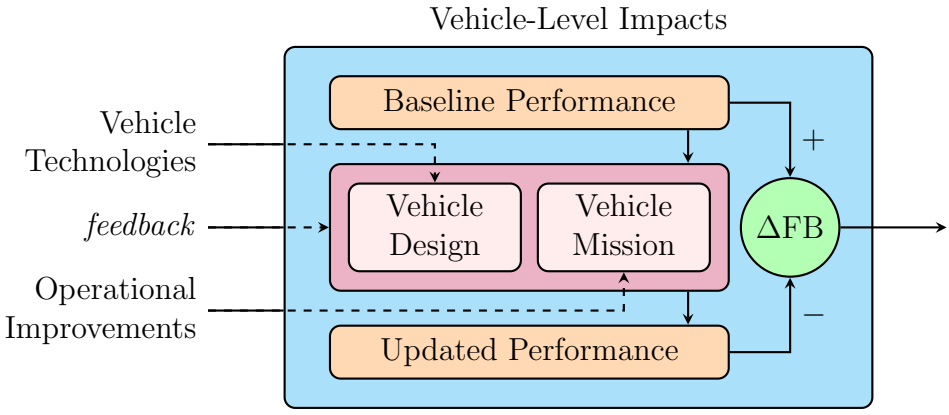

Figure 14: Building blocks required for the computation of vehicle-level impacts

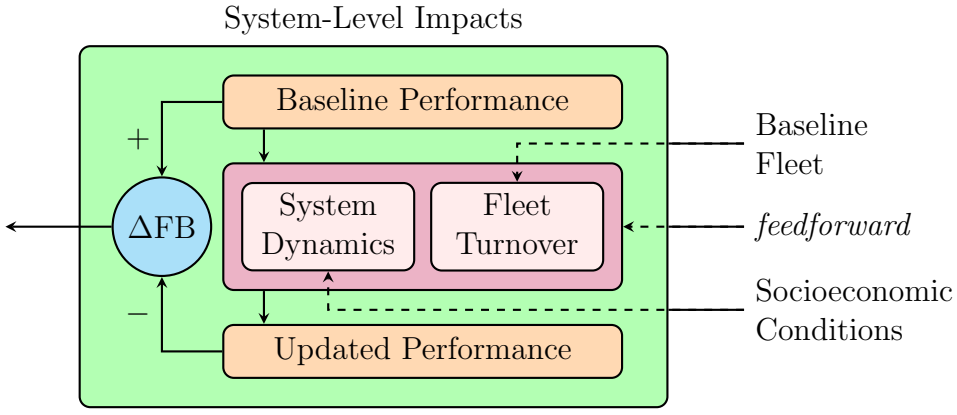

Figure 15: Building blocks required for the computation of system-level impacts

system-level impacts according to predefined socioeconomic conditions and a baseline operational fleet. Figures 14 and 15 further demonstrate the steps required to quantify vehicle-level and system-level impacts, respectively. As shown in the figures, a baseline reference needs to be established at both levels to quantify performance improvements. For vehicle-level analysis, an aircraft sizing capability should be utilized to map the impacts of technologies on vehicle design. Similarly, a flight optimization environment is necessary to map the impacts of operational improvements. At the system-level, a complete fleet turnover procedure should be employed to upgrade the baseline fleet and introduce new aircraft to the system. Additionally, the system dynamics need to be modeled to simulate the system's response to varying socioeconomic conditions.

As illustrated in Figures 13–15, vehicle-level and system-level analyses feed into one another (feedforward: $vehicle \Longrightarrow system$ and feedback: $vehicle \Longleftarrow system$). It is important to note that while these links are crucial to meet the research objective of this thesis, they remain optional and can be replaced with appropriate assumptions (i.e., within the framework, it is possible to conduct a vehicle-level analysis without conducting a system-level analysis and vice versa).

3.2 Building Blocks

In this section, the main building blocks of the methodological framework are detailed. First, the baseline performances for both vehicle-level and system-level analyses are established. Second, the two vehicle-level building blocks are discussed: vehicle design and vehicle mission. Last, the two system-level building blocks are described: system dynamics and fleet turnover.

3.2.1 Baseline Performance

In order to gauge the impacts of technological and operational changes on the vehicle and/or the system, a baseline performance needs to be defined at both analysis levels. The following subsections demonstrate how those baselines are modeled/determined.

Table 3: Baseline vehicles

	TP	RJ	SSA	LSA	STA	LTA	VLA
Passenger capacity	66	86	128	177	261	305	417
Design range (nmi)	1 000	1 980	3 330	2 960	5 920	7 530	7 060
Cruise Mach number	0.450	0.800	0.780	0.780	0.800	0.840	0.850
Service ceiling (ft)	25 000	41 000	41 000	41 000	43 200	43 000	45 100
Operating empty weight (lb)	28 537	47 360	82 949	91 300	198 133	317 088	403 008
Maximum ramp weight (lb)	49 965	85 165	154 859	174 900	412 052	656 229	874 027
Sea-level static thrust (lbf)	2× 6 997	2× 14 393	2× 25 911	2× 27 300	2× 59 901	2× 97 186	4× 56 599
Wing reference area (ft^2)	647	754	1 408	1 409	3 193	4 922	6 186
Wing span (ft)	88	76	113	113	155	199	207
Reference airframe	ATR-72	CRJ-900	737-700	737-800	767-300ER	777-200ER	747-400
Reference engine	PW127	CF34-8C5	CFM56-7B	CFM56-7B	CF6-80C2	GE90-94B	PW4056

3.2.1.1 Baseline Vehicle Performance

Performance varies by aircraft type and therefore, a baseline cannot be defined based on a single vehicle. Instead, vehicles are categorized by seating capacity and engine type into seven representative classes: Turboprop (TP), Regional Jet (RJ), Small Single Aisle (SSA), Large Single Aisle (LSA), Small Twin Aisle (STA), Large Twin Aisle (LTA), and Very Large Aircraft (VLA). For each class, an operational airframe/engine design combination is identified as reference. Performance of that reference design is used to model the baseline[2]. Table 3 summarizes design characteristics pertaining to the baseline vehicle classes.

To create fuel burn performance models for the baseline vehicles, the Flight Optimization System (FLOPS) software developed by NASA is utilized [44]. FLOPS is a multidisciplinary modeling capability used for the conceptual and preliminary design of aircraft concepts. While FLOPS can be used to optimize aircraft configuration, to generate/calibrate the baseline vehicle models, it is utilized in analysis mode in which the user provides fixed configuration inputs (including aircraft geometry and design mission) and FLOPS returns a detailed performance report that includes block fuel. Inputs for the seven reference vehicles are gathered from publicly available sources[3]. To model engine performance, FLOPS engine decks are generated beforehand using two additional NASA modules: the Numerical Propulsion System Simulation (NPSS) and the Weight Analysis of Turbine Engines (WATE) [45, 46].

The baseline models are calibrated such that the FLOPS output weights closely

[2]The *baseline* vehicle is a model that resembles the fuel burn performance of an existing *reference* vehicle (e.g., the LSA baseline is modeled/calibrated such that its performance closely matches that of the Boeing 737-800 with CFM56-7B engines).

[3]The following sources were used to obtain geometry, payload/range and weights data:
ATR-72: ATR, ATR family brochure
CRJ-900: Bombardier, CRJ900 aircraft airport planning manual
737-700/-800: Boeing, 737 airplane characteristics for airport planning
767-300ER: Boeing, 767 airplane characteristics for airport planning
777-200ER: Boeing, 777-200LR/-300ER/-Freighter airplane characteristics for airport planning
747-400: Boeing, 747-400 airplane characteristics for airport planning

match published values for the reference vehicles. After calibration, the models are run in FLOPS once again, this time in optimization mode. As explained by Nickol and Haller, this final step is necessary for proper accounting of technology benefit [47]. It ensures that the baseline vehicles are operating at optimum levels and that any further performance enhancement can only be achieved through technological or operational upgrades. The final optimized FLOPS models are the ones utilized in further analyses to represent baseline vehicle performance.

It is important to note that after optimization, the baseline models are no longer calibrated/identical to the reference vehicles since FLOPS in optimization mode will vary design variables such as wing area and thrust to meet predefined constraints [47]. However, the resulting models should still closely resemble the reference vehicles.

The previously described method for establishing baseline performance using the NASA software suite (FLOPS/NPSS/WATE) was successfully demonstrated in past works by different researchers, and is therefore implemented in this thesis [48, 49].

3.2.1.2 Baseline System Performance

In order to define a baseline for system performance, an appropriate fuel burn metric needs to be identified. Different metrics have been proposed and utilized in the past; however, most are similar and attempt to relate distance to fuel consumption. Among those metrics are the following:

- ASM/Gallon: the ratio of total available seat miles[4] to total fuel consumption. This metric was used by the FAA for its aerospace forecasts [4].
- MV: the Metric Value (MV) is defined as $SAR^{-1}/RGF^{0.24}$ where SAR is specific air range[5] and RGF is a reference geometry factor[6]. This metric is defined at the vehicle-level but can be averaged across fleet vehicles to give a representative

[4] Available seat miles, calculated as [no. of seats]·[distance], is a measure of capacity.
[5] Specific air range is the distance covered per unit fuel consumed at specific operating conditions.
[6] Reference geometry factor is the cabin floor area, defined by ICAO as a measure of aircraft size.

system-level value. This metric was recently introduced by ICAO [50].

- PFEI: the Payload Fuel Energy Intensity (PFEI) metric is defined as the ratio of fuel energy consumed to the product of total payload and great circle distance. This metric was used by Hileman et al [51].
- Fuel/RPK: the ratio of total fuel consumption to total revenue passenger kilometers[7]. This metric was utilized by Kharina and Rutherford [52].

There are different strengths and weaknesses to each metric. For example, the advantage of using PFEI is that it is based on fuel energy rather than fuel quantity, which allows for future concepts like hybrid-electric or fully electric vehicles to be accounted for. These concepts however, are not studied within the scope of this thesis. Similarly, while MV is being proposed as a first step towards achieving a global CO_2 emissions standard, it has been criticized for its derivation and its scientifically unjustified units (kilograms/kilometer/meter$^{0.48}$) [50].

Alternatively, the ASM/Gallon and Fuel/RPK metrics are very similar and could be considered as reciprocals of one another (since available seats are directly related to revenue passengers through load factor). For the purposes of this thesis, the metrics are equivalent. Unlike PFEI and MV, both metrics are straightforward and do not require any special conversions.

Given the previous, ASM/Gallon is selected as a metric for system performance. Current fuel burn performance, derived from BTS historical data, is used to establish a baseline value for ASM/Gallon. This value will get updated based on technological and/or operational changes.

3.2.2 Vehicle Design

The vehicle design block of the methodological framework reflects design changes due to the implementation of technology. It is important for those changes to occur about

[7]Revenue passenger kilometers, calculated as [no. of passengers]·[distance], is a measure of traffic.

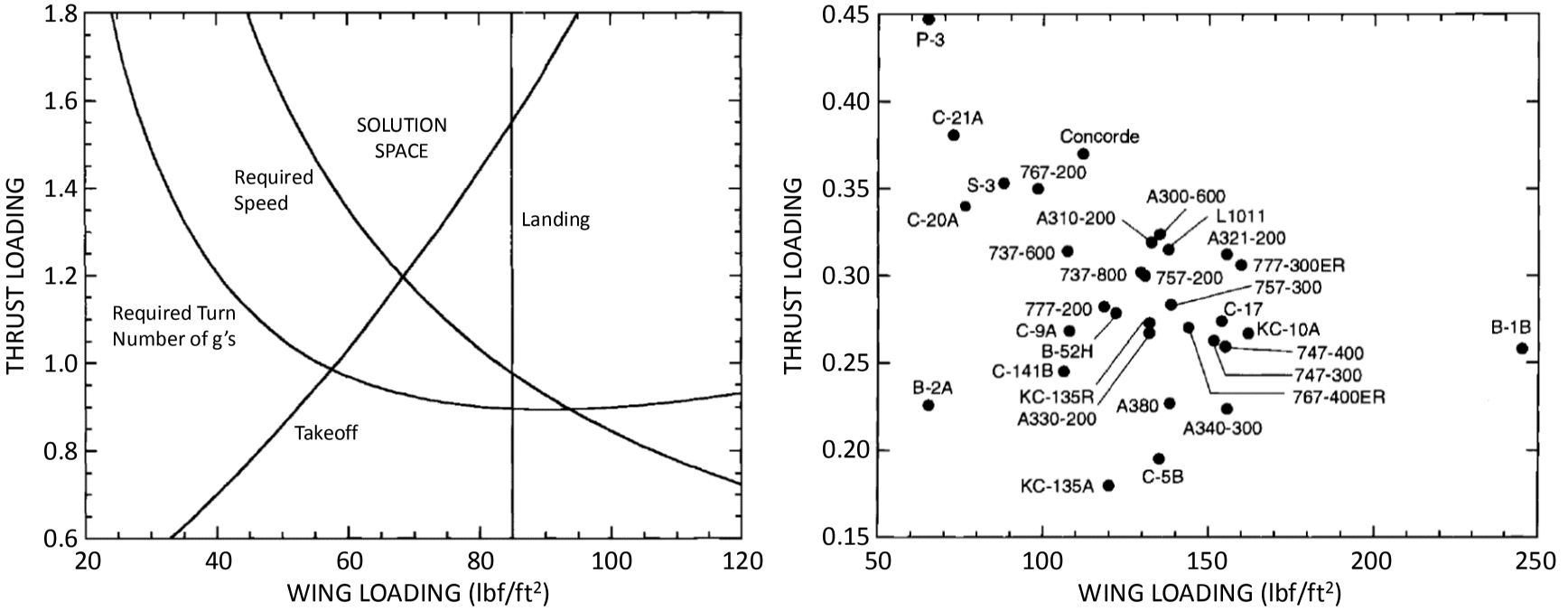

Figure 16: Thrust loading versus wing loading (left: scehmatic constraint analysis; right: cargo and passenger aircraft) [53]

a fixed 'design point'. Furthermore, if multiple technologies are being implemented, it is crucial for their compatibility to be determined in advance. Finally, a clear mapping between the technologies and the metrics they impact needs to be constructed. These issues are addressed in the next subsections.

3.2.2.1 Aircraft Sizing

Sizing an aircraft typically commences with a constraint analysis. The latter is based on performance requirements originally defined in a Request for Proposal (RFP), and translated into functional relationships between thrust loading (T_{SL}/W_{TO}) and wing loading (W_{TO}/S) of the general form:

$$\frac{T_{SL}}{W_{TO}} = \frac{\beta}{\alpha}\left\{\frac{qS}{\beta W_{TO}}\left[K_1\left(\frac{n\beta}{q}\frac{W_{TO}}{S}\right)^2 + K_2\left(\frac{n\beta}{q}\frac{W_{TO}}{S}\right) + C_{D0} + C_{DR}\right] + \frac{P_S}{V}\right\} \quad (14)$$

where T_{SL} is sea-level thrust, W_{TO} is takeoff weight, S is wing area, n is load factor, q is dynamic pressure, $\alpha = T/T_{SL}$ is the installed full throttle thrust lapse, $\beta = W/W_{TO}$ is the ratio of instantaneous weight to takeoff weight, $[K_1; K_2; C_{D0}]$ are the coefficients of the parabolic lift-drag polar, C_{DR} represents additional drag caused by, for example, flaps or ground friction, P_S is the weight specific excess power, and V is velocity [53]. Figure 16 presents a schematic constraint analysis. The selection of a thrust loading and wing loading combination in the solution space resulting from the analysis defines a vehicle design point.

For the baseline vehicles, the design points are determined based on the information of Table 3 (Table 4). Although the baseline models are re-optimized to reflect the impact of technology implementation, the design points need to be fixed throughout.

Table 4: Design points of the baseline vehicles

	TP	RJ	SSA	LSA	STA	LTA	VLA
Thrust loading	0.280	0.338	0.335	0.312	0.291	0.296	0.259
Wing loading (lbf/ft^2)	77.21	112.96	110.02	124.15	129.08	133.34	141.39

	T1	T2	T3	T4
T1	1	1	1	0
T2	1	1	1	0
T3	1	1	1	1
T4	0	0	1	1

	M1	M2	M3	M4	M5	M6
T1	+1.1%	+2.3%	0.0%	0.0%	−0.3%	+4.1%
T2	−0.2%	0.0%	+3.7%	0.0%	0.0%	+0.1%
T3	−0.2%	−0.9%	+1.4%	+1.2%	+0.1%	−0.7%
T4	0.0%	+1.4%	−1.1%	−0.1%	−2.1%	−0.6%

Figure 17: Notional technology compatibility (left) and impact (right) matrices

This is to ensure that the vehicles remain within the feasible space of their respective constraint analyses (i.e., the updated vehicles should meet the same requirements of the baseline ones).

3.2.2.2 Technology Implementation

To ensure that all vehicle technologies implemented are compatible with one another, a compatibility matrix is constructed beforehand. This is a symmetric square matrix with binary elements where 0 indicates incompatibility and 1 indicates compatibility. Another equally important matrix that needs to be defined is the technology impact matrix. The matrix maps all technologies to the different metrics they directly affect. Figure 17 shows notional examples of both matrices.

Vehicle technologies target different aircraft design areas including aerodynamics, structures, propulsion, etc. Those areas interact and this interaction affects the design of the vehicle as a whole. Therefore, to determine the full impact of a given technology package, it is crucial for those different design areas to be considered simultaneously.

Technology impact on vehicle performance is typically determined through computational modeling and physical experimentation. Once a technology is fully matured[8], its precise impact is determined and it is ready for introduction to service. Since technologies require years (sometimes decades) to mature, various modeling capabilities

[8]The Technology Readiness Level (TRL) is a measurement system used to assess the maturity of technologies under development [54, 55]. There are nine TRLs ranging from 1 to 9. The uncertainty in performance of a particular technology decreases as its TRL increases [56].

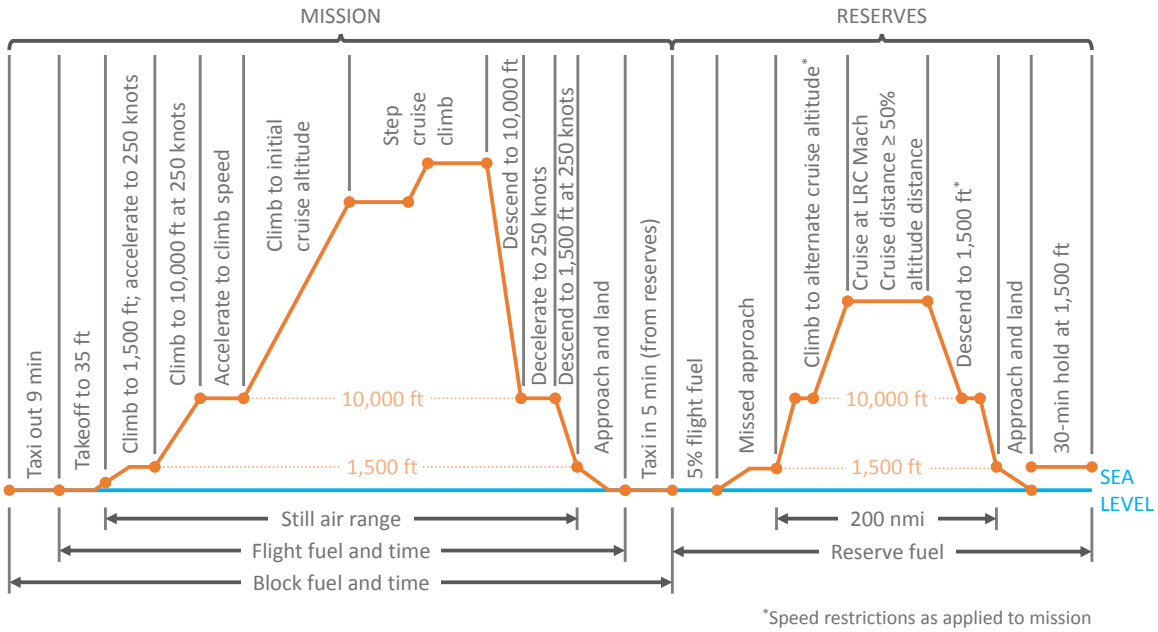

Figure 18: Example mission profile [57]

have been developed to predict their impact on vehicle performance in the conceptual and preliminary design phases. As will be shown in Chapter 4, most of those modeling capabilities rely on Multidisciplinary Design Optimization (MDO) methods.

3.2.3 Vehicle Mission

The vehicle mission block of the methodological framework reflects changes in mission profile due to the implementation of operational improvements (an example mission profile is shown in Figure 18). Unlike aircraft technologies, operational improvements are assumed to not instigate any changes in vehicle design. Instead, the sized vehicle is treated as a point mass that is flown different profiles for a fixed design range (still air range). This assumption is made to isolate the impact of operational improvements on performance, and to ensure that such impact does not include any re-design effects[9].

[9]If an operational improvement does require the implementation of technology or the installation of specific equipment, its impact is determined by first re-designing the vehicle to accommodate the required technology (vehicle design block), and second by altering the mission profile to reflect the operational improvement (vehicle mission block). Within the context of this thesis, such improvement is not considered to be purely operational, but a hybrid one that combines both technological and operational elements.

Since operational changes seek to enhance vehicle performance along the different segments of the mission profile, an overview of mission fuel consumption is presented. Further, minimum/optimal fuel and time paths for certain segments are discussed.

3.2.3.1 Mission Fuel Consumption

The goal of conducting a fuel consumption analysis along the vehicle's design mission is to determine takeoff gross weight (W_{TO}), which is simply the sum of payload weight (W_P), operational empty weight (W_E), and flight fuel weight (W_F):

$$\begin{aligned} W_{TO} &= W_P + W_E + W_F \\ &= (W_P + W_E) \Bigg/ \left(1 - \frac{W_F}{W_{TO}}\right) \end{aligned} \tag{15}$$

Both W_P and W_E are easily obtained since the vehicle design is known. Alternatively, the unknowns W_{TO} and W_F are determined using an iterative process that starts with an initial estimate of either W_{TO} or W_F/W_{TO}. The latter is computed as follows:

$$\frac{W_F}{W_{TO}} = 1 - \prod_{k=1}^{n} \left[\frac{W_f}{W_i}\right]_k \tag{16}$$

where n is the number of mission segments, and $(W_f/W_i)_k$ is the ratio of aircraft final weight at the end of segment k to initial weight at the beginning of that segment. The weight fractions are determined for every segment based on the value of P_S [58]:

$$\frac{W_f}{W_i} \approx \begin{cases} \exp\left[-\dfrac{TSFC \cdot (D+R)}{W}\Delta t\right], & \text{if } P_s = 0 \\ \exp\left[-\dfrac{TSFC \cdot T}{V(T-(D+R))}\Delta z_e\right], & \text{if } P_s > 0 \end{cases} \tag{17}$$

where $TSFC$ is the installed thrust specific fuel consumption, $[T; W; (D+R)]$ are the instantaneous thrust, weight and drag forces, respectively, V is velocity, Δt is total segment flight time, and Δz_e is total change in segment energy height[10]. For segments of the first type ($P_S = 0$), all thrust work is dissipated resulting in no speed and/or

[10]The energy height represents the sum of the instantaneous potential and kinetic energies of the aircraft $z_e = h + V^2/2g$, and is related to the weight specific excess power through $P_S = \mathrm{d}z_e/\mathrm{d}t$ [58].

altitude variation. Examples include constant speed cruise, best cruise Mach number and altitude, and loiter. For segments of the second type ($P_S > 0$), some thrust work is converted to mechanical energy in order to vary speed and/or altitude. Examples include constant speed climb, takeoff acceleration, and horizontal acceleration.

The previous analysis yields the fuel required and the corresponding takeoff gross weight to fly a given mission. However, surface operations such as taxiing and towing are not considered. Instead, they are accounted for in the determination of block fuel, which is the sum of flight fuel and ground fuel (Figure 18). The latter is a function of engine idle fuel flow and time spent on the ground (typically a direct proportionality):

$$W_{F,G} = f(\dot{W}_{F,\text{idle}}, \Delta t_G) \quad \Rightarrow \quad W_{F,G} \propto \dot{W}_{F,\text{idle}} \cdot \Delta t_G \tag{18}$$

Accordingly, for subsequent analyses, block fuel is used to gauge the impact of vehicle technologies and operational improvements on vehicle fuel burn performance.

3.2.3.2 Minimum Fuel and Time Paths

For mission segments with $P_S > 0$, it is possible to mathematically derive paths that minimize either fuel or time from the vehicle's rate of fuel consumption given as [58]:

$$\frac{\mathrm{d}W_F}{\mathrm{d}t} = T \cdot TSFC \quad \Rightarrow \quad \mathrm{d}W_F = \alpha T_{SL} \cdot TSFC \cdot \frac{\mathrm{d}z_e}{P_S} \tag{19}$$

Defining $[\alpha \cdot TSFC/P_S]$ as the fuel consumed specific work (f_S) and integrating yields:

$$\Delta W_F = \int_1^2 \mathrm{d}W_F = T_{SL} \int_{z_{e1}}^{z_{e2}} \frac{\mathrm{d}z_e}{f_S} \tag{20}$$

From Eq. 20, it is deduced that the minimum fuel-to-climb path from energy height z_{e1} to energy height z_{e2} is one that maximizes the value of f_S at every z_e. Similarly, to determine the minimum time to climb, the relation between P_S and z_e is integrated:

$$\Delta t = \int_1^2 \mathrm{d}t = \int_{z_{e1}}^{z_{e2}} \frac{\mathrm{d}z_e}{P_S} \tag{21}$$

From Eq. 21, it is deduced that the minimum time-to-climb path from energy height z_{e1} to energy height z_{e2} is one that maximizes the value of P_S at every z_e. Graphically, Figure 19 highlights both paths on example contour plots of f_S and P_S.

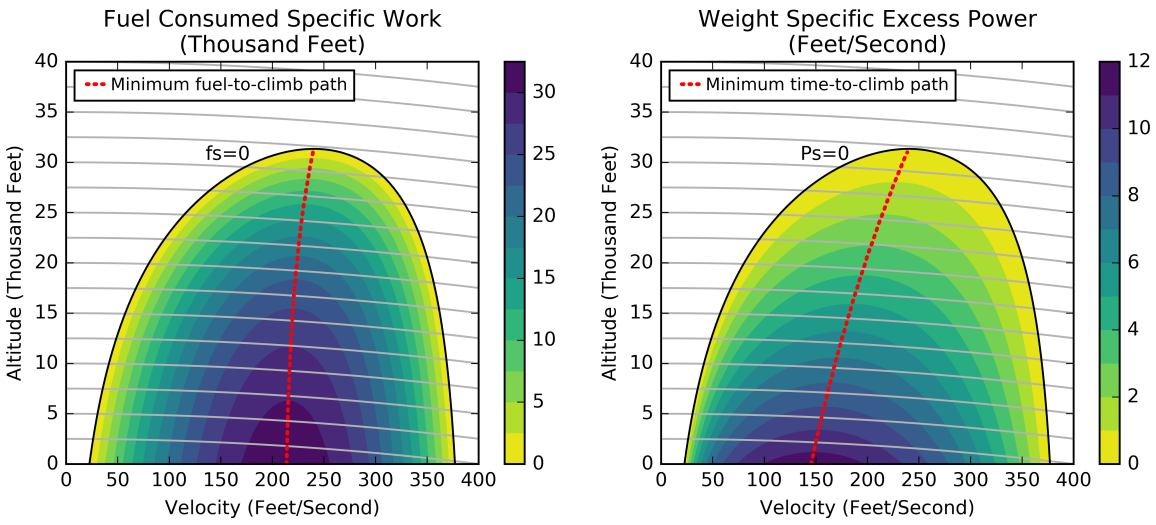

Figure 19: Example contour plots of fuel consumed specific work (f_S) and weight specific excess power (P_S) for the DHC-6 Twin Otter aircraft (constant energy height (z_e) contours overlaid in grey)

Due to various regulations concerning both safety and noise, current aircraft do not necessarily climb and/or descend at optimal settings. Some operational improvements seek to remedy that, however. In order to quantify the impacts of those improvements, the previously discussed paths need to be considered.

3.2.4 System Dynamics

In 1978, the US Congress passed and President Carter signed the Airline Deregulation Act. Prior to that, domestic aviation activity was regulated by the Civil Aeronautics Board (CAB). The CAB was authorized to "control route entry and exit of air carriers, regulate fares, award subsidies, and control mergers and inter-carrier agreements" [59]. However, an economic and political consensus was reached that regulation as practiced by the CAB was inefficient and hindered the growth of the aviation industry. The act effectively stripped the CAB of its regulation authority. Since deregulation, for almost all airlines, the decision to fly a specific route is driven solely by economic profitability. In the next subsections, an overview of airline economics is presented followed by an economics based representation of the aviation system, conveniently developed for the

purposes of this methodological framework.

3.2.4.1 Airline Economics[11]

The route selection process takes into account a number of factors including demand, operating cost, revenue, market share and airport capacity, most of which require sophisticated economic forecasts. In addition, the expected competitor response needs to be simulated and accounted for. Airlines typically utilize optimization based computer models that require detailed inputs to evaluate the profitability of candidate routes. The accuracy of these models depends entirely on the accuracy of the forecasts used and the nature of the embedded assumptions.

The previously described represents a *bottom-up* approach to airline route planning in which detailed analysis is required. Alternatively, a *top-down* approach is based on a relatively high-level aggregate analysis in which only principal knowledge of market demand and operating costs is necessary. Simplified relationships are used to estimate total demand and the corresponding supply. In its most simplistic multiplicative form, demand (D) along an origin-destination (OD) pair can be represented as:

$$D = M \cdot P^a \cdot T^b \tag{22}$$

where M is a constant sizing parameter that accounts for OD market demographics, P is average trip price, T is total trip time, a is price elasticity, and b is time elasticity[12]. The values of M, a and b could be estimated using regression techniques applied to historical values of D, P and T. Supply is then derived from demand through another simple multiplicative relationship:

$$D = S \cdot LF \tag{23}$$

where S is supply and LF is passenger load factor ($LF \in [0, 1]$).

[11] This discussion is primarily based on reference [60].

[12] Price elasticity (a) is defined as the percent change in market demand in response to a 1% increase in average trip price. Similarly, time elasticity (b) is defined as the percent change in market demand in response to a 1% increase in total trip time. Both a and b are negative.

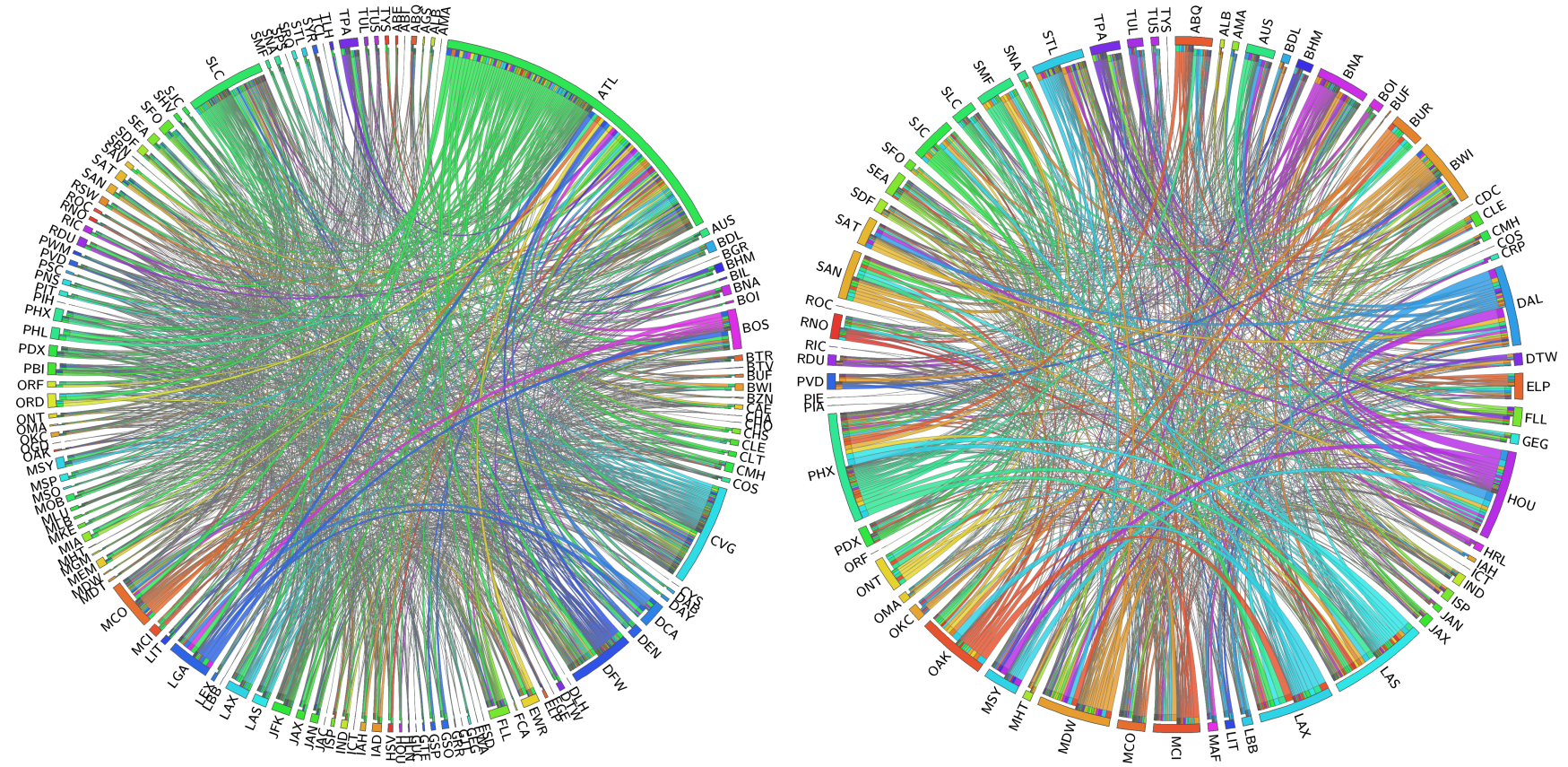

Figure 20: Network of operations for two US airlines in 2000 (left: Delta Air Lines operating a hub-and-spoke network with a main hub in Atlanta Hartsfield-Jackson; right: Southwest Airlines operating a decentralized point-to-point network) [19]

On a system-level, where multiple airlines are considered, it is difficult to adopt a bottom-up approach. Airlines are typically classified into either legacy carriers or low cost carriers [61, 62]. While the former tend to operate in hub-and-spoke networks, the latter tend to operate in point-to-point networks (Figure 20). Not only do the business strategies differ significantly between legacy and low cost carriers, but also within each class various strategies exist. Therefore, implementing a bottom-up approach at the system-level would require the consideration of each airline individually. This is cost prohibitive and will lead to results associated with high levels of inherent uncertainty (since more assumptions and forecasts will be utilized).

Alternatively, a top-down approach allows all airlines operating within the system to be accounted for simultaneously in an aggregate analysis. As previously discussed, information regarding market demand and operating costs are sufficient to construct a high-level system model, without the need for individual airline schedules or route networks. Based on the above-mentioned, a top-down approach is selected for this methodological framework, and will be the basis for the aviation system representation introduced next.

3.2.4.2 Aviation System Representation

An examination of airline operating costs over the last 30 years reveals that, on average, almost 49% of the total costs are due to fuel and labor expenses (Figure 21) [63]:

$$TOC \approx \frac{FC + LC}{0.49} \tag{24}$$

where FC is fuel cost, LC is labor cost, and TOC is total operating cost. Therefore, given both FC and LC, TOC can be easily approximated using Eq. 24. Alternatively, if $[FC;FC/TOC]$ or $[LC;LC/TOC]$ are known, TOC can be directly determined:

$$TOC = \frac{FC}{FC/TOC} = \frac{LC}{LC/TOC} \tag{25}$$

Unlike FC, which is computed as the product of both fuel price and fuel quantity, LC cannot be computed in a straightforward manner since detailed information regarding

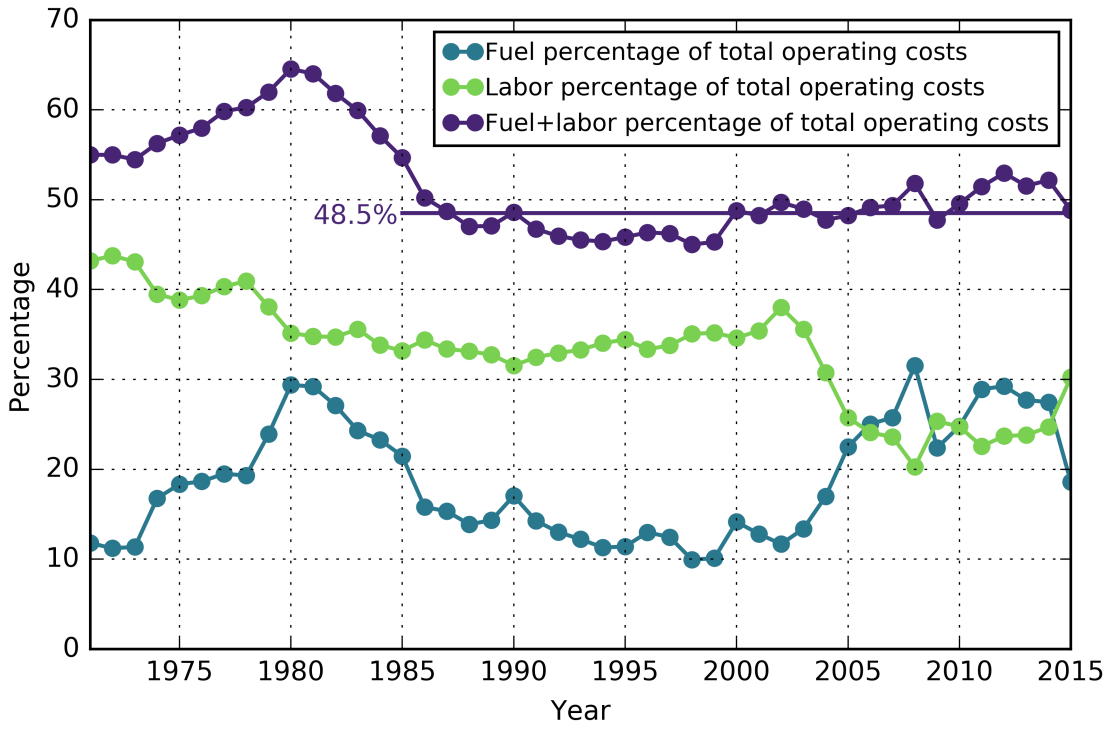

Figure 21: US airlines fuel and labor expenses relative to total operating costs [63]

salaries and related benefits for all personnel needs to be known. Because Eq. 24 would require the computation of LC, it is not utilized. Instead, Eq. 25 is used, along with appropriate assumptions regarding the fuel fraction FC/TOC, to compute TOC.

Given that demand is derived from the input socioeconomic conditions (Figure 15), and given the previous method for determining TOC, a high-level representation of the aviation system may be constructed based on top-down economics.

Figure 22 presents an overview of such representation. Simply, passenger demand for commercial aviation dictates the amount of air traffic and hence, fuel consumption. Fuel cost is an important driver of airline operating cost, which itself influences ticket price. The latter then feeds back to passenger demand, closing the system loop. Those six main system-level quantities are related through six factors, as shown in Figure 22. By definition, passenger load factor is the ratio of demand to supply (Eq. 23). Supply, along with a system-wide fuel efficiency metric (ASM/Gallon), determines system fuel consumption. Fuel cost is calculated based on both consumption and unit price.

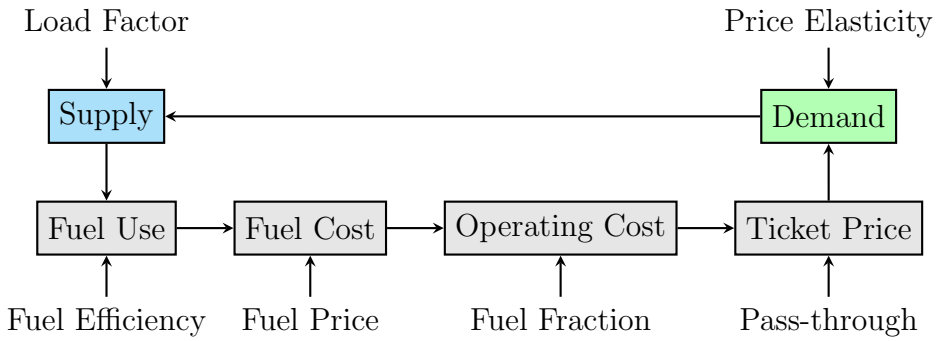

Figure 22: Block diagram of the aviation system

Accordingly, total airline operating cost is determined given a predefined fuel fraction. The 'pass-through' factor then represents a valve that controls how much change in operating cost is reflected in ticket price. Pass-through values are non-negative with zero indicating a fixed ticket price regardless, and positive values indicating changes in ticket price (typically, pass-through values are close to unity). Finally, price elasticity translates any change in ticket price to an inverse change in demand. This is the only negative relationship in the system feedback loop and thus, is the one that guarantees system convergence towards equilibrium.

The system-level representation described above is linked to the vehicle-level analysis through the fuel efficiency metric, as shown in Figure 23. Since vehicle technologies instigate design changes, their system-level impacts can only be realized through the introduction of new vehicles and therefore, a fleet turnover procedure is required. Conversely, operational improvements are assumed to not instigate any design changes and thus, they are applicable to vehicles in the baseline fleet. As a result, the impacts of operational improvements can be directly realized at the system-level.

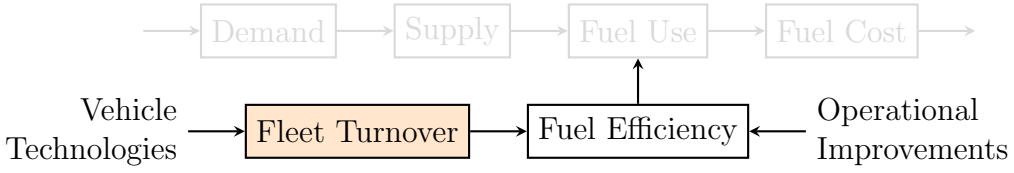

Figure 23: System-level fuel efficiency

3.2.5 Fleet Turnover

To accommodate changes in vehicle design due to the introduction of technologies, the input baseline fleet (Figure 15) needs to be upgraded. Previous works considered three aspects for the turnover of aviation fleets: aircraft retirements, aircraft replacements, and required fleet growth [38, 64]. For its relevance, the retire-replace-grow procedure is incorporated in this methodological framework.

3.2.5.1 Aircraft Retirements

Aircraft age distributions of the baseline fleet are required to initialize the retirement process. Empirically derived aircraft retirement curves (also known as aircraft survival curves) are utilized to determine which vehicles of the fleet are retired (Figure 24) [65, 66]. These curves assign a survival percentage to a vehicle based on its age and type. Accordingly, retirements across the entire fleet are calculated. This approach assumes that vehicles are assigned operations with no preference to age, and that retirements are applied uniformly across the system [38].

To account for deviations from historical trends, parametric retirement curves are

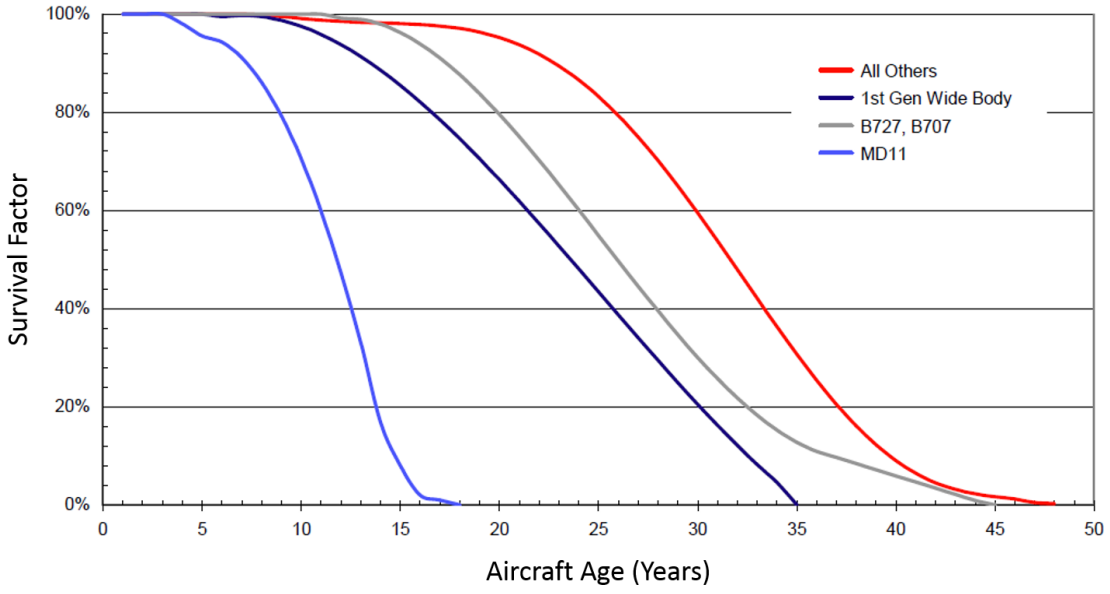

Figure 24: Emperically derived aircraft retirement curves [65]

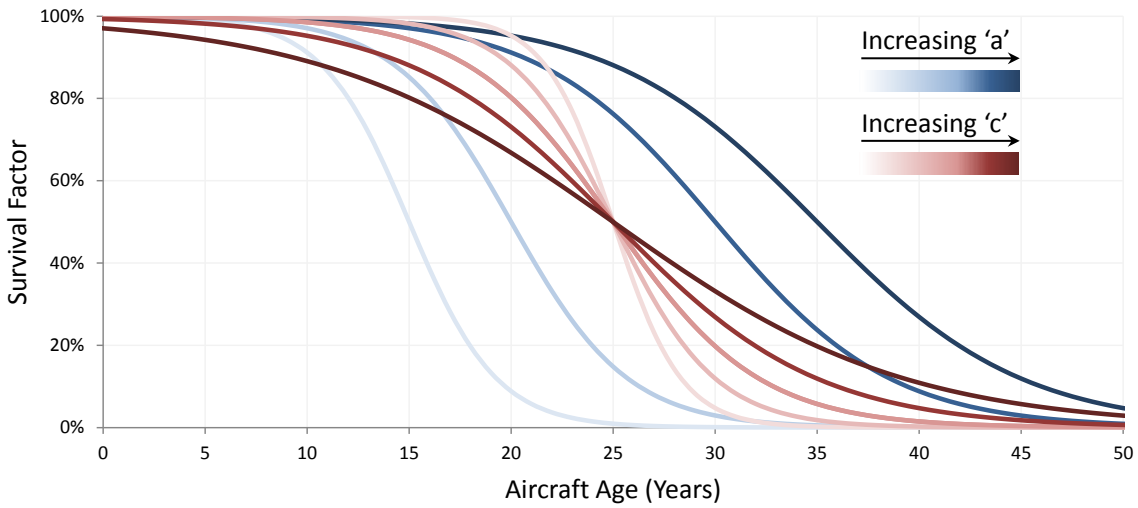

Figure 25: Parametric aircraft retirement curves

formulated using a logistic function of the following form:

$$L(t) = 1 - \frac{1}{1 + \exp((a - t)/c)} \tag{26}$$

where a and c are the location and scale parameters, respectively (Figure 25). Careful consideration should be given to the definition of retirement curves since they directly influence fleet evolution and consequently, system-level performance (Figure 26).

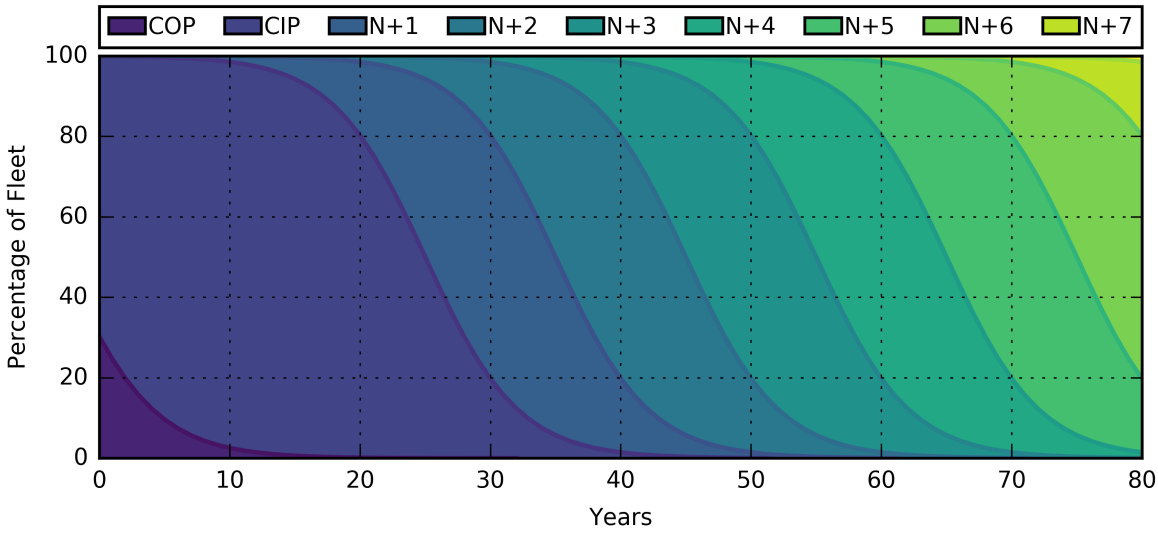

Figure 26: Example fleet evolution according to aircraft retirement curves (COP: current out-of-production vehicles; CIP: current in-production vehicles; N+i: future i-th generation vehicles)

3.2.5.2 Aircraft Replacements

Aircraft replacements are commonly determined on a seating capacity basis, in which fleet vehicles are categorized into several seat classes and retirements/replacements occur within the same class [31, 35]. Although the approach is generally favored for its reduced complexity, Jimenez et al. highlight its limitations through two examples [38]. Assuming the traditional seating classification in which the (211–300 seats) class and the (301–400 seats) class are distinct:

1. The approach would allow a Boeing 757 (220 seats) to be replaced with a Boeing 777 (290 seats) since they fall in the same category (211–300 seats). In reality however, this replacement is unlikely to happen given that the two vehicles are utilized very differently by airlines.
2. Alternatively, the approach would not allow a Boeing 777 (290 seats) to be replaced with another Boeing 777 (305 seats) because the latter falls in a different category (301–400 seats). Nevertheless, the replacement would be reasonably considered in reality.

Instead, Jimenez et al. proposed replacements to occur based on the vehicle's mission capabilities (i.e., a replacement aircraft "must have a mission range and payload/seat capacity that are comparable to or exceed those of the aircraft it replaces" [38]). Their approach has its own drawbacks since it requires the availability of payload/range data for all current and future vehicles.

Within this methodological framework, replacements are determined on a seating capacity basis. However, the limitations discussed above are taken into consideration. The classification of vehicles of the baseline fleet is not subject to rigid cut-off seating values as is the case in traditional fleet turnover procedures. Instead, some flexibility and judgment are exercised in order to avoid cases such as the ones illustrated above and to avoid possible fleet distortions.

3.2.5.3 Fleet Growth

Theoretically, demand growth could be accommodated through increasing passenger load factors and without the addition of new vehicles. However, airlines are currently operating near what forecasts project to be the limit load factor (∼84%) and therefore, fleet growth is inevitable [4]. Future growth in passenger jet aircraft of US mainline air carriers, as predicted by the FAA 2016–2036 aerospace forecast, is shown in Figure 27.

The overall growth in fleet size, as determined by the growth in passenger demand (Figure 22), is related to the growth in vehicle class proportions as follows:

$$[\text{total no. of aircraft}] = \sum_{i=1}^{n} \gamma_i \cdot [\text{no. of aircraft}]_i \tag{27}$$

where γ_i is a vehicle class growth factor and n is the number of vehicle classes of the fleet. However, the determination of the γ_i's requires a detailed bottom-up analysis which, as discussed in section 3.2.4.1, is cost prohibitive and impractical. To overcome such complexity, the fleet is assumed to grow proportionally across all vehicle classes (i.e., vehicle class proportions remain constant):

$$[\text{total no. of aircraft}] = \gamma \cdot \sum_{i=1}^{n} [\text{no. of aircraft}]_i \tag{28}$$

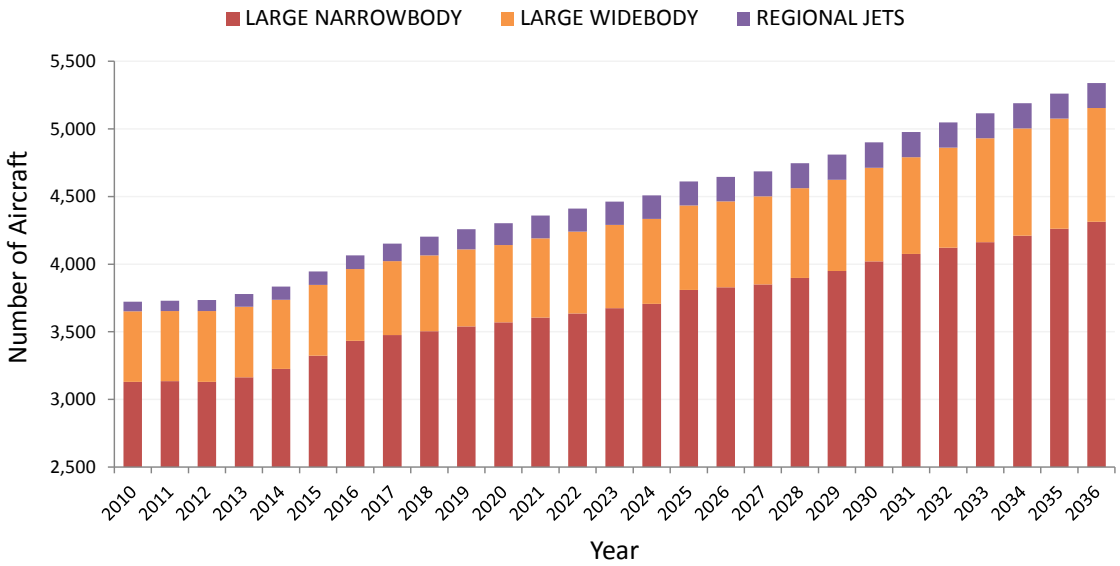

Figure 27: Forecast growth in passenger jet aircraft of US mainline air carriers [4]

where γ is an overall fleet growth factor. This assumption reduces computational complexity and is in line with historical trends and forecast projections (see Appendix A).

3.3 Managing Uncertainty Using Scenarios

Scenarios are typically utilized for uncertainty management when the ambiguity of the working environment is high, the rate and degree of change within such environment is accelerating, and the planning horizon stretches for a long period of time [67]. As quoted below, the goal of scenario based assessments is not to quantify uncertainty, but rather to bound it [67]:

> "When scenarios are used for planning, the intent is not to predict what the market will be and then build a master plan, but rather to ask what the future might hold and then identify the actions that can be taken today that will work no matter how the future turns out."

Scenario planning has been previously utilized as an effective tool in various fields of study [68, 69].

Within the methodological framework, there exists multiple sources of uncertainty. At the vehicle-level, the impacts of both vehicle technologies, especially ones with low TRL, and operational improvements are associated with epistemic uncertainty. At the system-level, socioeconomic conditions that dictate both passenger demand and fuel price are associated with aleatory uncertainty. To tackle those sources of uncertainty, scenarios are utilized at the system-level (Figure 28).

Vehicle-level impacts are used to set performance bounds for fleet vehicles at the system-level. Within those bounds, numerous scenarios are considered to account for uncertainties in vehicle performance. Socioeconomic scenarios are also considered in order to account for uncertain passenger demand growth rates and fuel prices. As will be demonstrated in Chapter 4, the scenarios are generated randomly within Monte Carlo simulations.

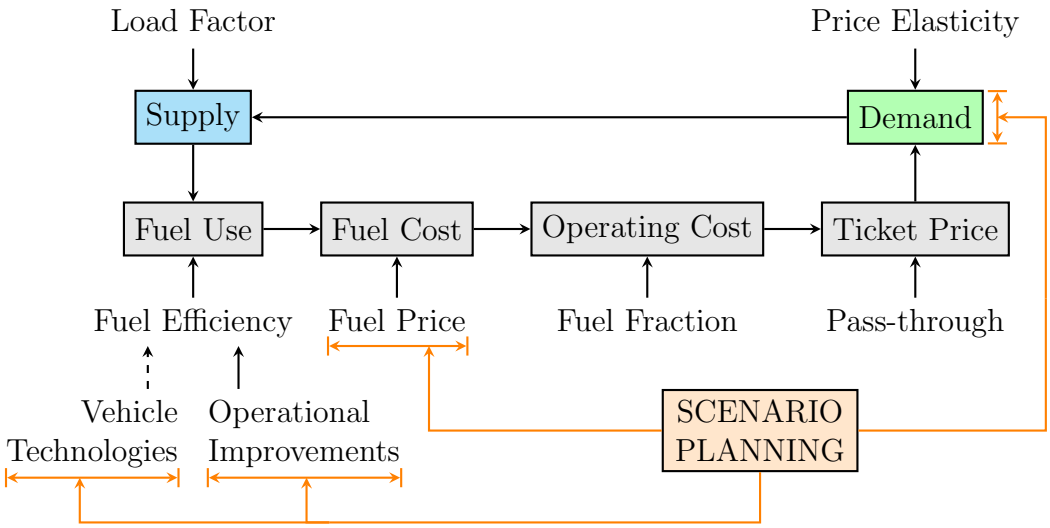

Figure 28: Block diagram of the aviation system showing the different sources of uncertainty managed using scenario planning

CHAPTER IV

MODELING APPROACH

The methodology constructed in the previous chapter identified the elements required to meet the research objective of this thesis. In this chapter, the models and methods implemented within that methodological framework are presented. While most of the modeling is required to evaluate the vehicle-level and system-level impacts of vehicle technologies and operational improvements, the linkage between both impacts needs to be clearly defined beforehand.

4.1 Decoupling of Vehicle-Level and System-Level Impacts

As depicted in Figure 13 and further illustrated in Figure 28, vehicle-level and system-level analyses of the methodological framework are directly linked. This linkage can severely limit the framework's capability if vehicle-level impacts are to be re-evaluated for every technological scenario considered at the system-level, or if system-level impacts are to be re-evaluated for every socioeconomic scenario considered at the vehicle-level. In this thesis, in order to reduce such complexity, the vehicle-level and system-level analyses are decoupled so that they are not reliant on one another (Figure 29).

Decoupling analyses in the engineering design process has been investigated in the past as a means to improve performance and decrease computational run time [70–73]. Within the methodological framework, decoupling allows for the analyses to be conducted independently and at varying fidelity levels. Further, it enables the evaluation of numerous system-level scenarios that adequately cover wide ranges of uncertainty at diminished complexity.

To decouple both analyses, vehicle technologies and operational improvements are not accounted for directly within the system model and instead, are represented by

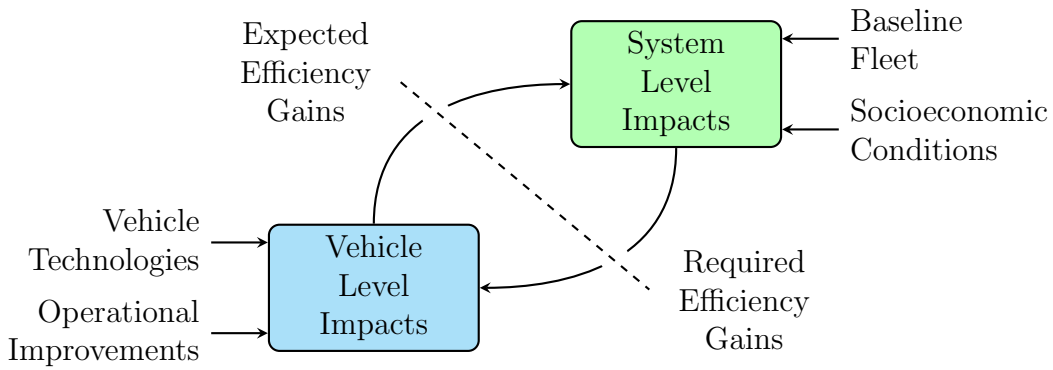

Figure 29: Decoupling of vehicle-level and system-level impacts

efficiency gains/factors that act on the system-level fuel efficiency metric (Figure 23). As a result, the role of the vehicle-level analysis is to either set the values of those efficiency gains or set the bounds from which their values are sampled. Similarly, system performance is not accounted for directly within the vehicle-level analysis. Instead, the role of the system-level analysis is to provide feasible and/or viable efficiency gain values for which the system meets specified performance targets.

4.2 Modeling Vehicle-Level Impacts

In this section, modeling methods implemented within the vehicle design and vehicle mission blocks of the methodological framework are detailed. The modeling approach implemented to evaluate the vehicle-level performance impact of vehicle technologies is discussed first. This is followed by a description of the modeling approach utilized to determine the vehicle-level performance impact of operational improvements.

4.2.1 Modeling Vehicle Technology Impact

To meet the environmental targets set at both the vehicle-level and the system-level, a multitude of technological concepts are currently under investigation. Those concepts typically impact aspects of vehicle design that are airframe related (aerodynamics and structures) or engine related. In addition, some technologies are aimed at enhancing specific vehicle metrics such as noise (Table 2). Although noise technologies are also

airframe or engine related, they are usually handled separately. Tables 5 and 6 list some of the airframe, engine and noise technologies in the NASA portfolio for introduction in the mid term and far term [74, 75].

Recent environmental concerns have shifted the focus of the traditional design process for commercial aircraft [76]. Vehicles have long been designed to meet predefined performance goals while minimizing operating costs. Environmental performance has been typically considered post-design to meet certification standards that required minor adjustments. The recent push to reduce the environmental impact of aviation has led to the tightening of certification requirements. The traditional design process no longer guarantees that a cost efficient design will be environmentally compliant.

In response to this gradual shift towards design for environmental performance, several aircraft design tools have been developed over the years. Those tools attempt to accommodate the impact of technologies under development during the conceptual and preliminary design phases. Many of the tools rely on the definition of an Overall Evaluation Criterion (OEC) that accounts for different design objectives concurrently (in which case, MDO techniques are utilized); otherwise, if the objectives are not to be combined in a single criterion, more complex Multi-Objective Optimization (MOO) methods are used. In the next subsections, a review of existing vehicle design tools is presented followed by the selection of a modeling and simulation environment to be utilized within the vehicle design block of the methodological framework.

4.2.1.1 Existing Vehicle Design Tools

EDS: Kirby and Mavris developed the Environmental Design Space (EDS) as a modeling and simulation environment for aircraft design [77]. EDS provides a capability to generate an integrated analysis of vehicle-level performance, source noise and exhaust emissions using core modules originally developed by NASA including: FLOPS for vehicle sizing, NPSS for engine thermodynamic cycle analysis, WATE for analysis

Table 5: NASA N+2 (mid term) vehicle technologies [74]

Technologies	2015 TRL
Aircraft Aerodynamics and Structures	
T3 – Damage arresting stitched composites	6
T6 – Electro-mechanical flight control actuators	7
T7 – Solid oxide fuel cell auxiliary power unit	3
T10 – Hybrid laminar flow control using suction devices	5
T11 – Natural laminar flow control	5
T12 – Riblets	6
T66 – Tail active flow control	3
T69 – Hybrid laminar flow control using discrete roughness elements	4
T83 – Unitized metallic structures	6
T84 – Tow steered composite structures	4
T96 – Adaptive compliant trailing edge	3
Engine Performance	
T20 – Active compressor clearance control	3
T21 – Active compressor flow control	3
T22 – Active compressor cooling	3
T23 – Active turbine clearance control	5
T24 – Active turbine flow control	4
T25 – Active film cooling	2
T26 – Powder metallurgy disks bonded to single crystal rims	2
T28 – Turbine superalloys	4
T61 – Active combustion control	5
T64 – Lean burn combustor and twin annual premixing swirler	9
T65 – Rich-quench-lean combustor	6
Noise Reduction	
T14 – Flap continuous mold-line link	4
T15 – Flap side edge fence	3
T16 – Landing gear integration	5
T18 – Slat inner surface acoustic liner	3
T47 – Fluidic chevrons	3
T52 – Fan and compressor lip liner	6
T53 – Over the rotor metal foam liner	4
T54 – Fan compound rotor sweep	7
T56 – Soft vanes	3
T57 – Stator sweep and lean	5
T59 – Variable geometry chevrons	6

Table 6: NASA N+3 (far term) vehicle technologies [75]

Technologies	2015 TRL
Aircraft Aerodynamics and Structures	
T165 – Advanced aerodynamic wing circulation control	4
T166 – Cruise slotted flap	5
T187 – Curvilinear stiffened structures	5
T188 – Hybrid nano-composites	3
T189 – Functionally graded materials	4
T190 – Aeroelastically tailored structural wing design	3
T191 – Continuous distributed control surfaces	3
T192 – Variable camber continuous trailing edge flap	4
T193 – Adaptive aeroelastic wing shape control	2
T195 – Morphing skin	5
T196 – Active structural control	4
Engine Performance	
T144 – Low pressure ratio fan	4
T154 – Boundary layer ingestion inlet and flow control	1
T164 – Lean direct injection and active combustion control	3
T170 – Variable fan blade using shape memory alloy	2
T172 – Distortion tolerant fan	3
T174 – 1500 °F hybrid disk	3
T175 – 1500 °F non-contacting seal	3
T176 – 1500 °F corrosion coating	3
T179 – Toughened composite fan blade	3
T180 – Boundary layer ingestion inlet and distortion tolerant fan	3
T182 – Tip clearance loss mitigation	2
Noise Reduction	
T142 – Ceramic matrix composite based acoustic liner	3
T148 – Flap side edge acoustic liner	4
T150 – Landing gear acoustic liner	2
T152 – Flap side edge treatment	3
T153 – Slat cove filler	4
T156 – Fan bypass duct acoustic splitter	3
T157 – Blade tone control using trailing edge blowing	4
T158 – Noise cancelling stator	3
T159 – Mission adaptive duct liner	3
T161 – Over the rotor acoustic treatment	3
T168 – Active pylon shaping and/or blowing	3

of engine flow path and weight estimation, CMPGEN for compressor map generation within engine design, and ANOPP for noise [44–46, 78, 79]. EDS has been successfully demonstrated in previous works and has been calibrated based on publicly available data [80–83].

PASS: Kroo and Takai proposed a computational Program for Aircraft Synthesis Studies (PASS) which implements an MOO approach for the design of novel aircraft concepts [84]. PASS consists of a collection of disciplinary analysis routines combined with a numerical optimizer. The design modules of PASS analyze vehicle aerodynamics, performance, structural weights, stability and control, and associated economics. The optimizer allows for the reconfiguration of a baseline vehicle through the addition, removal and modification of design variables, value objectives and constraints [85, 86]. Previous applications of PASS implemented sequential quadratic programming and genetic algorithms for optimization [76, 87, 88].

TASOPT: The Transport Aircraft System OPTimization (TASOPT) program was developed at Massachusetts Institute of Technology (MIT) to design and analyze future air transport aircraft carrying N+3 technologies [89, 90]. TASOPT does not rely on historical correlations and empirical data except where absolutely necessary and instead, depends on low-order physics based models that implement fundamental aerodynamic, structural, and thermodynamic theory. Aerodynamic models use Computational Fluid Dynamics (CFD) to predict wing, fuselage, and tail drag. Structural models assume an aircraft weight breakdown and compute gross weight as an aggregate of component weights. Engine performance is predicted using a thermodynamic cycle analysis turbofan model [91, 92]. An iterative procedure determines the optimum vehicle based on minimized fuel consumption.

WingMOD: Developed by Wakayama, WingMOD follows an MDO approach to balance and reconfigure the unconventional Blended-Wing-Body (BWB) design [93]. The intermediate fidelity program follows a sequential optimization process to define

and calibrate a baseline planform of the BWB. Each optimization step has a single objective function along with constraints that are defined such that certain structural and aerodynamic conditions are met. Although the BWB is radically different from the conventional tube-and-wing designs, the code uses several empirical relations for aerodynamic analyses. Structural weight calculations are based on maximum loads the vehicle is subjected to through simulated flight conditions [94, 95].

4.2.1.2 Modeling and Simulation Environment

As described in section 3.2.2, the modeling and simulation environment utilized should handle the different vehicle design aspects simultaneously, to properly map the impact of technologies on vehicle-level performance. All the above-mentioned tools provide this required capability. However, since WingMOD is primarily focused on the BWB concept, it is not favored. Moreover, given that TASOPT has not undergone extensive validation and has only been demonstrated in the design of another unconventional configuration (Double Bubble [96]), it is also not selected. Between PASS and EDS, the latter is chosen to be the modeling and simulation environment. This is to ensure a consistent vehicle-level performance analysis since EDS utilizes the NASA software suite (FLOPS/NPSS/WATE), which was also used in section 3.2.1 to establish baseline performance. Figure 30 highlights the core modules of EDS and shows the basic information flow.

Models for the seven baseline vehicles shown in Table 3 are embedded within EDS. Based on the technology package being implemented, different model parameters are altered to reflect the impact of vehicle technologies. This mapping is according to the technology impact matrix constructed in advance (Figure 17). The vehicle models are then re-optimized to determine the updated fuel burn performance, while maintaining their respective design points (Table 4). Last, performance improvements relative to the baseline are translated to efficiency gains fed forward to the system-level analysis.

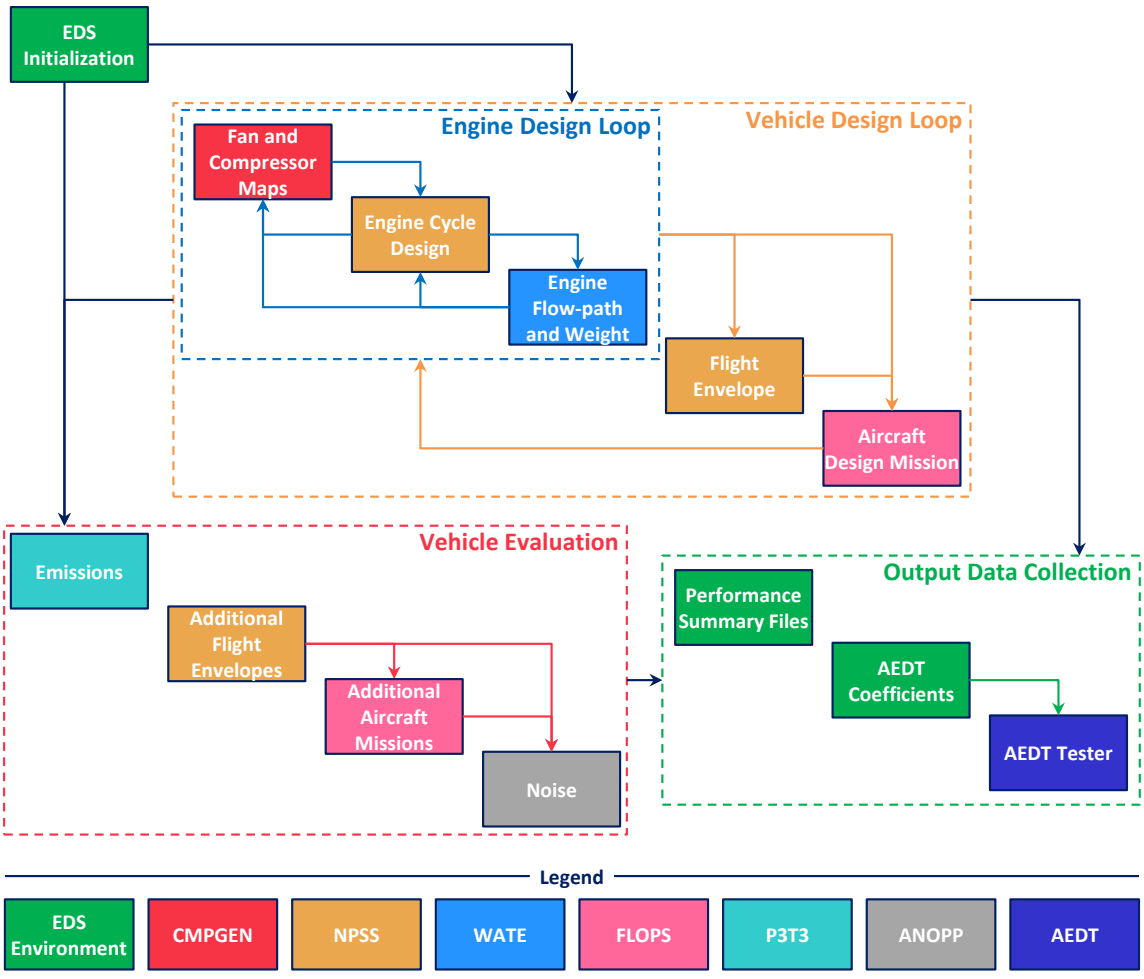

Figure 30: Environmental Design Space (EDS) [81]

4.2.2 Modeling Operational Improvement Impact

In 2012, Marais et al. compiled a comprehensive list of 61 operational improvements that can be implemented in the next 5–10 years (a shortened list is shown in Table 7). To demonstrate the capability of the methodological framework, only a subset of those improvements are considered, specifically: [S1; S3; S5], [D4; D5], [C2; C3; C4; C5], and [A1; A4]. The previous improvements were selected since they are purely operational and do not require technology implementation or infrastructure enhancement.

To model the impact of operational improvements on vehicle performance, FLOPS is utilized. This is because the baseline vehicles were modeled using FLOPS, and only the mission profiles are being changed (since the improvements are purely operational, no vehicle re-design is required). FLOPS is sufficiently flexible to simulate the selected operational improvements through mission definition, as will be shown next.

4.2.2.1 Surface Improvements

As explained in section 3.2.3.1, ground fuel burn is a function of both engine idle fuel flow and ground time. Surface improvements [S1; S3; S5] simply seek to minimize the latter. This is modeled in FLOPS by varying taxi in/out times to establish functional relationships between block fuel reduction and ground time reduction for the different vehicle classes.

4.2.2.2 Departure Improvements

Departure improvements [D4; D5] are modeled differently using FLOPS. To maximize the rate of climb upon takeoff (D4), FLOPS is set to override the FAA restriction for maximum rate of climb and optimize the departure for minimum time-to-climb. Alternatively, a continuous climb procedure (D5) is modeled by eliminating any level-offs between takeoff and initial cruising altitude and setting FLOPS to optimize the departure for minimum fuel-to-climb. Both improvements are graphically depicted in Figure 31.

Table 7: Near term operational improvements [37]

Improvements	Ease of Implementation
Surface	
S1 – Procedure-based congestion management systems	Easy
S2 – Technology-based congestion management systems	Medium
S3 – Taxi route optimization	Easy
S4 – Reduced-engine taxi	Easy
S5 – Operational tow-outs	Medium
S6 – Auxiliary power unit management	Easy
Departure	
D1 – Noise abatement departure procedures	Easy
D2 – Trajectories to minimize population noise exposure	Medium
D3 – Operating in best noise configuration	Medium
D4 – Maximum climb on takeoff	Easy
D5 – Continuous climb	Medium
D6 – Dispersal headings	Easy
Cruise	
C1 – Reduced horizontal separation minima	Hard
C2 – Reduced vertical separation minima	Easy
C3 – Increased directional airways	Medium
C4 – Cruise climb	Medium
C5 – Domestic step climb	Easy
C6 – Fuel-optimized cruise speeds	Hard
C7 – Cruise Mach reductions	Easy
C8 – More efficient passing options	Medium
Approach	
A1 – Optimized profile descents	Medium
A2 – Steeper descent and approach	Medium
A3 – Delayed deceleration approach	Medium
A4 – Absorbing delay enroute instead of terminal area	Medium
A5 – Reduced thrust reverser usage	Easy
A6 – Reduced flap landing	Easy
Policy	
P1 – Increase priority for environmental performance	Hard
P2 – Redesign airspace to increase efficiency	Hard
P3 – Integrate terminal and en route control facilities	Hard

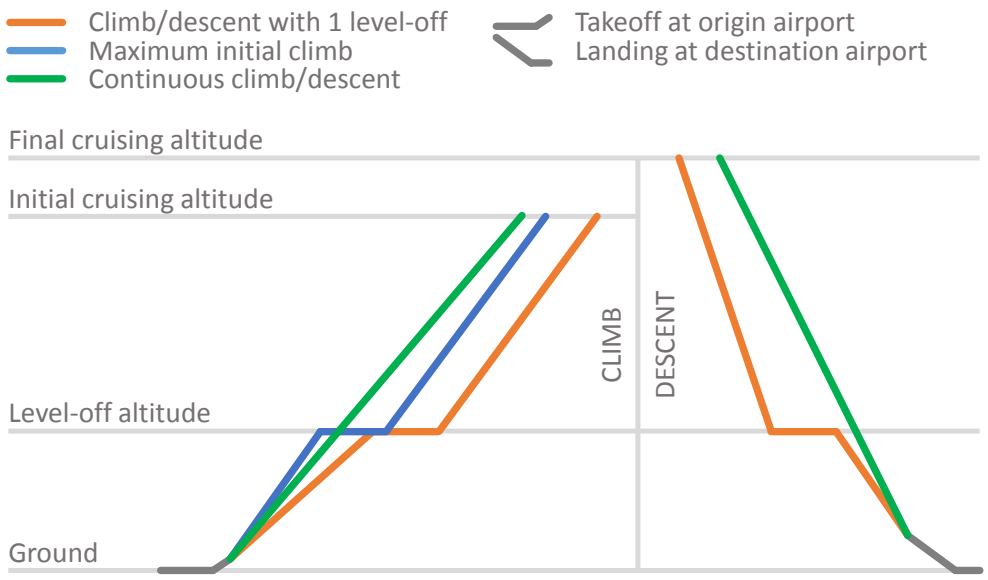

Figure 31: Departure and approach improvements

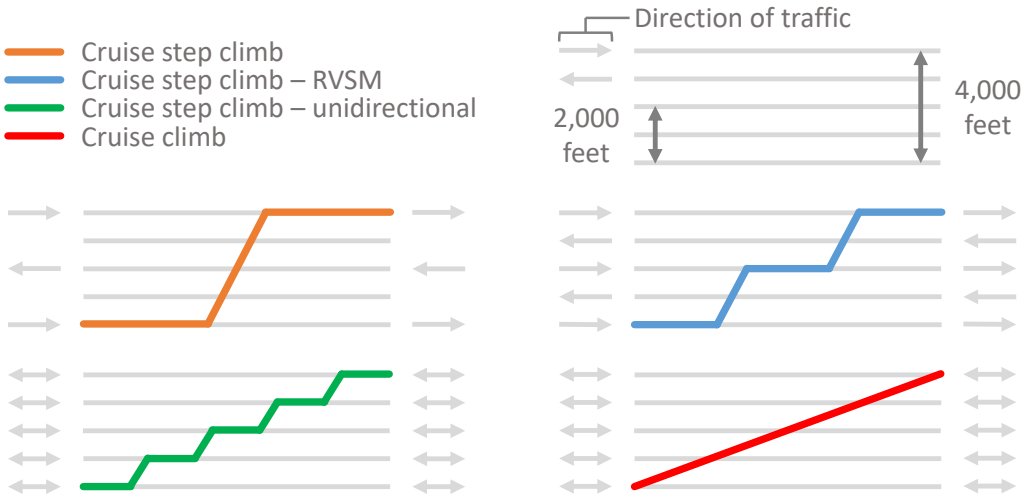

Figure 32: Cruise improvements

4.2.2.3 Cruise Improvements

The cruise segment of the mission is named the "free" segment in FLOPS. Different settings apply to this segment in which detailed cruise altitude and speed schedules are permitted. There are also options to optimize altitude and Mach automatically without the definition of schedules. Both methods are utilized to simulate the four cruise improvements (Figure 32). Specifically, [C2; C3; C5] are modeled using predefined schedules, while C4 is optimized in an unconstrained manner.

4.2.2.4 Approach Improvements

Similar to continuous climb, an optimized descent profile (A1) requires the removal of level-offs and holding patterns between final cruising altitude and landing (Figure 31). Alternatively, absorbing delay enroute (A4) is simulated by reducing cruise Mach such that flight time is increased by an amount equivalent to that spent in a descent level-off or holding pattern.

4.3 Modeling System-Level Impacts

In this section, methods to evaluate the performance of the aviation system (as represented in Figure 22) are detailed. The representation of both vehicle technologies and operational improvements at the system-level using efficiency factors, is discussed. In addition, to utilize the methodological framework to assess the feasibility of the IATA environmental targets, biofuels are accounted for at a basic analysis level. But first, necessary assumptions pertaining to the aviation system are stated and justified.

4.3.1 Assumptions

- **Aviation CO_2 emissions are computed on a life cycle basis.**

  Recent studies have shown that aircraft combustion CO_2 emissions do not vary much, regardless of the type of fuel being used [97]. Unlike conventional fossil fuels however, most biofuels offer 'biomass credits' during production that offset

the combustion CO_2 emissions. Hence, a 'well-to-wake' life cycle analysis should be conducted in order to quantify the full environmental benefits of biofuels. This assumption was previously utilized by the FAA and Stratton et al. [15, 97].

- **Aviation CO_2 emissions are directly proportional to fuel burn.**
  In the literature, CO_2 emissions and fuel burn are consistently related through a direct proportionality ($CO2 \propto FB \Rightarrow CO2 = \kappa \cdot FB$). The proportionality constant κ indicates the amount of life cycle CO_2 emitted from the consumption of a unit amount of fuel, and is determined through experimentation. Representative values of κ are routinely published for various types of fuel [98]. This assumption was previously utilized by Stratton et al. and Hassan et al. [97, 99].

- **Aviation system achieves partial equilibrium.**
  Aviation supply in terms of available seat miles is assumed to meet aviation demand in terms of revenue passenger miles (for any predefined passenger load factor), such that the aviation system is in partial equilibrium. In this thesis, the impact of the aviation industry on the entire economy is not considered and therefore, general equilibrium is not guaranteed. This assumption was utilized in previous works by Hofer et al. and Winchester et al. [100, 101].

- **Aviation system performance is driven by passenger transport.**
  Historical performance of the NAS shows that passenger transport is responsible for 86% of aviation system fuel burn, with the remaining 14% primarily due to cargo operations [19]. While the share of cargo transport is not insignificant, it has been steadily declining since 2005. Passenger transport is assumed to remain the dominant driver of system-level performance and thus, cargo operations are not considered. This assumption was recently utilized by Krammer et al. [102].

Besides the aforementioned, assumptions specific to the modeling methods discussed in the next subsections will be stated and justified as they arise.

4.3.2 System Fuel Burn and Emissions

Partial equilibrium of the aviation system, as represented in Figure 22, is posed as an optimization problem with the following objective function and constraint [103]:

$$\textbf{min.} \quad f(\text{ASM}) = \left(\frac{\left(\text{RPM}_D - \text{ASM}_D \cdot \text{LF}_D\right)^2}{\text{ASM}_D \cdot \text{LF}_D} + \frac{\left(\text{RPM}_I - \text{ASM}_I \cdot \text{LF}_I\right)^2}{\text{ASM}_I \cdot \text{LF}_I} \right) \tag{29}$$

$$\textbf{s.t.} \quad \text{ASM} \geq 0$$

where ASM is available seat miles, RPM is revenue passenger miles, and LF is load factor. The subscripts D and I denote domestic and international terms, respectively. Clearly, the function seeks to match aviation supply and demand so that the system is in partial equilibrium. All system factors, except for fuel efficiency, are predefined and fixed for every iteration. Fuel efficiency is dependent on fleet growth as dictated by ASM and therefore, is recomputed every function call.

Although a top-down approach was selected to model the dynamics of the system (section 3.2.4), a reference scenario based on bottom-up analyses is utilized to initiate the optimization process. For an input demand growth scenario, the six system-level quantities are computed relative to the reference scenario, and the system is optimized such that supply meets the input demand (Figure 33). In this thesis, the FAA 2016–2036 aerospace forecast is used as a reference [4]. Optimization of the system based on relative quantities has the advantage of simplifying computations, especially regarding operating costs and ticket prices (which are hard to quantify). Yet, the disadvantage is that the model inherits all assumptions embedded in the reference scenario.

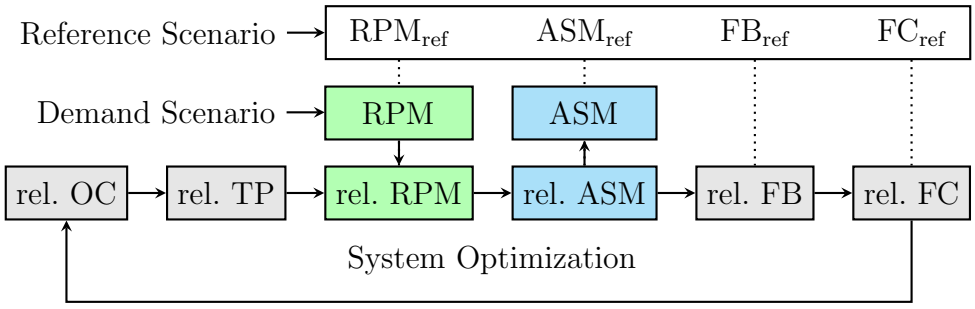

Figure 33: Block diagram of system optimization method

While technologies and operations reduce CO_2 emissions by enhancing system fuel efficiency, biofuels reduce CO_2 emissions through life cycle biomass credits. Therefore, their impact cannot be captured through fuel efficiency. The benefits of biofuels are alternatively determined based on quantities consumed. System fuel consumption is first computed from the converged values of available seat miles and fuel efficiency:

$$\begin{aligned} \text{FB} &= \text{ASM} \cdot (\text{ASM/Gallon})^{-1} \\ &= \text{FBC} + \text{FBB} \end{aligned} \tag{30}$$

where FBC and FBB are the quantities of conventional jet fuel and biofuel, respectively. Biofuel availability is predefined and dictates both FBC and FBB. System CO_2 emissions are then derived from fuel burn based on emission factors (proportionality constants), as previously discussed in section 4.3.1:

$$\text{CO2} = \kappa_c \cdot \text{FBC} + \kappa_b \cdot \text{FBB} \tag{31}$$

where κ_c and κ_b are the emission factors of conventional jet fuel and biofuel, respectively. The environmental benefits of biofuels are accounted for using those factors where, in most cases, $\kappa_c > \kappa_b$ and the net reduction in system CO_2 emissions due to biofuels is $(\kappa_c - \kappa_b) \cdot \text{FBB}$.

Modeling biofuel impact as described above implicitly assumes that biofuels are equivalent to conventional jet fuel (in terms of energy content), and that availability is the only constraint preventing their full adoption by the aviation industry. However, there are several other constraining factors that have not been accounted for [104]. One such factor is the higher production costs, and therefore the higher sale prices, of biofuels as compared to conventional jet fuel. This difference in fuel price was not considered beforehand when seeking equilibrium of the aviation system. Even though those constraints have not been modeled directly (partially due to the lack of available data), the uncertainty in biofuel impact is captured indirectly using multiple scenario evaluations, as will be shown.

4.3.3 Modeling Enabler Impact on System Fuel Efficiency

As previously discussed in section 3.2.1, the fuel efficiency metric is ASM/Gallon, the reciprocal of which is fuel intensity (η) defined as:

$$\eta = \left[\sum_{i}^{\text{AC}} \sum_{j}^{\text{OD}} [\text{fuel burn}]_{ij}\right] \cdot \left[\sum_{i}^{\text{AC}} \sum_{j}^{\text{OD}} [\text{seats}]_{i} \cdot [\text{distance}]_{j} \cdot [\text{operations}]_{ij}\right]^{-1} \tag{32}$$

where indices i and j represent aircraft types and origin-destination pairs, respectively. This value can be easily calculated for any system with known fleet composition and network structure. However, in this thesis, the objective is to evaluate system performance for future years in which both fleet and network are uncertain (i.e., the goal is to calculate system fuel consumption based on efficiency/intensity, not the contrary). Forecasting network changes is beyond the scope of the methodological framework, although previously investigated [105, 106]. Instead, the FAA forecast assumption for fuel efficiency is used to establish a baseline trend (the FAA assumes 1.0% annual improvement in ASM/Gallon) [4]. By leveraging the fleet turnover procedure discussed in section 3.2.5, this trend is adjusted to account for the introduction of technologies. The procedure outputs the number of aircraft by type based on demand growth, while preserving fleet proportions. Accordingly, fuel intensity is approximated as:

$$\eta_{\text{Tech}} \approx \frac{\eta_{\text{FAA}}}{[\text{total no. of aircraft}]} \sum_{i}^{\text{AC}} \alpha_i \cdot \omega_i \cdot [\text{no. of aircraft}]_{i} \tag{33}$$

where α is a relative fuel intensity factor and ω is a normalized weighting. Within each vehicle class, aircraft types are assigned α values based on fuel consumption such that $\alpha = 1$ represents current state-of-the-art aircraft, $\alpha \geq 1$ represents older aircraft, and $0 < \alpha \leq 1$ represents new aircraft (e.g., in the STA vehicle class, the Boeing 787 is assigned $\alpha = 1$ while the Boeing 767 is assigned $\alpha > 1$). Alternatively, ω values are assigned to aircraft types based on their respective contributions to system capacity. Without those weightings, η_{Tech} would be solely influenced by the number of aircraft of each type, which is not necessarily indicative of capacity share.

Eq. 33 updates the FAA prediction using the fleet weighted average relative fuel intensity ($\eta_{\text{Tech}} \approx \bar{\alpha} \cdot \eta_{\text{FAA}}$). The approximation implies that if all old aircraft in the fleet are retired and/or replaced by the *current* state-of-the-art, the system fuel efficiency will match that of the FAA, which is reasonable since η_{FAA} is derived from business as usual efficiency improvement trends. Further, Eq. 33 assumes that η is primarily driven by fuel consumption and not capacity. This is a justifiable assumption given that the FAA estimates a very slow progression ($< 0.5\%$ per year) in both seats per aircraft mile and passenger trip length [4]. Because the number of operations is not a factor since it affects both fuel consumption and capacity proportionally, the former can be assumed the sole driver of system fuel efficiency.

To account for the impact of operational improvements, the FAA trend (η_{FAA}) is adjusted in a similar manner. Unlike vehicle technologies, operational improvements impact system fuel efficiency/intensity directly without the need for a fleet turnover procedure, as previously discussed (Figure 23):

$$\eta_{\text{Ops}} \approx \beta \cdot \eta_{\text{FAA}} \tag{34}$$

where β is a relative fuel intensity factor such that $0 < \beta \leq 1$.

Eqs. 33 and 34 represent the individual enabler impacts on fuel intensity. Assuming the FAA trend corresponds to the 'no action' curve of Figure 6, the total impact of implementing vehicle technologies and operational improvements simultaneously is derived using Eq. 4:

$$\begin{aligned} \Delta &= \delta_{\text{Tech}} + \delta_{\text{Ops}} \\ \text{ASM} \cdot (\eta_{\text{FAA}} - \eta) &\approx \text{ASM} \cdot \left[(\eta_{\text{FAA}} - \eta_{\text{Tech}}) + (\eta_{\text{FAA}} - \eta_{\text{Ops}}) \right] \\ (\eta_{\text{FAA}} - \eta) &\approx (\eta_{\text{FAA}} - \bar{\alpha} \cdot \eta_{\text{FAA}}) + (\eta_{\text{FAA}} - \beta \cdot \eta_{\text{FAA}}) \\ \eta &\approx (\bar{\alpha} + \beta - 1) \cdot \eta_{\text{FAA}} \end{aligned} \tag{35}$$

Although Eq. 4 implies the independence of technological and operational changes, it is used to derive a first estimate for the fuel efficiency/intensity of the system based

on $\bar{\alpha}$ and β. In this thesis, it is argued that given this initial guess, the system could achieve equilibrium such that fuel intensity, and hence fuel consumption, is reduced ($\eta_{\text{final}} < \eta_{\text{initial}}$).

4.3.4 Input Parameters and Variables

Eq. 35 defines the system fuel intensity and hence, fuel efficiency (η^{-1}). The remaining system factors of Figure 22 and other necessary model inputs are defined next. Unlike *parameters* which are determined and fixed based on literature review, *variables* are considered within scenarios to accommodate their associated uncertainty. All inputs and their corresponding values/bounds are summarized in Table 8.

4.3.4.1 Input Parameters

There are four system factors that are determined using literature findings and fixed throughout: load factor, fuel fraction, pass-through, and price elasticity. Load factor is determined based on the reference scenario considered where $\text{LF} = \text{ASM}_{\text{ref}}/\text{RPM}_{\text{ref}}$ (Figure 33). The FAA predicts that load factor plateaus for both domestic (0.86) and international (0.82) air travel such that the system load factor is 0.85 [4]. In addition, the baseline fuel fraction of total airline operating cost is assumed 0.3 (30%). This is according to cost data reported by major airlines that showed fuel fraction in 2014 and 2015 to be 0.333 and 0.264, respectively [108]. Although this baseline value is fixed within the model, the effective fuel fraction of the system is updated according to fuel price and fleet efficiency such that total airline operating cost, relative to the

Table 8: Input parameters and variables

Parameter		Value
Load factor	(–)	0.85
Fuel fraction	(–)	0.3
Pass-through	(–)	1.0
Price elasticity	(–)	[107]
κ_c	(gCO_2/gal)	11 474

Variable		Bounds
Vehicle fuel intensity	α	$[x, 1.0]$
Ops. fuel intensity	β	$[y, 1.0]$
ABF scaling	ϕ_{ABF}	$[0.0, 1.0]$
FP scaling	ϕ_{FP}	$[0.0, 1.0]$
$\dot{\text{RPM}}$ scaling	$\phi_{\dot{\text{RPM}}}$	$[0.0, 1.0]$

baseline, is calculated as follows:

$$\text{rel. OC} = 1 + \text{FF} \cdot \left[\left(\text{rel. FP} \cdot \frac{\eta}{\eta_{\text{FAA}}} \right) - 1 \right] \tag{36}$$

where OC is operating cost, FF is the baseline fuel fraction and FP is fuel price (see Appendix A).

Further, pass-through is set to 1.0 (100%), in agreement with prior studies that investigated airlines' response to cost changes under competitive market conditions [109, 110]. Price elasticity values utilized in this thesis are based on estimates published by Gillen et al. in 2003 [107]. Gillen et al. empirically estimated price elasticity ranges for different short-haul/long-haul, business/leisure, and domestic/international market segments (Table 9). In addition, it is assumed that of all US flights, 72% are short-haul ($< 1\,500$ statute miles) and 42% are business, according to historical trends [14, 111]. Pfaender and Mavris previously noted that the price elasticity values only represent the rate/slope at which demand changes about a fixed reference point, and that the construction of a complete demand curve is necessary using an appropriate inverse function [112]. The following inverse function is used to relate demand to ticket price:

$$\text{rel. RPM} = \frac{1 + \text{PE} \otimes \left[(\text{rel. TP} - 1)/(\text{rel. TP} + 1) \right]}{1 - \text{PE} \otimes \left[(\text{rel. TP} - 1)/(\text{rel. TP} + 1) \right]} \tag{37}$$

where PE is price elasticity and TP is ticket price. A graphical representation of this function using the price elasticity values presented in Table 9 is shown in Figure 34 (note: the fixed reference point is [rel. TP, rel. RPM] = [1.0, 1.0]).

Besides the above-mentioned system factors, additional input parameters are required for the complete definition of the model, including: $[a; c]$ in Eq. 26, $[\kappa_c; \kappa_b]$ in

Table 9: Median price elasticity values [107]

	Short-Haul		Long-Haul	
	Domestic	International	Domestic	International
Business	–0.700	–0.700	–1.150	–0.265
Leisure	–1.520	–1.520	–1.104	–1.040

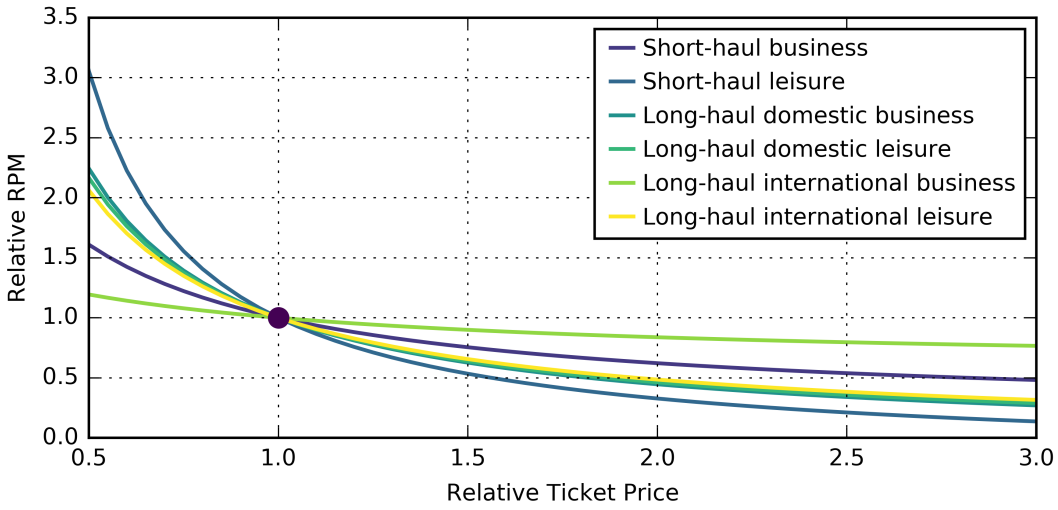

Figure 34: Demand response to changes in ticke price

Eq. 31, and $[\alpha_i; \omega_i]$ in Eq. 32.

The shape parameters $[a; c]$ are determined based on the empirically derived aircraft retirement curves shown in Figure 24. To fit the 'All Others' curve, the values for a and c were: $a = 31.5$ and $c = 4$. The location parameter a corresponds to the average aircraft retirement age (the age at which an aircraft is 50% likely to be retired from service). Although its value can be varied to simulate accelerated/delayed retirements, the reference age of 31.5 is fixed in light of recent literature findings suggesting that current retirement patterns will remain the same for future aircraft [66].

Emission factors $[\kappa_c; \kappa_b]$ are determined using estimates of well-to-wake life cycle emissions by Stratton et al., derived from data published by Argonne National Laboratory [97, 98]. The estimates were in terms of CO_2 mass per unit energy consumed (gCO_2/MJ), consistent with prior studies [113]. For conventional jet fuel, that value is 87.5, from which κ_c is calculated as follows:

$$\kappa_c = 87.5\frac{\mathrm{gCO_2}}{\mathrm{MJ}} \times 43.2\frac{\mathrm{MJ}}{\mathrm{kg}} \times 0.802\frac{\mathrm{kg}}{\mathrm{L}} \times 3.785\frac{\mathrm{L}}{\mathrm{gal}} = 11\,474\frac{\mathrm{gCO_2}}{\mathrm{gal}} \tag{38}$$

where the heating value (in MJ/kg) and density (in kg/L) of conventional jet fuel are those used by Stratton et al. The emission factor of biofuel κ_b is assumed 0.25 times that of conventional jet fuel. This assumption is in line with the estimates provided

by Stratton et al. and was previously utilized by the FAA [15].

Finally, the values of $[\alpha_i; \omega_i]$ are defined based on the baseline fleet (Figure 13). In this thesis, the operational fleet of 2015 is the system baseline fleet, and is established using historical data published by the BTS. Specifically, the T-100 database is used to identify operational aircraft types and their respective system capacity shares [14] such that ω values are computed as:

$$\forall k \in \text{AC}: \quad \omega_k = \text{ASM}_k/[\text{total ASM}] \tag{39}$$

where piston aircraft, helicopters and business jets are filtered out and not included in the computation of [total ASM]. Remaining aircraft types are categorized into the seven vehicle classes discussed before. Within each class, α values are calculated using the T-2 database that summarizes traffic data and includes fuel data [19]:

$$\forall k \in \text{AC}: \quad \alpha_k = [\text{ASM/Gallon}]^{\text{best-}}_{\text{in-class}}/[\text{ASM/Gallon}]_k \tag{40}$$

Aircraft counts are established using the BTS aircraft inventory reported in schedule B-43 [114]. This schedule is also used to determine age distributions for all aircraft types, which are required for the fleet turnover procedure.

4.3.4.2 Input Variables

There are five input variables within the system model: two intensity variables $[\alpha; \beta]$ and three scaling variables $[\phi_{\text{ABF}}; \phi_{\text{FP}}; \phi_{\dot{\text{RPM}}}]$. By definition, $[\alpha; \beta]$ have upper limits of 1.0 that indicate no efficiency gain. Their lower limits are set using either a vehicle-level analysis or literature findings. Alternatively, $[\phi_{\text{ABF}}; \phi_{\text{FP}}; \phi_{\dot{\text{RPM}}}]$ scale reference trends for available biofuel (ABF), fuel price (FP) and demand growth rate ($\dot{\text{RPM}}$) based on upper/lower limits determined through literature review (reference, upper and lower trends correspond to $\phi = 0.5$, $\phi = 1.0$ and $\phi = 0.0$, respectively).

The 2016 billion-ton report prepared for the US Department of Energy by Oak Ridge National Laboratory is utilized to determine the reference and bound limits of

ABF [115]. The report includes multiple projections for biomass availability based on different biomass prices. The trends corresponding to \$40/dry ton, \$60/dry ton and \$80/dry ton were utilized to define the lower, reference and upper trends of biomass availability, respectively. ABF is computed under the assumption that a third of the biomass would be converted to biofuel at a conversion efficiency of 45 gallons per ton, an assumption that was recently utilized by the FAA in a 2015 study [15].

As for FP and $\dot{\text{RPM}}$, the reference trends are defined using the reference scenario of the system model (Figure 33), which in this thesis is the FAA 2016–2036 aerospace forecast [4]. The reference FP trend is bounded by the high and low jet fuel price projections published by the US Energy Information Administration in its 2016 annual energy outlook [116]. Moreover, the FAA reference $\dot{\text{RPM}}$ of 2.6% per year is bounded by an upper limit of 3.4% per year based on alternative aerospace forecasts [2, 3], and a pessimistic lower limit of 0.0% per year.

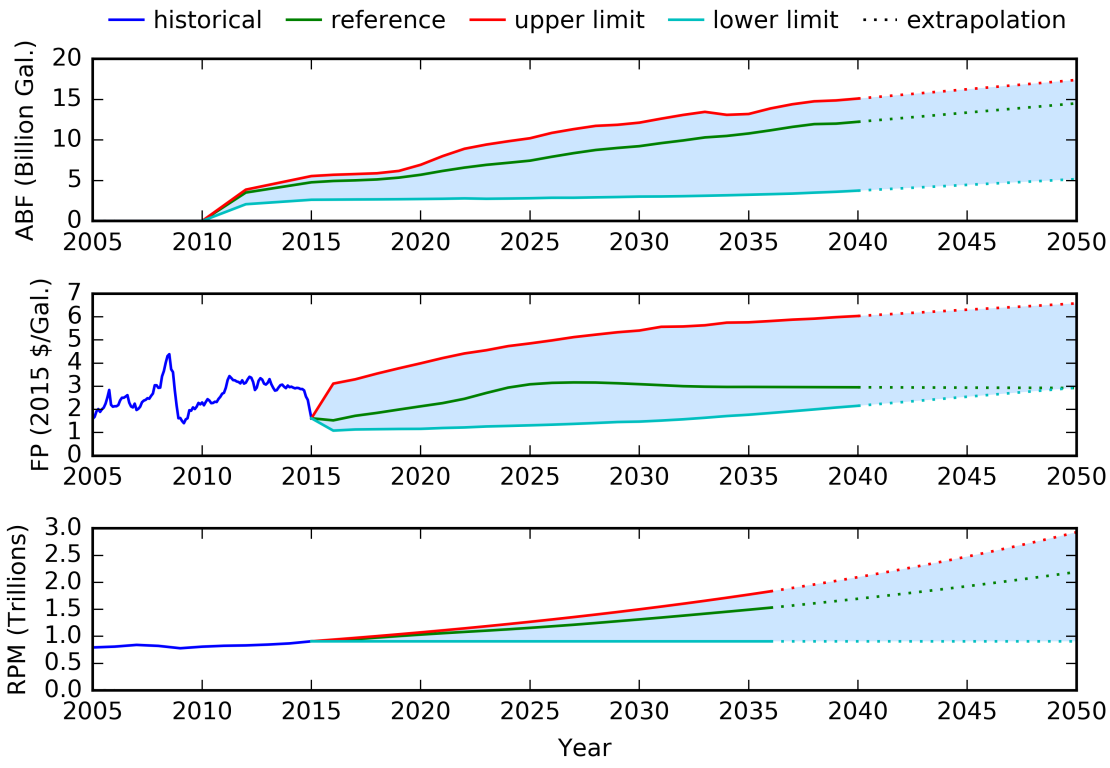

Figure 35: Reference and bound trends for available biofuel, fuel price and passenger demand

To assess the feasibility of the IATA environmental targets (Figure 1), the previous trends are extrapolated either linearly (ABF and FP) or exponentially ($\dot{\text{RPM}}$) up to 2050. Figure 35 shows all reference and bound trends for the three variables.

Finally, it is important to note the difference between the α value in Table 8 and the α values calculated using Eq. 40. The latter represent the relative fuel intensity of aircraft types in the baseline fleet. They are derived using BTS historical data and are *fixed* throughout the analysis. Alternatively, the α in Table 8 is a *variable* that represents the fuel efficiency of future aircraft. It is an array of six values that assigns relative fuel intensity factors to all replacement vehicles entering service starting 2020 based on the lower bound value x, which represents the maximum fuel efficiency gain attainable during the forecast period (note: lower α implies lower fuel burn and higher efficiency). From 2020 till 2050, fuel intensity is enhanced through six increments of $\xi = (1.0 - x)/6$ such that the six values of the α array are as follows:

$$\begin{aligned}
&\alpha_{2020} \in \big[(1.0-\xi), 1.0\big] && \alpha_{2025} \in \big[(\alpha_{2020}-\xi), \alpha_{2020}\big] \\
&\alpha_{2030} \in \big[(\alpha_{2025}-\xi), \alpha_{2025}\big] && \alpha_{2035} \in \big[(\alpha_{2030}-\xi), \alpha_{2030}\big] \\
&\alpha_{2040} \in \big[(\alpha_{2035}-\xi), \alpha_{2035}\big] && \alpha_{2045} \in \big[(\alpha_{2040}-\xi), \alpha_{2040}\big]
\end{aligned} \tag{41}$$

where the subscripts indicate the year in which the replacement vehicle is available for introduction to service. Eq. 41 assumes a continuous progression of fuel efficiency such that new aircraft are at least as efficient as ones introduced five years earlier. It also assumes that new vehicles can only enter service in specific years in the future, which is a simplifying assumption made for computational purposes.

4.3.5 Evaluation Procedure

In order to evaluate the system model, all variables need to be assigned values within the bounds shown in Table 8. Those values are generated randomly through Monte Carlo simulations. Two probability distributions are considered from which variable values are sampled: rectangular and triangular. Once variable values are generated, a

sequential evaluation procedure repeatedly seeks convergence of the aviation system (as shown in Figure 33) according to the optimization problem of Eq. 29, for every set of $[\alpha; \beta; \phi_{\mathrm{ABF}}; \phi_{\mathrm{FP}};\ \phi_{\mathrm{R\dot{P}M}}]$. The steps of the procedure are as follows:

1. Load the baseline fleet along with the aviation and energy forecasts.
2. Scale the forecast reference trends according to $[\phi_{\mathrm{ABF}}; \phi_{\mathrm{FP}}; \phi_{\mathrm{R\dot{P}M}}]$.
3. Calculate ASM using RPM from step 2 and LF from step 1.
4. Solve Eq. 29 using ASM from step 3 as an initial guess.
5. Calculate FB (Eq. 30) using the converged value of ASM from step 4.
6. Calculate CO2 (Eq. 31) using FB from step 5 and ABF from step 2.
7. Repeat steps 2–6 for a different set of $[\alpha; \beta; \phi_{\mathrm{ABF}}; \phi_{\mathrm{FP}}; \phi_{\mathrm{R\dot{P}M}}]$.

This procedure is computationally implemented in Anaconda 4.2.0 powered by Python 3.5 (check Algorithm 1 for pseudocode) [117]. Optimization is based on a Sequential Least SQuares Programming (SLSQP) algorithm, which is executed using a built-in Python solver [118, 119].

Algorithm 1

Input: α, PE (array); $\beta, \kappa_c, \kappa_b, \phi_{\mathrm{ABF}}, \phi_{\mathrm{FP}}, \phi_{\mathrm{R\dot{P}M}}, \mathrm{FF}, \mathrm{PT}$ (scalar)
Output: CO2 (time series)

```
procedure
    load baseline fleet
    load aerospace and energy forecasts
    function ScaleForecasts(φ_ABF, φ_FP, φ_RṖM)
        ABF ← f(φ_ABF, ABF_ref, ABF_min, ABF_max)          ▷ available biofuel
        FP ← f(φ_FP, FP_FAA, FP_min, FP_max)               ▷ fuel price
        RṖM ← f(φ_RṖM, RṖM_FAA, RṖM_min, RṖM_max)          ▷ demand growth rate
        calculate RPM_scaled
    end function
    rel. FP ← FP/FP_FAA                                    ▷ relative fuel price
    ASM ← RPM_scaled/LF_FAA                                ▷ initial guess
    procedure SystemEquilibrium(ASM)                       ▷ SLSQP solver
        repeat
            growth ← AṠM
            procedure FleetTurnover(growth)
                calculate retirements
                calculate replacements
                return no. of aircraft by type
            end procedure
            calculate ᾱ
            rel. OC ← 1 + FF · ((rel. FP · (ᾱ + β − 1)) − 1)
            rel. TP ← 1 + PT · rel. OC
            rel. RPM ← (1 + PE ⊗ ((rel. TP − 1)/(rel. TP + 1)))/
                       (1 − PE ⊗ ((rel. TP − 1)/(rel. TP + 1)))
            RPM ← rel. RPM · RPM_scaled
            calculate f                                    ▷ objective function
            update ASM
        until f ≤ ε                                        ▷ ε ≈ 0
        return ASM, ᾱ
    end procedure
    FB ← ASM · η_FAA · (ᾱ + β − 1)                         ▷ system fuel burn
    if FB ≤ ABF then
        FBC ← 0
        FBB ← FB
    else
        FBC ← FB − ABF
        FBB ← ABF
    end if
    CO2 ← κ_c · FBC + κ_b · FBB                            ▷ system CO2 emissions
    return CO2
end procedure
```

CHAPTER V

RESULTS

The research objective of this thesis is met by embedding the models of Chapter 4 in the methodological framework of Chapter 3, and evaluating the system-level impacts of vehicle technologies and operational improvements. In this chapter, the evaluation results are presented. First, vehicle-level performance is analyzed, where the impacts of technological and operational changes on block fuel are quantified. Second, system-level performance is evaluated through two Monte Carlo simulations, where numerous socioeconomic and technological scenarios are accounted for in a probabilistic manner.

5.1 Vehicle-Level Results

As discussed in Chapter 3, mission block fuel is an appropriate metric for evaluating vehicle-level performance. For all vehicle classes, baseline performance is established using the NASA software suite (Table 10). The mission flown by the baseline vehicles includes: a level-off after takeoff at 10 000 feet, a cruise segment in which step climb is permitted and same-direction traffic is separated by 4 000 feet, and no level-offs during descent. For vehicle technologies, the same mission is flown with the upgraded vehicle. For operational improvements, the baseline vehicles are flown the upgraded profiles for the same mission range.

It is important to note that, in order to quantify the performance impacts for some

Table 10: Fuel burn performance of the baseline vehicles

	TP	RJ	SSA	LSA	STA	LTA	VLA
Range (nmi)	1 000	1 980	3 330	2 960	5 920	7 530	7 060
Block fuel (lb)	4 710	15 621	37 345	38 196	141 404	248 365	344 776

operational improvements, the baseline mission profile needs to be altered negatively. For example, since the baseline mission does not include level-offs during descent, the impact of a continuous descent improvement is quantified by adding an artificial hold before landing. Likewise, the impact of a step cruise climb improvement is quantified by fixing the cruising altitude.

5.1.1 Vehicle Technologies

The impact of vehicle technologies on the turboprop vehicle class was not investigated since EDS is calibrated and more suitable to handle aircraft carrying turbofan engines. Instead, the performance impact of technologies on the second smallest vehicle (RJ) is assumed to be representative of the performance impact on turboprops.

The baseline vehicles were upgraded to represent the full implementation of NASA N+1, N+2 and N+3 technologies (Tables 5 and 6). Table 11 summarizes the impacts of these technologies on vehicle design and performance [75]. The results indicate huge reductions in aircraft structural weight ranging from a minimum of 29.3% (RJ) to a maximum of 51.4% (LTA). Those weight reductions, along with drag reductions from aerodynamic technologies and propulsive efficiency enhancements from engine technologies, led to significant reductions in required thrust. The thrust reductions ranged from a minimum of 26.7% (RJ) to a maximum of 53.9% (LTA). Takeoff gross weight and wing reference area were reduced by the same amounts as thrust since both thrust loading and wing loading were kept fixed. Decreases in wing reference area translated into decreases in wing span for all vehicles ranging from a minimum decrease of 0.5% (RJ) to a maximum decrease of 15.9% (LTA).

Further, Figures 36 and 37 provide a breakdown of contributions from the different N+3 technology packages to the total reduction in block fuel. The figures show that airframe technologies (aerodynamics and structures) are responsible for most of the N+3 block fuel reductions, with the impacts of engine and noise technologies almost

Table 11: Impact of NASA N+1, N+2 and N+3 technologies on block fuel, operating empty weight, sea-level static thrust and wing span [75]

	TP*	RJ	SSA	LSA	STA	LTA	VLA
Block fuel	–66.1%	–66.1%	–63.6%	–62.4%	–67.9%	–68.6%	–71.4%
Operating empty weight	–29.3%	–29.3%	–34.5%	–32.6%	–44.4%	–51.4%	–42.2%
Sea-level static thrust†	–26.7%	–26.7%	–37.1%	–33.7%	–47.7%	–53.9%	–51.3%
Wing span	–0.5%	–0.5%	–6.6%	–4.2%	–6.6%	–15.9%	–7.1%

* Technology impact on TP is assumed to be equivalent to that on RJ
† Since the design points are fixed (Table 4), reductions in sea-level static thrust are identical to reductions in takeoff gross weight and wing reference area

canceling out. The minor contribution from engine technologies is not surprising since most of their impact is expected in the near/mid term (N+1 and N+2 time frames).

Last, the vehicle-level results are compared to the NASA vehicle fuel consumption goals presented in Table 2. Only three of the six vehicle classes met the mid term goal of 50–60% reduction in block fuel: RJ (52.3%), STA (50.4%) and VLA (53.3%); the other three classes were close, however: SSA (45.9%), LSA (44.1%) and LTA (48.8%). Alternatively, all vehicle classes achieved the far term goal of 60–80% reduction with the LSA having the least reduction (62.4%) and the VLA having the most (71.4%).

Based on the above results, vehicle efficiency gains (α) for the system-level analysis were determined. To simulate the impact of NASA N+1, N+2 and N+3 technologies, an α array of [0.70, 0.60, 0.50, 0.40, 0.30, 0.20] (Eq. 41) was utilized. The array reflects a steady progression in fuel efficiency at a rate of 2% per year starting 2020 such that vehicles entering service in 2045 are 80% more fuel efficient, which is in line with the results of Table 11. For the Monte Carlo simulations in which α values are sampled, a lower bound of $x = 0.10$ was enforced such that the maximum, yet highly improbable, efficiency gain by 2045 was 90%.

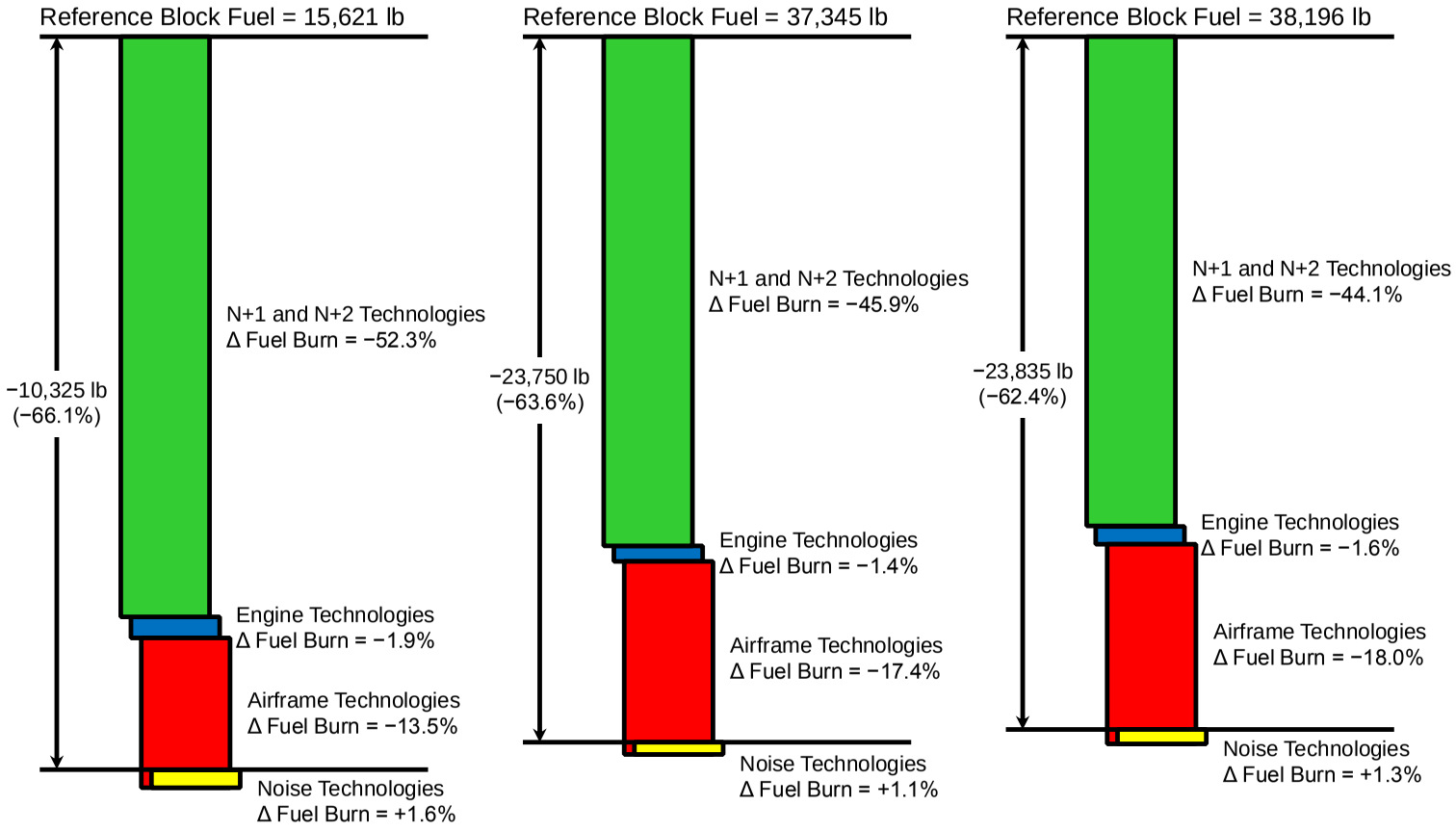

Figure 36: Impact of NASA N+1, N+2 and N+3 technologies on fuel burn performance of RJ (left), SSA (center) and LSA (right)

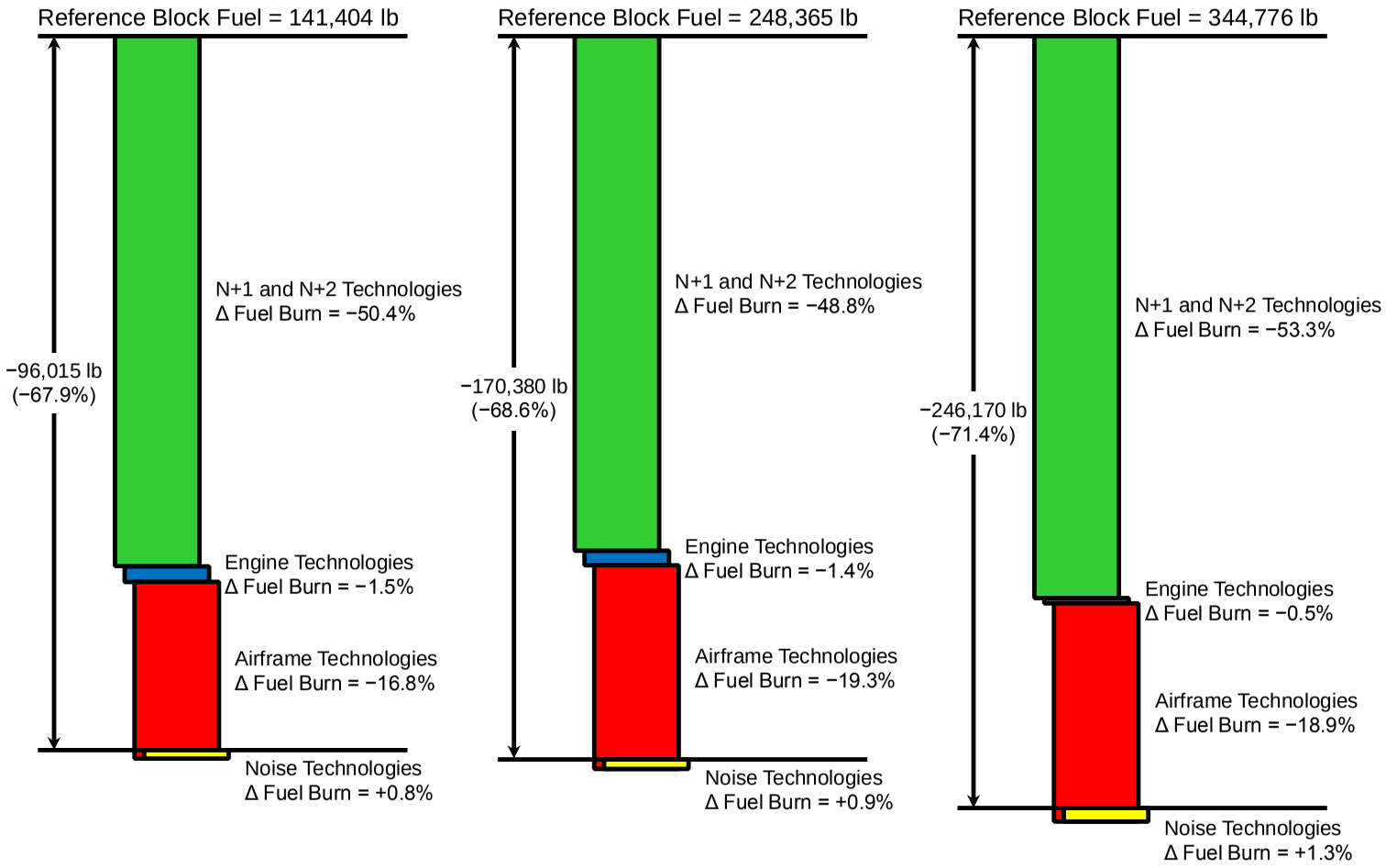

Figure 37: Impact of NASA N+1, N+2 and N+3 technologies on fuel burn performance of STA (left), LTA (center) and VLA (right)

5.1.2 Operational Improvements

The baseline mission profile was modified to accommodate operational improvements [S1; S3; S5], [D4; D5], [C2; C3; C4; C5], and [A1; A4] of Table 7, individually. Table 12 summarizes the maximum impacts of these improvements on vehicle performance.

Surface improvements were modeled by altering taxiing times in FLOPS. Figure 38 plots the resulting relationships. From the figure, it is clear that the smaller vehicles benefited more (percentage wise) than the larger ones. This is because the former fly shorter ranges and thus, the fuel saved on the ground represents a bigger proportion of their total block fuel. The biggest fuel savings were for the TP vehicle which saved 0.26% of its block fuel per minute saved on ground. This is almost ten times the rate of the LTA vehicle which saved the least fuel (0.029% per minute).

Departure improvements [D4; D5] were either to maximize the rate of climb after takeoff (primarily for noise mitigation) or to eliminate any level-offs before the initial cruising altitude. The results for both improvements are presented in Figure 39. The trends are somewhat similar for both operations as bigger vehicles appeared to benefit more. For maximum initial climb, the VLA had maximum benefit of 0.6% reduction in block fuel, while the SSA benefited the least with a reduction of only 0.02%. For continuous climb, the VLA saved 0.9% block fuel while the TP had almost no savings (turboprops fly at low altitudes and in most cases, no level-offs are required).

Similarly, for approach improvements [A1; A4], the goal was either to eliminate any

Table 12: Impact of select near term operational improvements on block fuel

	TP	RJ	SSA	LSA	STA	LTA	VLA
Surface*	–1.31%	–0.61%	–0.44%	–0.44%	–0.19%	–0.14%	–0.17%
Departure	–0.22%	–0.63%	–0.32%	–0.40%	–0.47%	–0.46%	–0.90%
Cruise	–0.00%	–0.76%	–0.68%	–0.52%	–1.22%	–2.00%	–2.42%
Approach	–3.29%	–2.02%	–1.06%	–1.22%	–0.73%	–0.98%	–0.68%
Total	–4.82%	–4.02%	–2.50%	–2.58%	–2.61%	–3.58%	–4.17%

* Based on a reduction in ground time of five minutes

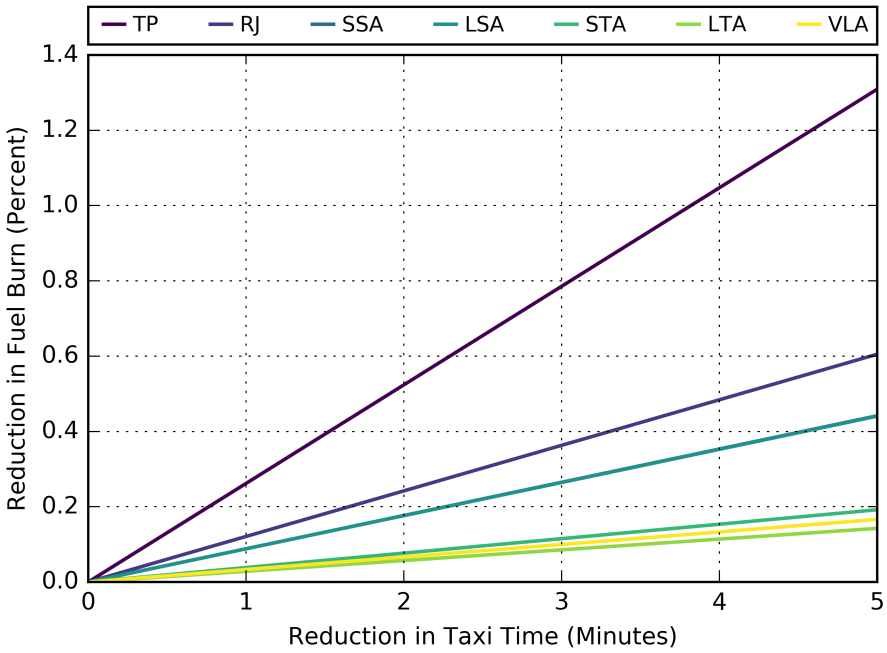

Figure 38: Impact of surface operational improvements on fuel burn performance of all vehicle classes

level-offs between the final cruising altitude and landing or to absorb delay enroute instead of holding near the terminal area. The impact of continuous optimized descent was simulated by adding a five minute hold/level-off before landing, and quantifying the increase in fuel burn (relative to the baseline mission which did not include any level-offs). An additional profile was flown in which cruise Mach was slightly reduced such that the total mission time was increased by five minutes. Fuel burn reductions from absorbing delay enroute were computed as the difference in fuel burn between those two mission profiles. The results are shown in Figure 39. Again, the trends are somewhat similar for both operations where larger vehicles benefited less in general. The TP vehicle saved the most on both operations with 2.7% reduction for continuous descent and 3.3% for absorbing delay enroute.

Finally, for improvements [C2; C3; C4; C5], the goal was to determine the benefits of flying a vehicle closer to or at its optimal altitude throughout the cruise segment. Step cruise climb (C5) was modeled by fixing the cruising altitude and comparing the

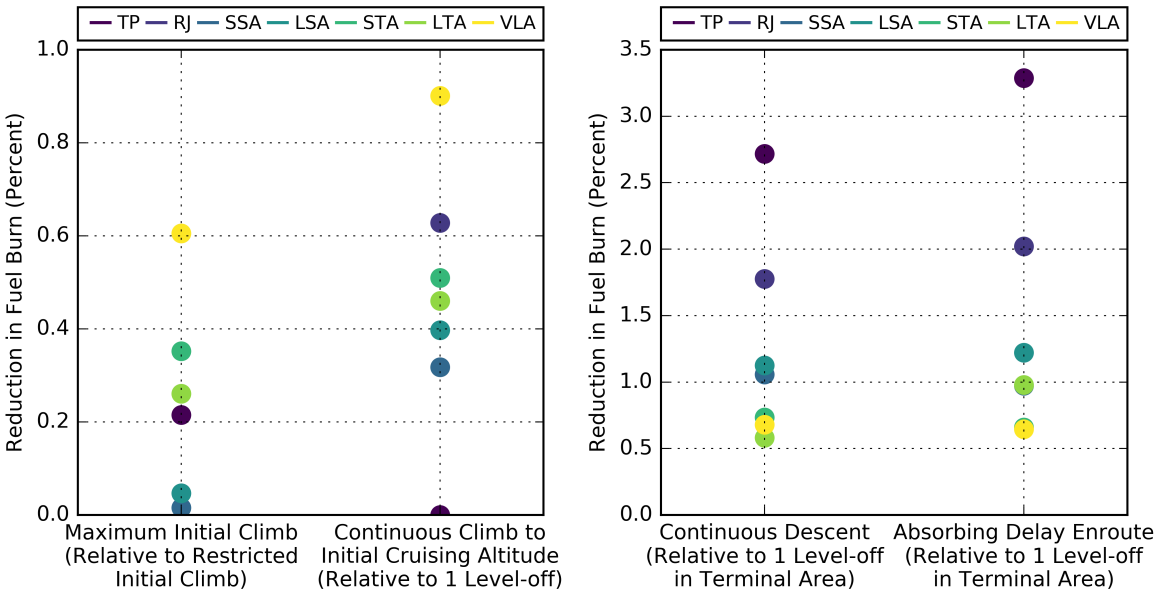

Figure 39: Impact of departure and approach operational improvements on fuel burn performance of all vehicle classes

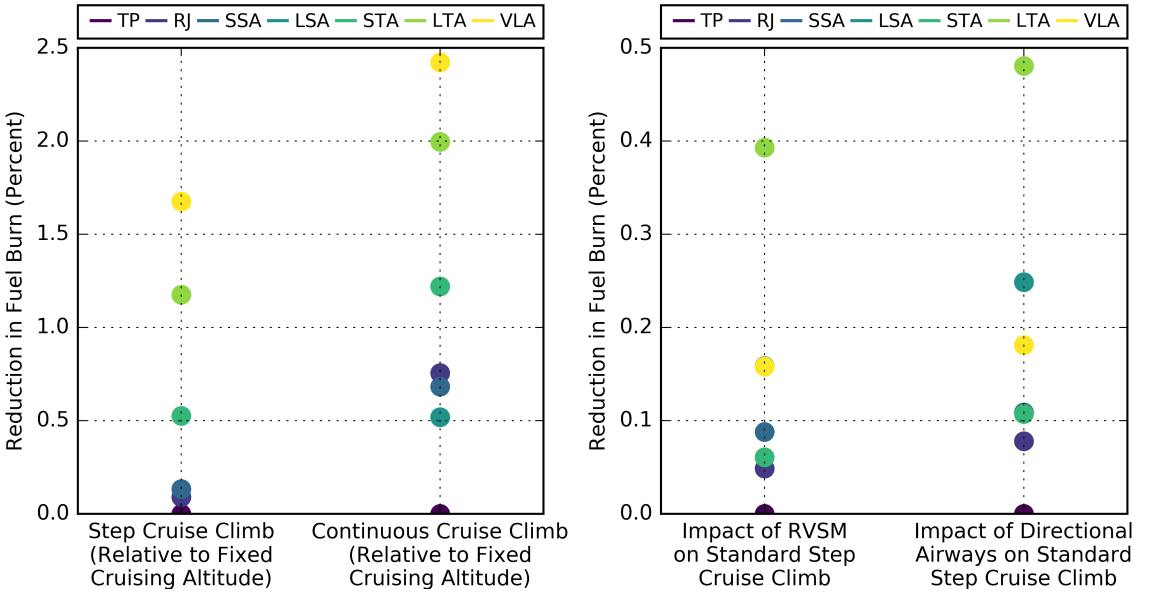

Figure 40: Impact of cruise operational improvements on fuel burn performance of all vehicle classes

results with those of the baseline mission (which permitted step cruise climb). Alternatively, cruise climb (C4) was simulated by setting FLOPS to optimize the vehicle's cruise path so that it maintains optimal altitude throughout. Improvements [C2; C3] were aimed at bridging the gap between improvements [C4; C5]. For RVSM, a reduction of the step size was modeled by altering the cruise schedule to include altitudes that are separated by 2 000 feet instead of 4 000 feet. And last, for the unidirectional airways, the cruise schedule included altitudes separated by 1 000 feet.

The results for the four cruise improvements are shown in Figure 40. As expected, larger vehicles that fly longer ranges benefited the most from the cruise improvements. The results indicate that vehicles which were forced to cruise at fixed altitudes (mostly domestically) ended up consuming up to 1.7% more fuel relative to a step cruise climb and up to 2.4% more relative to a continuous cruise climb. Furthermore, the impact of reducing vertical separation and allowing the vehicles to fly closer to their optimal altitudes was also clear. Fuel savings of up to 0.4% and 0.5% were achieved when vertical separations in step cruise climbs were reduced to 2 000 feet and 1 000 feet, respectively.

Based on the maximum results for the four mission phases (Table 12), operational efficiency gains (β) for the system-level analysis were defined. To simulate the impact of the improvements discussed above, a β value of 0.95 was utilized (i.e., 5% efficiency gain). For the Monte Carlo simulations in which β values are sampled, a lower bound of $y = 0.90$ was enforced. This is because several other improvements (Table 7) have not been accounted for. Their impact was accommodated through the definition of an optimistic upper limit of 10% system-wide efficiency improvement.

5.2 System-Level Results

Given the x and y values determined from the vehicle-level analysis, two Monte Carlo simulations were conducted, each consisting of 10 000 runs/cases. The first simulation

sampled all input variables (Table 8) from uniform/rectangular distributions. Alternatively, the second simulation sampled just the efficiency variables $[\alpha; \beta]$ uniformly, and used triangular distributions to sample the scaling variables $[\phi_{\text{ABF}}; \phi_{\text{FP}}; \phi_{\text{RPM}}]$ with modes $[0.0; 0.5; 0.5]$. While the first simulation attempted to account for every possible scenario within the bounds of input uncertainty, the second simulation focused on the more probable scenarios. This was done by skewing variable sampling towards the lower trend of biofuel availability (to simulate slow biofuel adoption) and the reference trends of fuel price and demand growth (Figure 35). The simulations were executed on a machine powered by an Intel® Core™ i7-2600 processor with 16GB of RAM. On average, each Monte Carlo run took 30–40 seconds to be executed, adding up to a computational run-time of approximately 8 days for both simulations.

The resulting contour plots of fuel burn and CO_2 emissions are shown in Figure 41. It is important to note that fuel burn contour plots are equivalent to 'zero-biofuel' CO_2 emissions (from Eqs. 30 and 31, if FBB = 0, then FB = FBC and $CO_2 = \kappa_c \cdot$FB). Figure 41 therefore signifies that a reduction of 50% in net carbon emissions by 2050 relative to 2005 levels (third IATA target) cannot be achieved without biofuels. In addition, fuel burn results suggest that carbon neutral growth (second IATA target) while possible without the utilization of biofuels, is hard to achieve starting 2020 as intended. Nevertheless, CO_2 emissions contour plots show that both IATA targets are probable with the adoption of biofuels, especially carbon neutrality (see Appendix B).

Overall, the resulting plots came out as expected. In both simulations, uncertainty bounds increased into the future with the all-uniform simulation having a lower mean and higher variance. Both simulations showed a clear peak just above 100% for 2016–2017, which then faded away as uncertainty grew. For the all-uniform simulation, a distinct collection of results appeared at 15–20% CO_2 emissions by 2045–2050. Those results were due to cases that combined low demand growth rates with high biofuel amounts and hence, they did not appear in the second simulation in which sampling

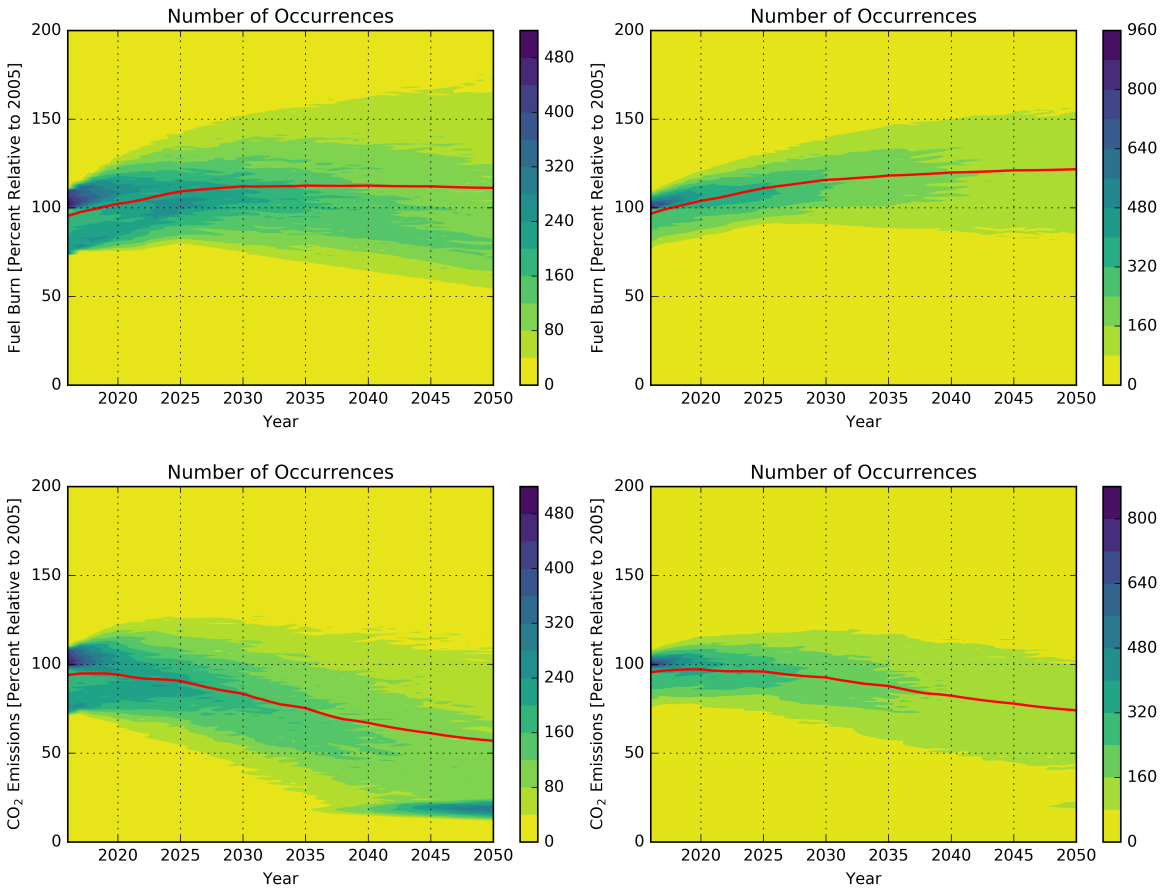

Figure 41: Contour plots of system fuel burn and CO_2 emissions for two Monte Carlo simulations (left: uniform sampling of all variables; right: uniform sampling of efficiency variables and triangular sampling of scaling variables; mean trends overlaid in red)

was skewed towards higher demand growth and lower biofuel availability.

Figure 42 further demonstrates the likelihoods of meeting all three IATA targets using cumulative distribution functions for fuel burn and CO_2 emissions in 2050. The distributions indicate that the probability of achieving the third IATA target without biofuels was virtually zero for both simulations. However, the probability of reaching carbon neutrality by 2050 (100% carbon emissions relative to 2005 levels) was found to be 50% for the all-uniform simulation and 26% for the second simulation. Biofuel utilization increased those chances significantly for both simulations such that meeting all IATA targets became 50% and 25% likely, and attaining carbon neutrality became 86% and 78% likely for the first and second simulations, respectively.

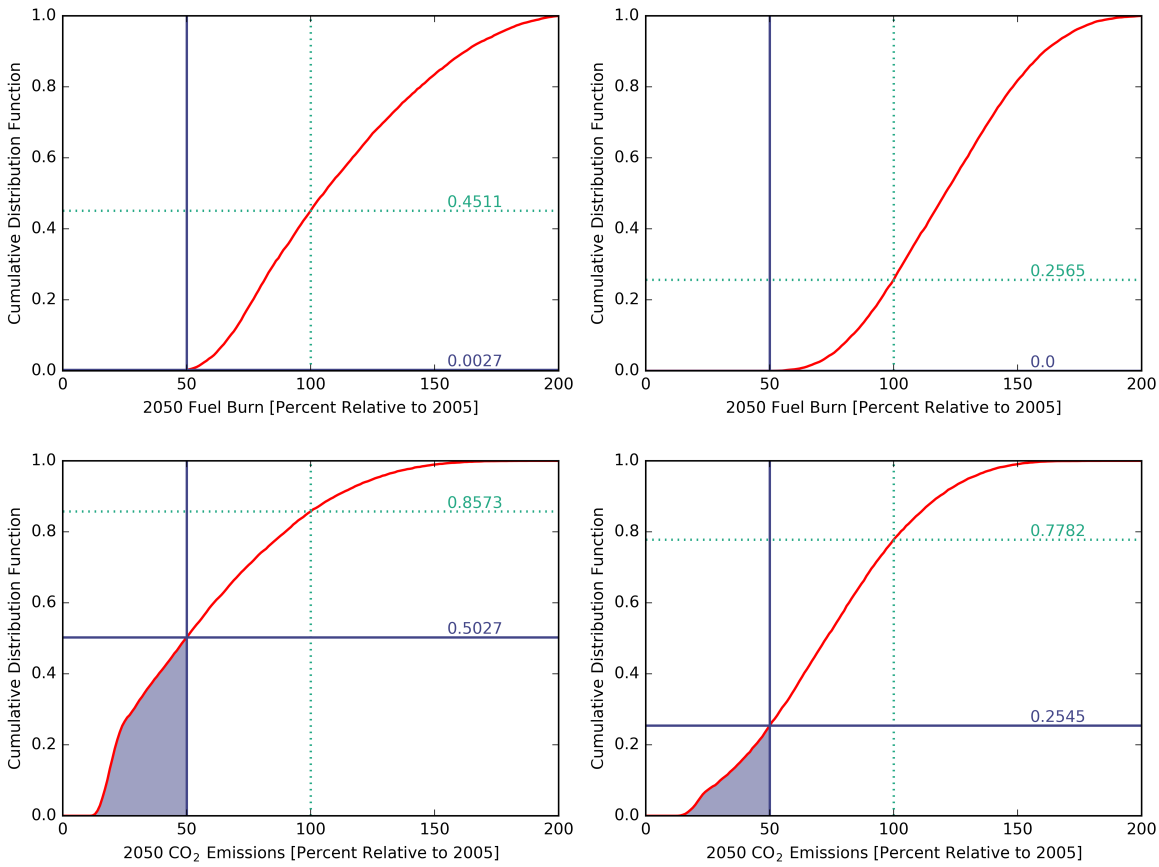

Figure 42: Cumulative distribution function of system fuel burn and CO_2 emissions in 2050 for two Monte Carlo simulations (left: uniform sampling of all variables; right: uniform sampling of efficiency variables and triangular sampling of scaling variables)

5.2.1 Discussion

Scenarios that met all IATA targets were investigated closely. As mentioned before, regardless of the input sampling distributions, those scenarios were characterized by low demand growth rates (Figure 43) and high biofuel availability, along with high fuel prices that helped suppress demand (Figure 44). The skewness of the histograms in Figures 43 and 44 identify $\dot{\text{RPM}}$ as the dominant factor affecting CO_2 emissions. This is significant since recent projections suggest $\dot{\text{RPM}}$ to be in the range of $[2.6, 3.4]$. For $\dot{\text{RPM}} \geq 2.6$, the likelihood of meeting all IATA targets drops to approximately zero. Even for moderate growth rates of $\dot{\text{RPM}} \geq 1.0$, most scenarios required excessive amounts of biofuel and high fuel prices (Figure 44). As for vehicle efficiency, results

indicate that α had a secondary impact on scenarios that met the IATA targets. The histograms of Figure 45 resemble the expected distributions from uniformly sampling Eq. 41, with some skewness towards higher α values, especially for the second simulation. Similarly, resulting β histograms implied that operational efficiency had little impact on the scenarios (Figure 46).

To generalize the above observations, the Monte Carlo cases were used to generate surrogate models that relate system fuel burn to the four variables it depends on $[\alpha; \beta; \phi_{\mathrm{FP}}; \phi_{\mathrm{R\dot{P}M}}]$. Two sets of surrogate models were generated using Response Surface Methodology (RSM) and Artificial Neural Networks (ANN) [120, 121]. Response values were chosen to be system fuel burn in 2030, 2040 and 2050 (see Appendix C for 'goodness-of-fit' measures for all surrogate models). Prediction profilers of the six models are shown in Figures 47 and 48.

The profilers re-emphasize the strong influence of socioeconomic factors on system fuel burn. Furthermore, they highlight that while the impact of vehicle technologies is modest in the near term, such impact intensifies in the far term. The response values have increasing dependence on vehicle efficiency values of later years. However, from Eq. 41, those values are dependent on earlier ones (e.g., a low α value in 2045 requires low α values for all previous years). This suggests that the system fuel burn trend is not necessarily dependent on the vehicle efficiency values, but more importantly on the technology introduction rate.

5.2.2 Case Study

The expected system-level impacts of vehicle technologies and operational improvements discussed in sections 5.1.1 and 5.1.2 were examined. Table 13 lists the enabler settings for four different scenarios. The first scenario represents the 'no action' curve of Figure 1 in which no vehicle technologies, operational improvements or biofuels are introduced into the system. Scenarios 1, 2 and 3 simulate the introduction of NASA

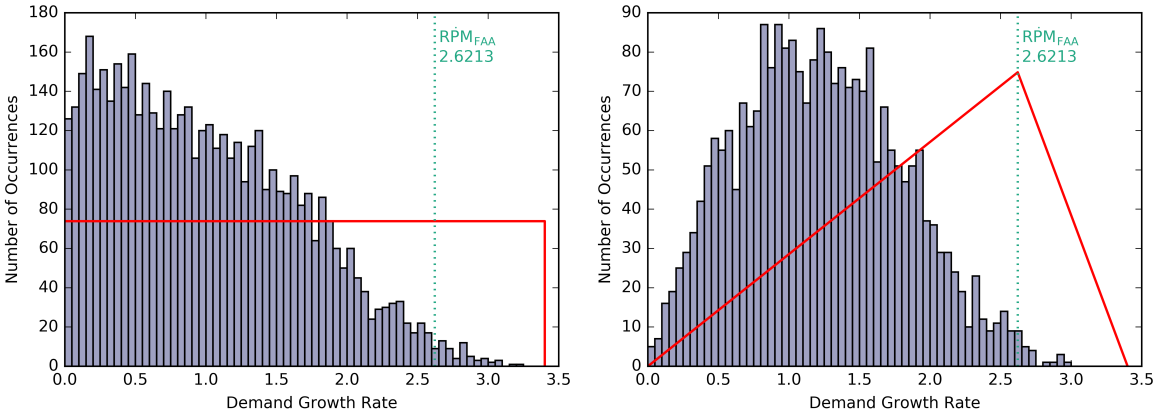

Figure 43: Histograms of RṖM for scenarios that met all IATA targets (left: uniform sampling of all variables; right: uniform sampling of efficiency variables and triangular sampling of scaling variables; sampling distributions overlaid in red)

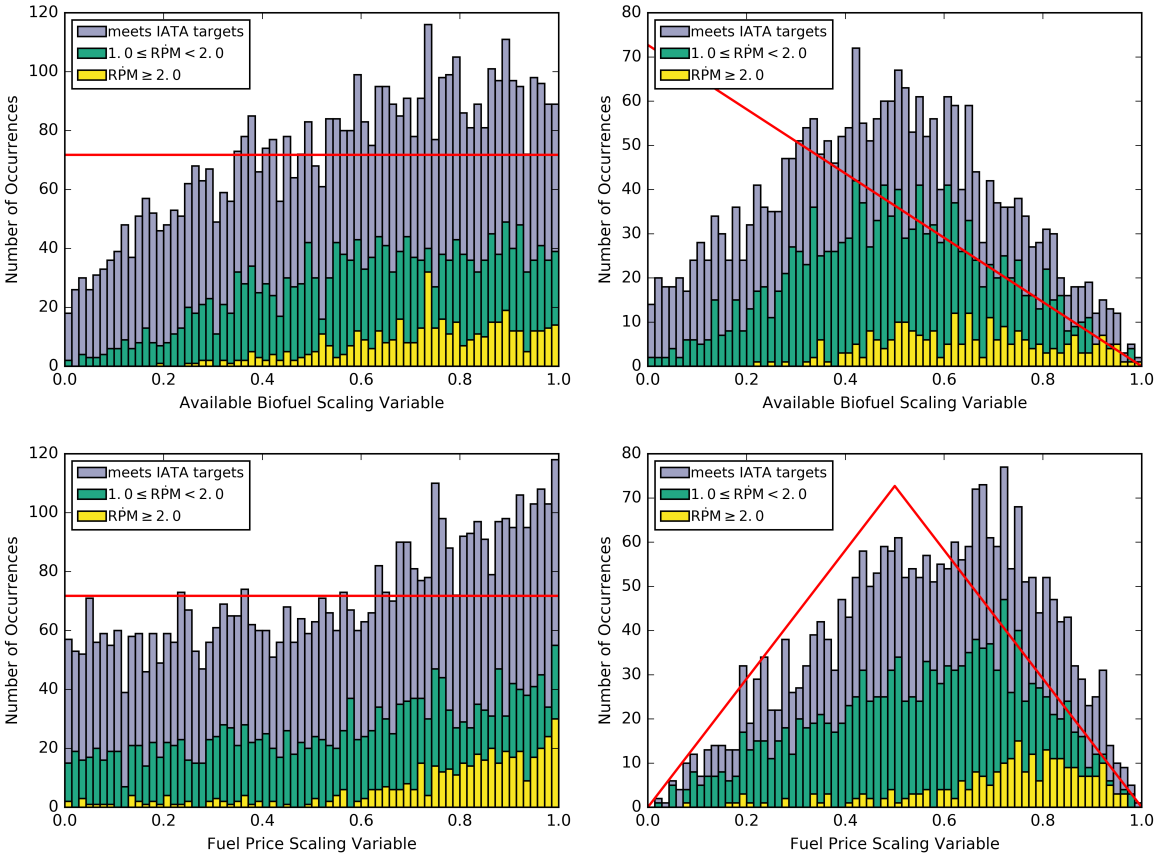

Figure 44: Overlaid histograms of ϕ_{ABF} and ϕ_{FP} for scenarios that met all IATA targets (left: uniform sampling of all variables; right: uniform sampling of efficiency variables and triangular sampling of scaling variables; sampling distributions overlaid in red)

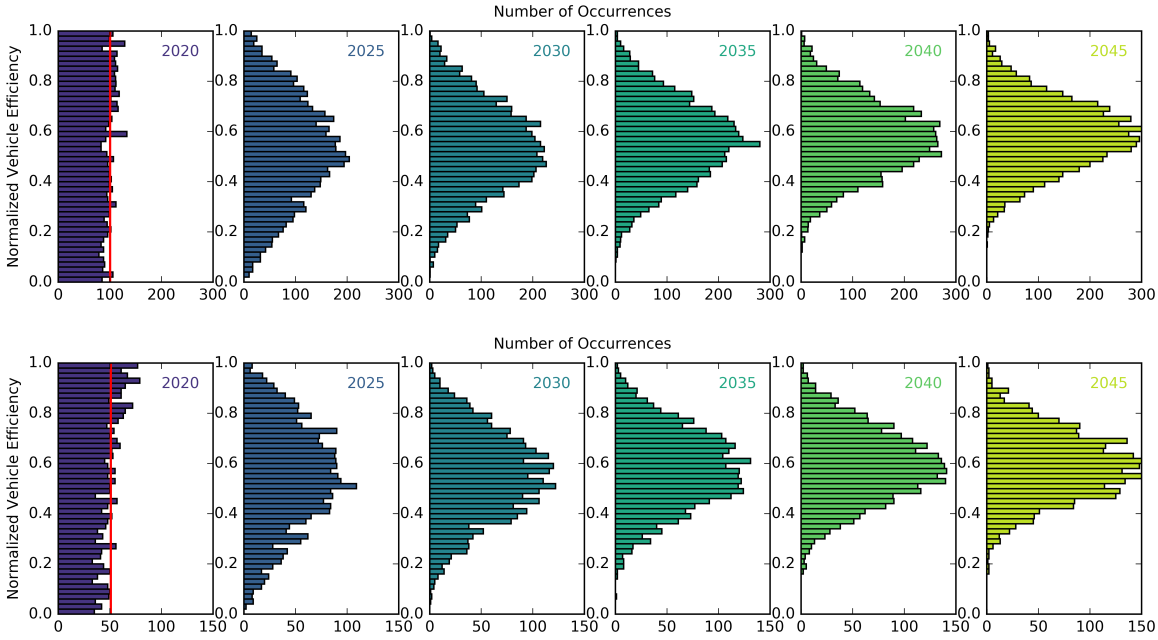

Figure 45: Histograms of normalized α values for scenarios that met all IATA targets (top: uniform sampling of all variables; bottom: uniform sampling of efficiency variables and triangular sampling of scaling variables; sampling distributions overlaid in red)

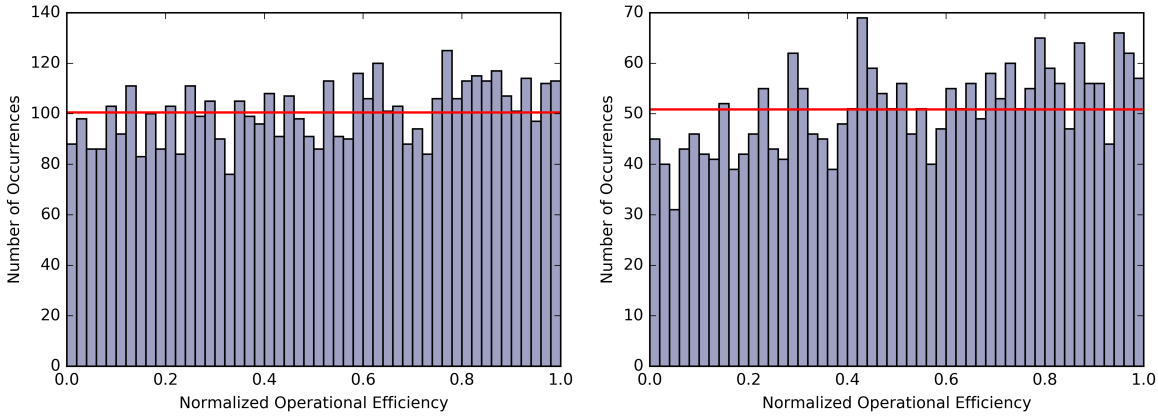

Figure 46: Histograms of normalized β values for scenarios that met all IATA targets (left: uniform sampling of all variables; right: uniform sampling of efficiency variables and triangular sampling of scaling variables; sampling distributions overlaid in red)

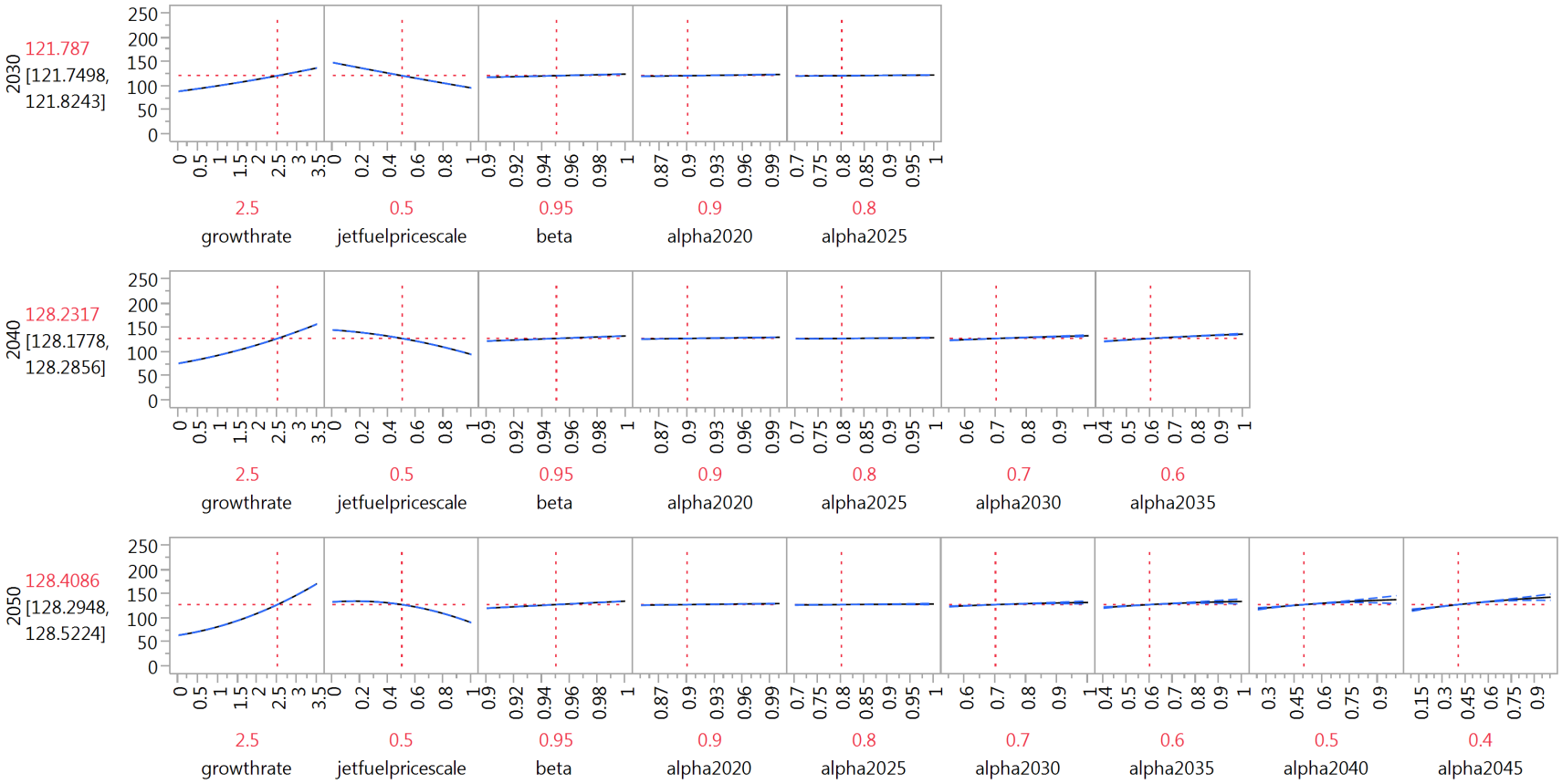

Figure 47: RSM models for system fuel burn in 2030, 2040 and 2050

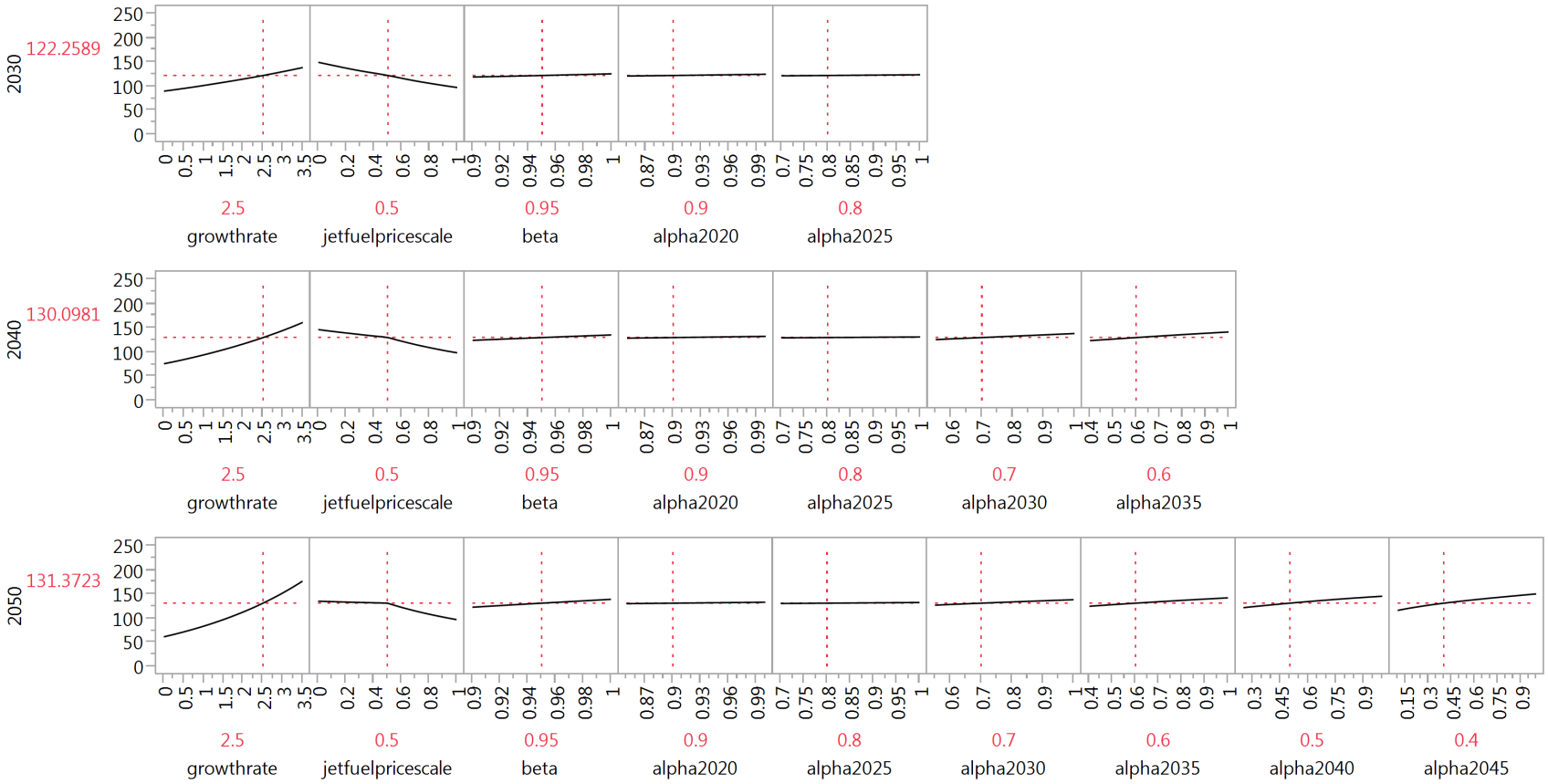

Figure 48: ANN models for system fuel burn in 2030, 2040 and 2050

[N+1], [N+1; N+2], and [N+1; N+2; N+3] technologies, respectively. Moreover, with the exception of the 'no action' scenario, all scenarios assumed an optimistic efficiency gain of 10% due to operational improvements and a pessimistic availability of biofuels according to the lower limit of Figure 35. Fuel price and passenger demand trends for all scenarios were based on the FAA 2016–36 aerospace forecast [4].

The resulting trends of system fuel burn and CO_2 emissions are shown in Figure 49. Although scenarios 1, 2 and 3 led to significant savings in fuel burn and CO_2 emissions, they still failed to meet the aggressive IATA target of 50% reduction in net carbon emissions by 2050 relative to 2005 levels. Nevertheless, they all achieved the carbon neutral growth target, primarily due to the adoption of biofuels. Figure 50 further illustrates the enablers' impact on the progression of system efficiency. From 2015 to 2050, scenario 3 resulted in the improvement of ASM/Gallon by more than three times; half of which was due to scenario 1 alone. The progression of system efficiency in terms of ASM/gCO_2 was also examined to capture the impact of biofuels. From 2015 to 2050, the three scenarios resulted in improvements in ASM/gCO_2 that ranged from 2.3 to 4.3 times, which again highlights the significance of biofuels.

Trends of operating costs and passenger demand, based on Eqs. 36 and 37, were also investigated. As shown in Figure 51, even though the input demand was such that $\dot{RPM} = 2.6$, the system converged towards a lower demand growth rate for the 'no action' scenario due to increasing operating costs and consequently, ticket prices. Conversely, scenarios 1–3 led to decreases in operating costs through the improvement of system fuel efficiency and therefore, resulted in increased demand.

Table 13: Enabler settings for four scenarios

	α_{2020}	α_{2025}	α_{2030}	α_{2035}	α_{2040}	α_{2045}	β	ϕ_{ABF}
No Action	1.0	1.0	1.0	1.0	1.0	1.0	1.0	N/A
Scenario 1	0.7	0.6	0.6	0.6	0.6	0.6	0.9	0.0
Scenario 2	0.7	0.6	0.5	0.4	0.4	0.4	0.9	0.0
Scenario 3	0.7	0.6	0.5	0.4	0.3	0.2	0.9	0.0

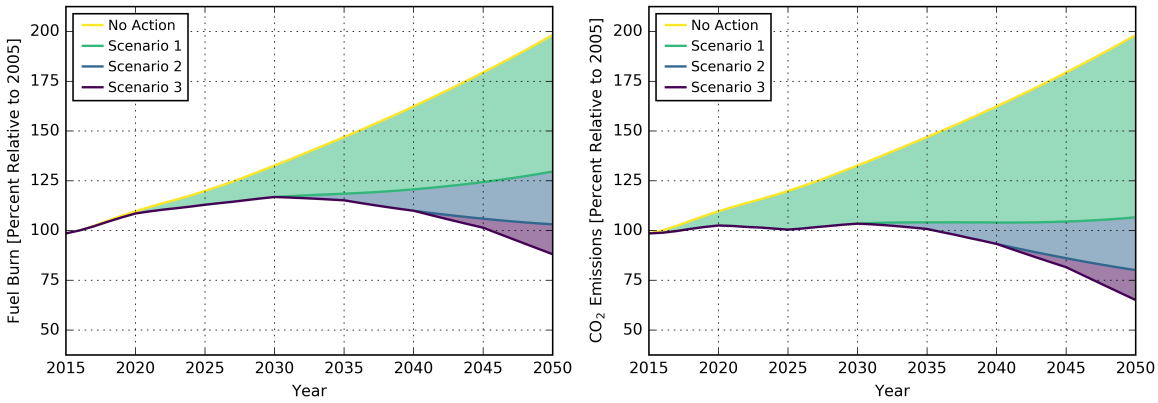

Figure 49: Trends of system fuel burn and CO_2 emissions for scenarios 1, 2 and 3

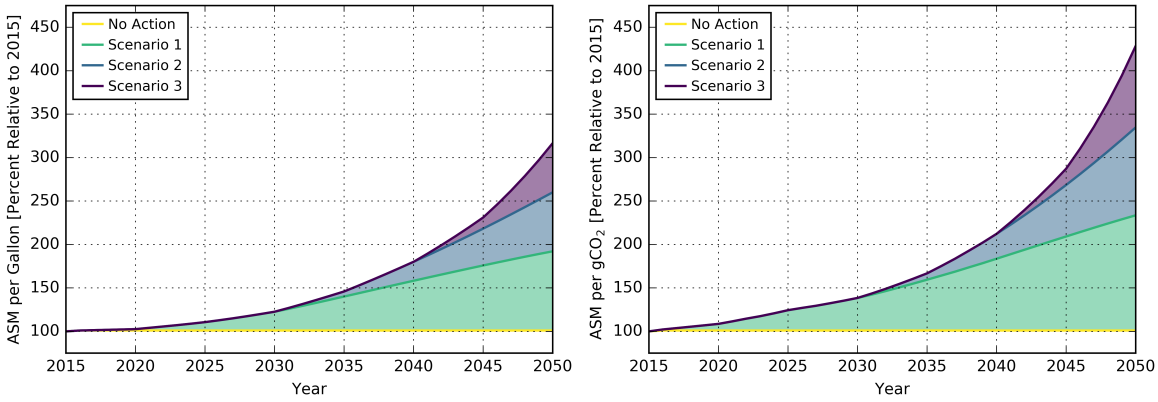

Figure 50: Trends of system efficiency in terms of ASM/Gallon and ASM/gCO_2 for scenarios 1, 2 and 3

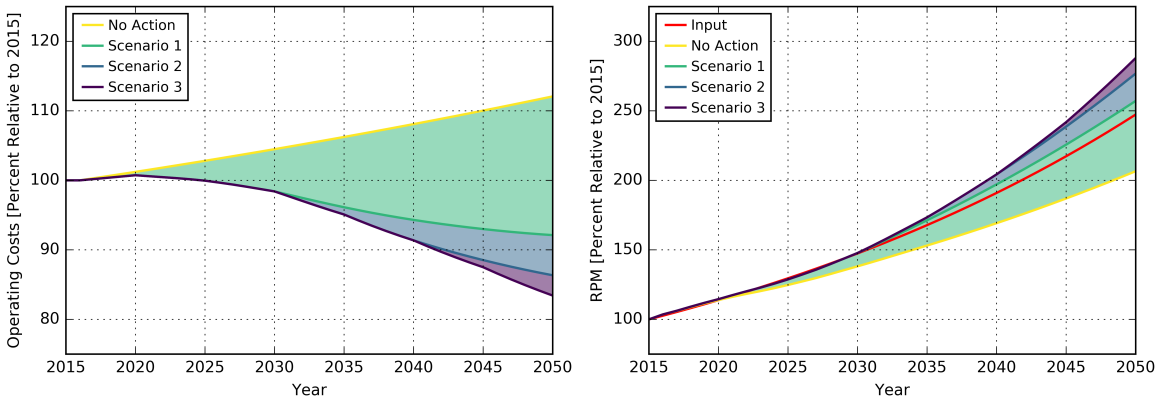

Figure 51: Trends of operating costs and demand growth for scenarios 1, 2 and 3

CHAPTER VI

HYPOTHESIS TESTING

In this chapter, hypothesis **H** is tested using the experimental plan of section 2.2.1. Testing **H** requires the isolation of technological and operational impacts on system fuel burn in order to compare the sum of their individual impacts to their combined impact. The Monte Carlo simulations of Chapter 5 were thus re-run three more times with the same values of ϕ_{FP} and $\phi_{\mathrm{R\dot{P}M}}$ (socioeconomic conditions) but with varying conditions for α and β (technological and operational improvements):

1. MC_0: both α and β set to zero
2. MC_α: same values of α but β set to zero
3. MC_β: same values of β but α set to zero

The individual impacts of α and β were then computed based on the fuel burn results of those three simulations such that:

$$\begin{aligned} \delta_{\mathrm{Tech}} &= \mathrm{FB}_{\mathrm{MC}_0} - \mathrm{FB}_{\mathrm{MC}_\alpha} \\ \delta_{\mathrm{Ops}} &= \mathrm{FB}_{\mathrm{MC}_0} - \mathrm{FB}_{\mathrm{MC}_\beta} \end{aligned} \tag{42}$$

In addition, the impact of inter-dependencies was determined using Eq. 12 as:

$$\begin{aligned} \delta_{\mathrm{Inter}} &= \Delta - \delta_{\mathrm{Tech}} - \delta_{\mathrm{Ops}} \\ &= (\mathrm{FB}_{\mathrm{MC}_0} - \mathrm{FB}_{\mathrm{MC}}) - (\mathrm{FB}_{\mathrm{MC}_0} - \mathrm{FB}_{\mathrm{MC}_\alpha}) - (\mathrm{FB}_{\mathrm{MC}_0} - \mathrm{FB}_{\mathrm{MC}_\beta}) \end{aligned} \tag{43}$$

where $\mathrm{FB}_{\mathrm{MC}}$ is the fuel burn of the original Monte Carlo simulations, which represent the combined impact of α and β. Eqs.42 and 43 are used for steps 1, 2 and 4 of the experimental plan. Experimental results are presented in the next section, followed by a discussion of findings.

6.1 Experimental Results

Contour plots of fuel burn reduction due to α and β, based on Eq. 42, are shown in Figure 52. Contour plots of fuel burn reduction due to inter-dependencies between α and β, based on Eq. 43, are shown in Figure 53.

The α plots of Figure 52 indicate that vehicle technologies had a gradual impact on system fuel burn, with minimal reductions in the near term. This is because of the slow fleet turnover where the newly introduced, more efficient vehicles required time to replace a considerable number of the older, less efficient ones. Hence, there exists a time lag between the input vehicle efficiency gain α and the resulting fleet efficiency gain $\bar{\alpha}$. Figure 52 illustrates that, on average, the rate of fuel burn reduction due to α ($-\Delta(\Delta\text{FB})/\Delta t$) increased from 0.2%/year 2016–2030 to 1.0%/year 2030–2050. The figure also shows that for both simulations, α had a similar impact on system fuel burn with slightly increased reductions, on average, for the second simulation, in which demand growth rates were higher. This slight increase in system efficiency can be attributed to the fact that all additional vehicles required to meet the higher demands were new vehicles of higher efficiency.

Alternatively, as emphasized in the β plots of Figure 52, operational improvements had an overall modest impact on system fuel burn. This result was expected since the maximum efficiency gain due to β was limited to 10% ($y = 0.90$). Unlike α, β does not have a gradual impact that intensifies with time, but instead has an immediate effect on CO_2 emissions reduction. This is because β is modeled as an overall improvement factor that directly affects system fuel efficiency (Eq. 34).

Last, the plots of Figure 53 show the difference between the sum of the individual impacts of α and β, and their combined impacts. The plots show clear discrepancies that intensify into the future. By 2050, the deviations range from a minimum of zero to a maximum of approximately 7.5% with an average value of 1.3%, relative to 2005 fuel burn levels.

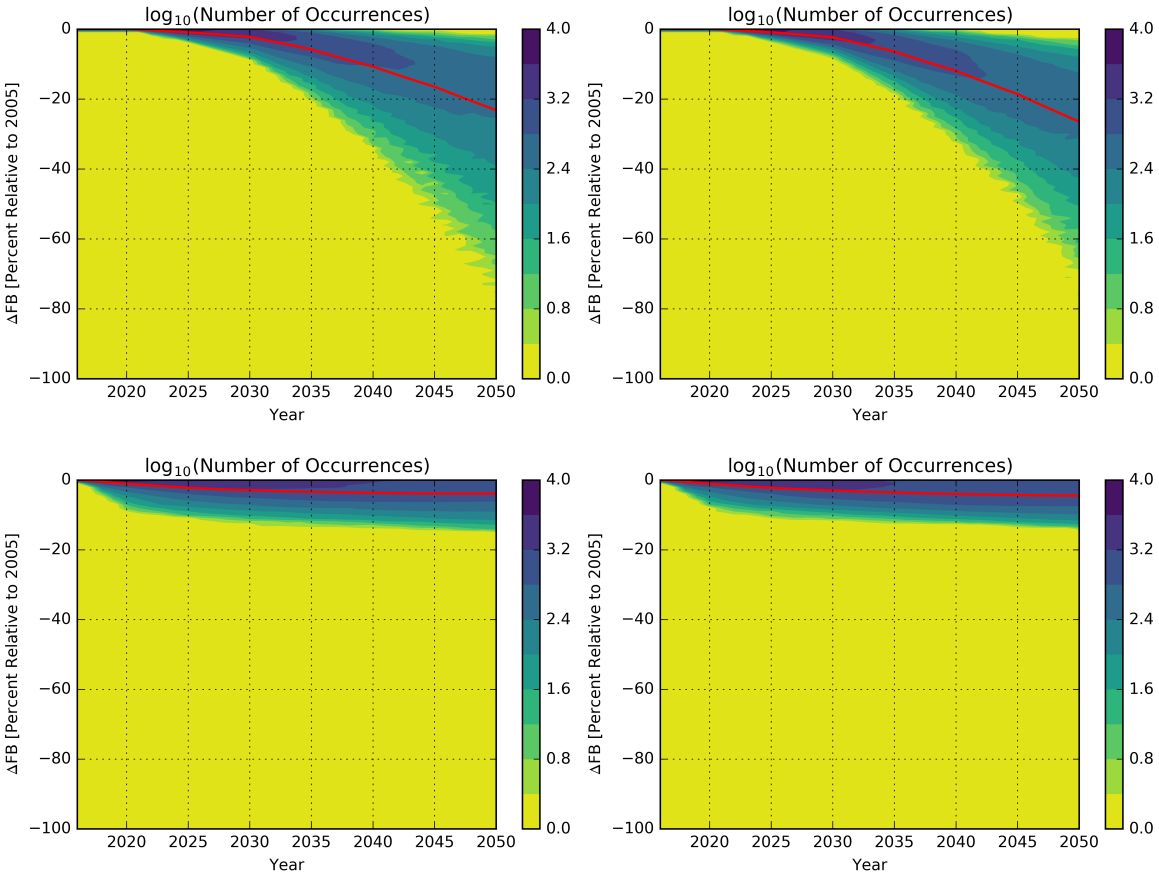

Figure 52: Contour plots of system fuel burn reduction due to α and β for two Monte Carlo simulations (left: uniform sampling of all variables; right: uniform sampling of efficiency variables and triangular sampling of scaling variables; top: α; bottom: β; mean trends overlaid in red)

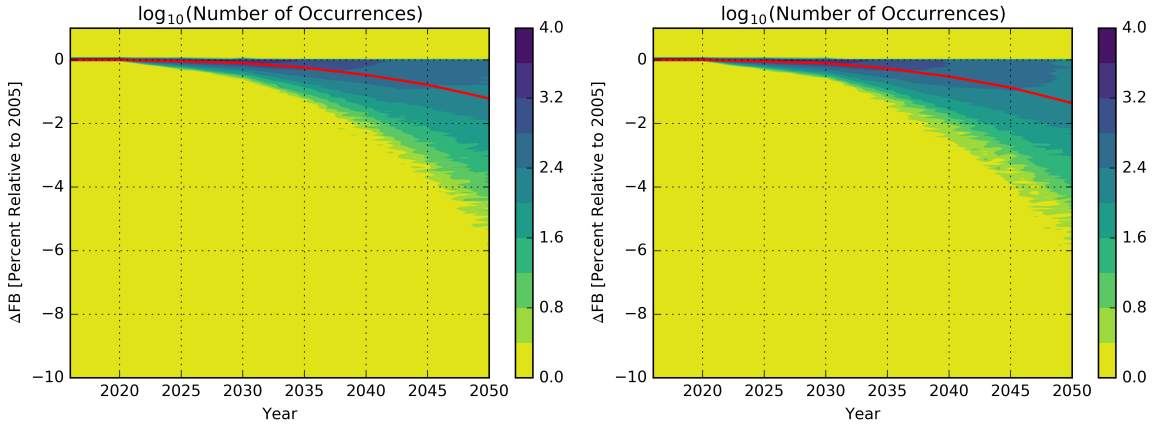

Figure 53: Contour plots of system fuel burn reduction due to α, β interaction for two Monte Carlo simulations (left: uniform sampling of all variables; right: uniform sampling of efficiency variables and triangular sampling of scaling variables; mean trends overlaid in red)

6.2 Discussion

As discussed in section 2.2, hypothesis **H** is accepted if the results show that $\delta_{\text{Inter}} \geq 0$ ($\Delta\text{FB} \leq 0$). From Figure 53, it is clear that this condition has been met and therefore, the hypothesis is *accepted*.

Although most scenarios resulted in system fuel burn reductions due to α, β interaction, Figure 54 highlights that approximately half of the Monte Carlo cases resulted in savings of 1% or less by 2050, relative to 2005 levels, which is not particularly significant. Nevertheless, this observation does not refute **H** because there were scenarios that have led to more significant savings. Those scenarios were investigated closely.

As shown in Figures 55–57, scenarios that resulted in system fuel burn reductions of 1.5% or more by 2050, relative to 2005 levels, were characterized by high demand growth rates and high dependency on enabler impacts, regardless of the input sampling distributions. With the exception of ϕ_{FP}, the variable histograms are noticeably skewed towards higher values of $\dot{\text{RPM}}$, α and β. This result was expected since, from Eqs. 11 and 12, system fuel burn reductions due to inter-dependencies rely on enabler impact ($\partial FB/\partial T$ and/or $\partial FB/\partial O$) and introduction rate ($\mathrm{d}T/\mathrm{d}t$ and/or $\mathrm{d}O/\mathrm{d}t$):

$$\delta_{\text{Inter}} = \int_a^b \left(\frac{\partial FB}{\partial T} \frac{\partial T}{\partial O} \frac{\mathrm{d}O}{\mathrm{d}t} \right) \mathrm{d}t = \int_a^b \left(\frac{\partial FB}{\partial O} \frac{\partial O}{\partial T} \frac{\mathrm{d}T}{\mathrm{d}t} \right) \mathrm{d}t \tag{44}$$

Enabler introduction rates, specifically of vehicle technologies, are influenced by $\dot{\text{RPM}}$. As previously discussed, high demand growth rates provide an opportunity for system fuel efficiency to be enhanced through the faster introduction of newer, more efficient vehicles.

To generalize the above observations, surrogate models were developed using the Monte Carlo cases to relate δ_{Inter} in 2030, 2040 and 2050 to the four variables that influence it $[\alpha; \beta; \phi_{\text{FP}}; \phi_{\dot{\text{RPM}}}]$. Two sets of surrogate models were generated using RSM and ANN (see Appendix C for 'goodness-of-fit' measures for all surrogate models). Prediction profilers of the six surrogate models are shown in Figures 58 and 59.

The profilers highlight several important trends. First, while the impact of inter-dependencies in the near term is almost nonexistent, such impact does intensify in the far term as the vehicle efficiency impact grows. In addition, the profilers re-emphasize the strong impact of demand growth rate, operational efficiency and vehicle efficiency. Last, the profilers show a slight inverse dependence on fuel price, where higher fuel prices result in lower values of δ_{Inter} (due to the consequent decrease in demand).

6.3 Case Study

The scenarios of section 5.2.2 are investigated further to analyze the impact of inter-dependencies on system fuel burn. Four additional scenarios were run to isolate the impacts of vehicle technologies and operational improvements in scenarios 1, 2 and 3 (Table 14). The additional scenarios were run using the same fuel price and passenger demand trends ($\phi_{\text{R\dot{P}M}} = \phi_{\text{FP}} = 0.5$). Eqs. 42 and 43 were then applied to the fuel burn results of all eight scenarios in order to quantify the individual impacts of α and β as well as the impact of α, β interaction.

Figures 60–62 show the system fuel burn trends for scenarios 1, 2 and 3 along with the enabler contributions for each. For all scenarios, the impact of inter-dependencies was negligible before 2040, but increased afterwards. In 2050, inter-dependencies contributed 3.9%, 5.8% and 6.8% to the overall reduction in fuel burn for scenarios 1, 2 and 3, respectively (Table 15). This progression in δ_{Inter} is attributed to the increased impact and introduction rate of vehicle technologies (since the impact of operational improvements was the same across all scenarios). The impact of inter-dependencies

Table 14: Enabler settings for four additional scenarios

	α_{2020}	α_{2025}	α_{2030}	α_{2035}	α_{2040}	α_{2045}	β
Operational Improvements	1.0	1.0	1.0	1.0	1.0	1.0	0.9
Scenario 1 Technologies	0.7	0.6	0.6	0.6	0.6	0.6	1.0
Scenario 2 Technologies	0.7	0.6	0.5	0.4	0.4	0.4	1.0
Scenario 3 Technologies	0.7	0.6	0.5	0.4	0.3	0.2	1.0

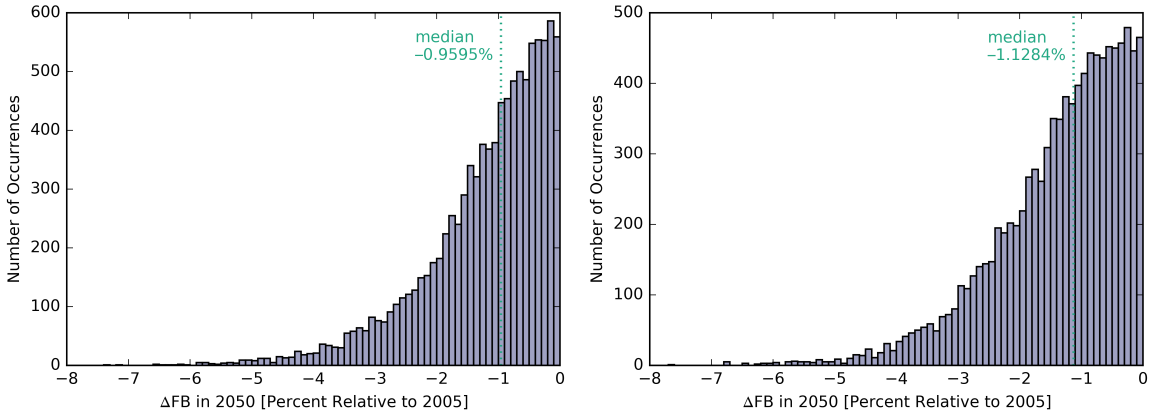

Figure 54: Histograms of system fuel burn savings in 2050 for all scenarios (left: uniform sampling of all variables; right: uniform sampling of efficiency variables and triangular sampling of scaling variables)

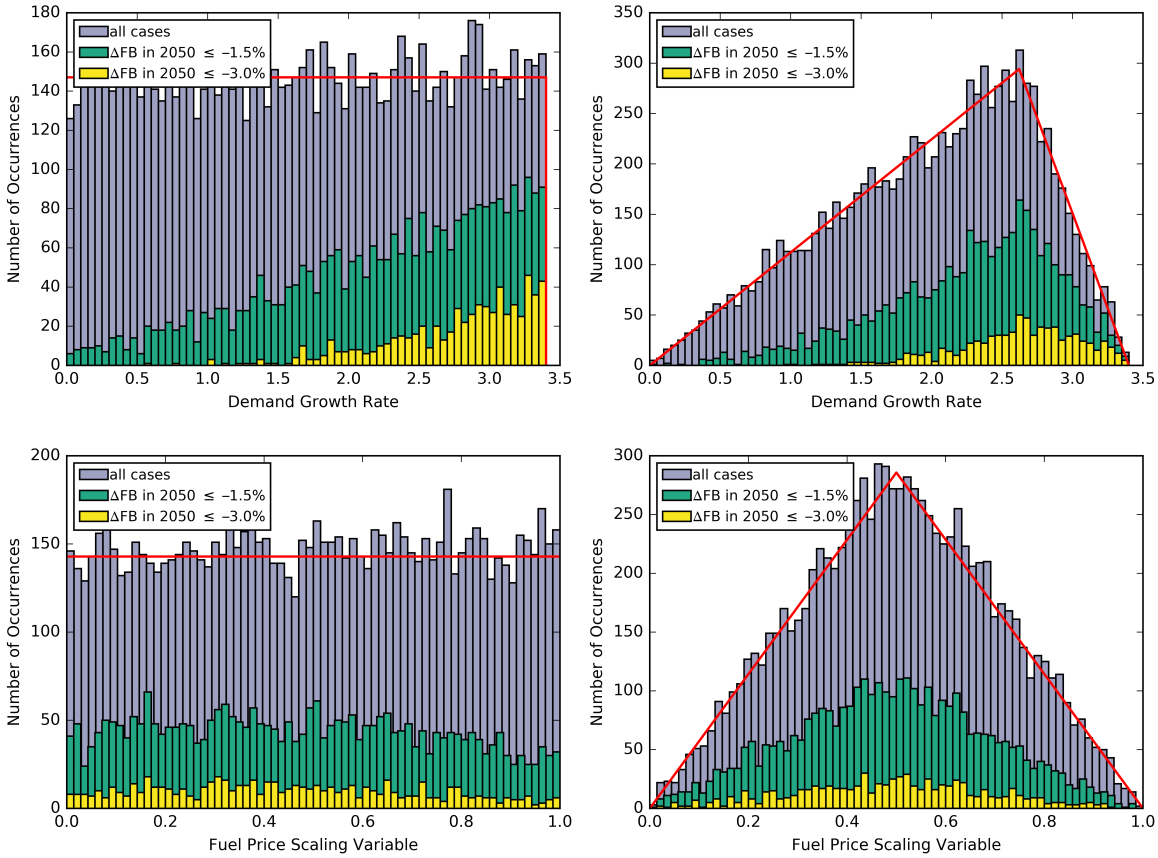

Figure 55: Overlaid histograms of $\dot{\text{RPM}}$ and ϕ_{FP} for all scenarios (left: uniform sampling of all variables; right: uniform sampling of efficiency variables and triangular sampling of scaling variables; sampling distributions overlaid in red)

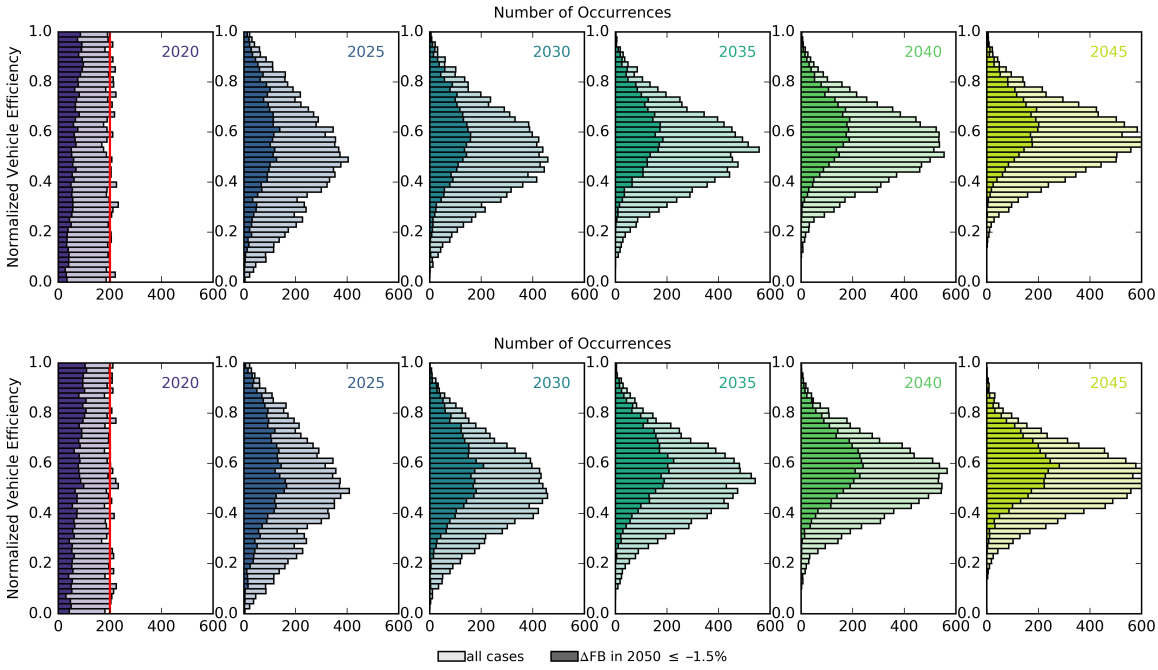

Figure 56: Overlaid histograms of normalized α values for all scenarios (top: uniform sampling of all variables; bottom: uniform sampling of efficiency variables and triangular sampling of scaling variables; sampling distributions overlaid in red)

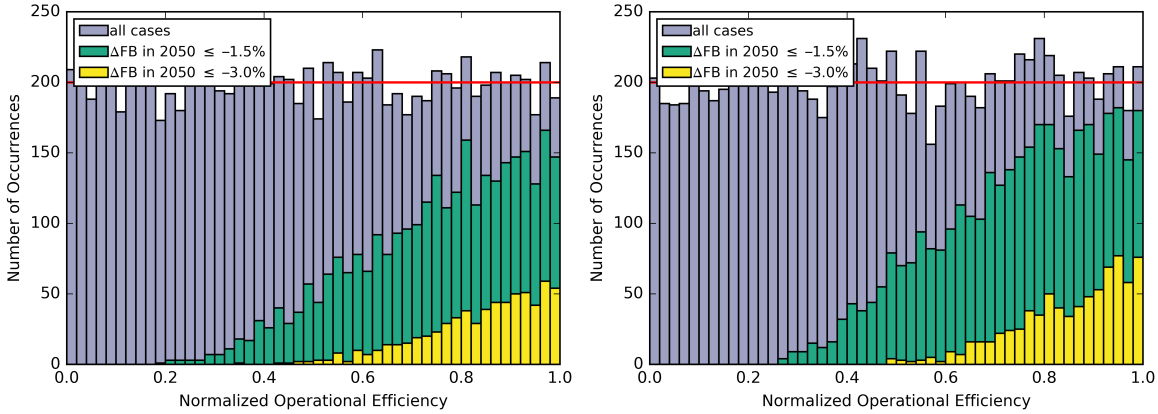

Figure 57: Overlaid histograms of normalized β values for all scenarios (left: uniform sampling of all variables; right: uniform sampling of efficiency variables and triangular sampling of scaling variables; sampling distributions overlaid in red)

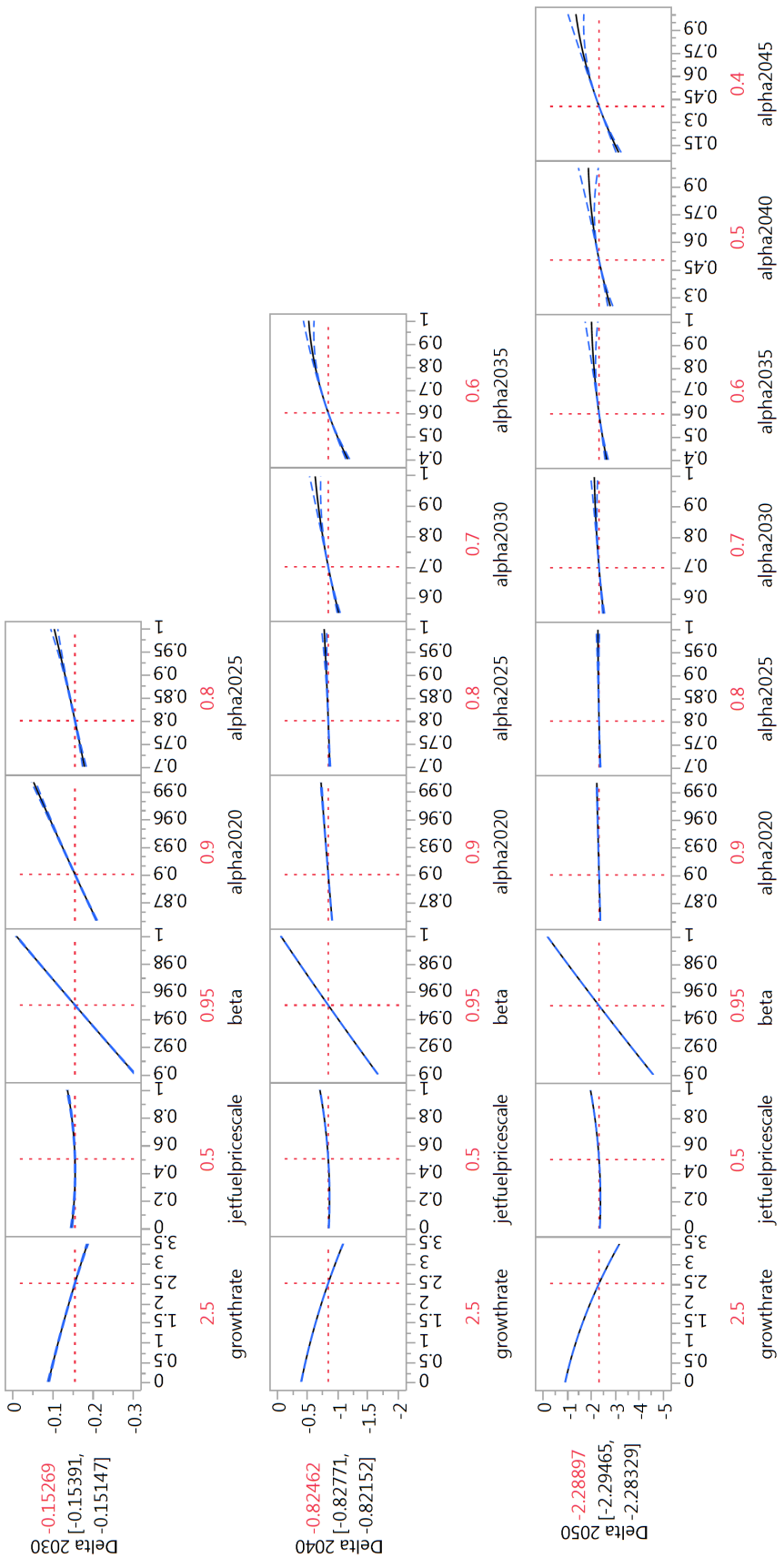

Figure 58: RSM models for system fuel burn reduction due to α, β interaction in 2030, 2040 and 2050

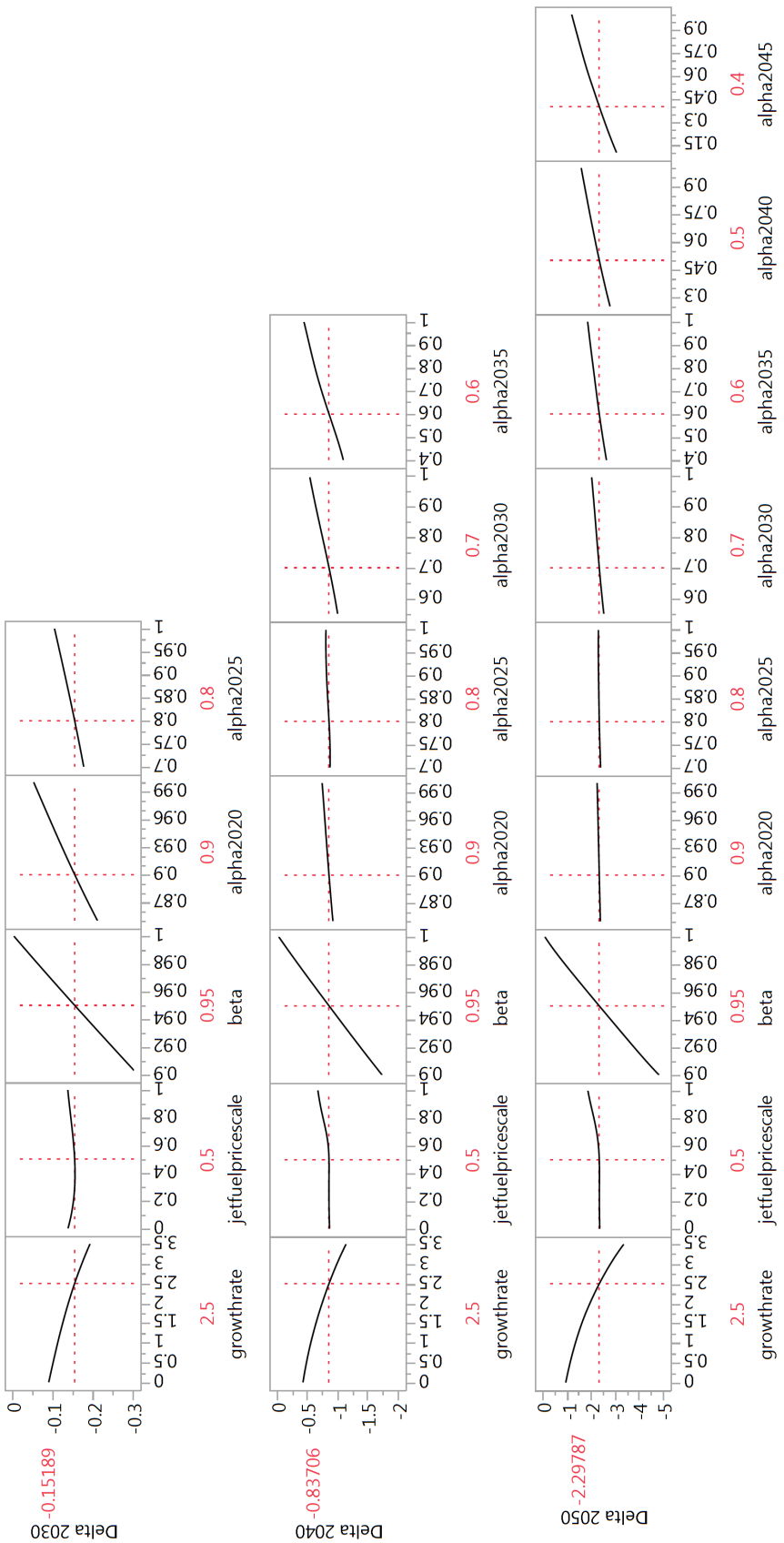

Figure 59: ANN models for system fuel burn reduction due to α, β interaction in 2030, 2040 and 2050

Table 15: Enabler contributions to the overall system fuel burn reduction for scenarios 1, 2 and 3 in 2040 and 2050

	Scenario 1		Scenario 2		Scenario 3	
	2040	2050	2040	2050	2040	2050
Operational Improvements	21.3%	20.8%	17.0%	15.0%	17.0%	13.0%
Vehicle Technologies	77.8%	75.3%	80.7%	79.2%	80.7%	80.2%
Inter-Dependencies	0.9%	3.9%	2.3%	5.8%	2.3%	6.8%

on system fuel burn reduction is signified when compared to that of operational improvements. As can be deduced from Table 15, δ_{Inter} was approximately 0.2, 0.4 and 0.5 times δ_{Ops} in 2050 for scenarios 1, 2 and 3, respectively.

The previous observations clearly suggest that inter-dependencies between vehicle technologies and operational improvements can be exploited to enhance system fuel burn performance, which again increases confidence in hypothesis **H**.

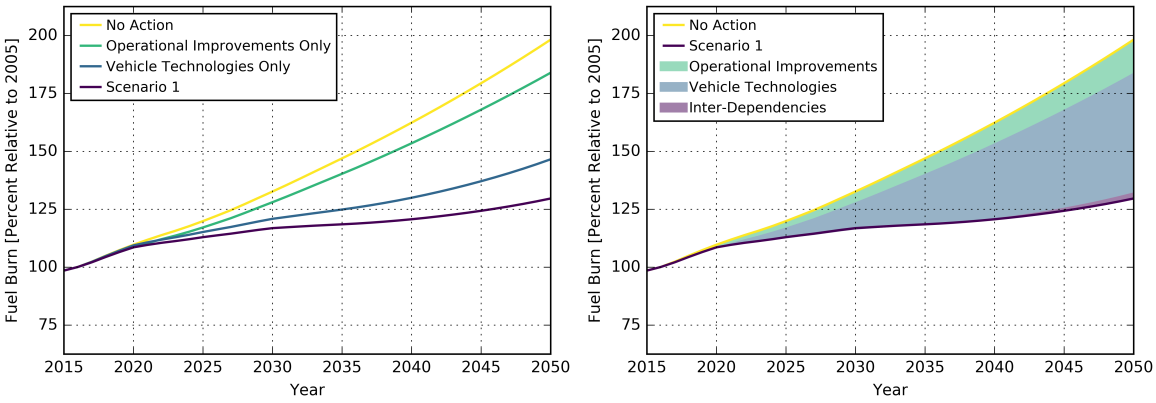

Figure 60: Trends of system fuel burn for scenario 1 (left: isolated and combined enabler impact trends; right: enabler contributions to fuel burn reduction)

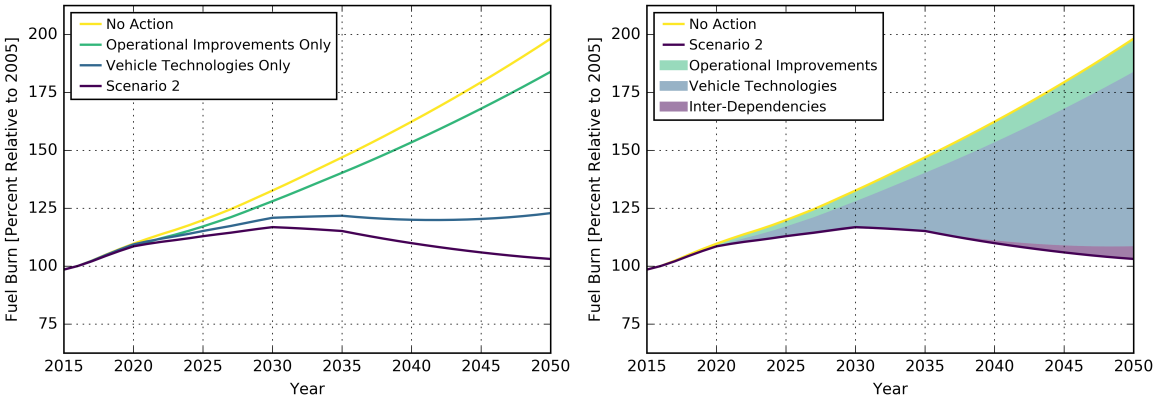

Figure 61: Trends of system fuel burn for scenario 2 (left: isolated and combined enabler impact trends; right: enabler contributions to fuel burn reduction)

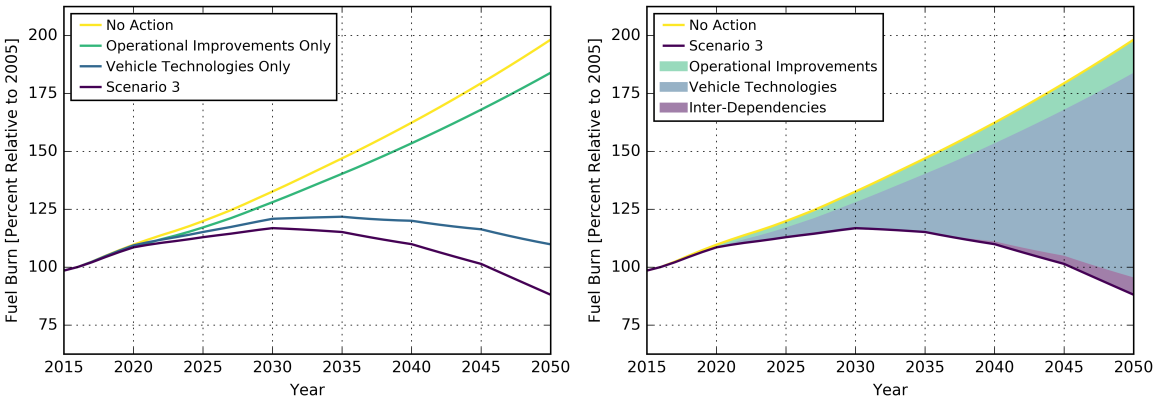

Figure 62: Trends of system fuel burn for scenario 3 (left: isolated and combined enabler impact trends; right: enabler contributions to fuel burn reduction)

CHAPTER VII

CONCLUSION

The **research objective** of this thesis was to provide a framework that incorporates vehicle technologies and operational improvements in order to evaluate their projected system-level impacts. Such framework fulfills a current need for an all-encompassing capability that evaluates system performance at reasonable accuracy and manageable uncertainty, and that can be used for the assessment of aviation environmental targets. Chapters 3 and 4 of this thesis were dedicated to the definition and development of that framework. In Chapter 5, the framework was employed to run different scenarios and evaluate performance impacts of vehicle technologies and operational improvements at the system-level.

The main thesis argument was formally presented in Chapter 2. It was concerned with the inter-dependencies between vehicle technologies and operational improvements and was posed in the form of a hypothesis:

H: Inter-dependencies between vehicle technologies and operational improvements can be exploited to further enhance the performance of aviation systems.

In order to test this argument, the methodological framework needed to be developed. In Chapter 6, the framework was utilized to test the hypothesis and it was accepted.

7.1 Contributions

The main contributions of this thesis are directly related to the research objective and main thesis argument. The former filled a current research gap in the literature for an evaluation capability that links vehicle-level and system-level analyses. Alternatively, hypothesis **H** challenged a commonly accepted assumption in system-level analyses.

7.1.1 Methodological Framework

The primary contribution of this thesis is the definition and development of a methodological framework that bridges the gap between the vehicle and the system. When the system environmental targets were first defined by IATA, vehicle technologies and operational improvements were considered essential enablers of the IATA vision. But while the targets were defined at the system-level, all vehicle technologies and many operational improvements were aimed at vehicle-level performance. Although previous works investigated the system-level impacts of either technologies or operations, their simultaneous consideration was overlooked. The assumption that the net system performance impact is the summation of the individual enabler impacts is commonly accepted. A framework that considered vehicle technologies and operational improvements simultaneously needed to be realized to test such assumption.

The developed framework enables a two way link between vehicle-level and system-level analyses. In the feedforward direction, vehicle-level impacts are evaluated to set bounds (or feed direct figures) to the system-level analysis. Those bounds are used to run numerous scenarios to accommodate inherent sources of epistemic and aleatory uncertainty. Once those scenarios are evaluated, a feedback can be initiated to the vehicle-level analysis in order to set technology and/or operational requirements. The exploratory and normative aspects together formulate a feedback loop that is of great significance to stakeholders. Since informed decision making is vital for investment resource allocation and the development of research strategies, such a framework is valuable in its ability to quantify the return on investment for multiple technological and operational upgrades.

7.1.2 Hypothesis

Another major contribution of this thesis is the assessment of the system-level impact of inter-dependencies between vehicle technologies and operational improvements. It

was hypothesized that such impact should not be generally disregarded and that opportunities can be identified where system performance is augmented through the exploitation of inter-dependencies. The hypothesis was tested and accepted. It was shown through numerous scenario evaluations that the inter-dependencies are indeed reinforcing and could lead to significant reductions in fuel burn for certain combinations of technological and operational upgrades.

The main implication of the thesis argument is the need for simultaneous consideration of vehicle technologies and operational improvements for certain scenarios. This is to account for the impact of inter-dependencies on system performance. Technologies and operations are considered means and ways to achieve the system performance and environmental targets. Hypothesis **H** provides guidance to accurate quantification of system-level technological and operational impacts. Opportunities exist for policy makers and stakeholders to identify appropriate actions and/or options for the enhancement of system performance by means of exploiting inter-dependencies.

7.2 Directions for Future Work

There are several directions for future works based on this thesis; however, there are two main avenues: either build on the current framework by adding other components to it, or increase its accuracy and fidelity by tackling its assumptions.

IATA envisioned achieving its environmental targets through four enablers and not just two. Even though this thesis focused on technologies and operations, there is a lot of potential from the other enablers. Some enablers such as economic measures were not accounted for, while others such as biofuels were handled at a basic analysis level. Those enablers are unlike technologies and operations as they primarily impact system performance. The system-level response to all the enablers being implemented may instigate or enforce requirements for technologies and operations at the vehicle-level. Such interplay would be interesting to observe and quantify if possible.

In addition, operational improvements considered in this thesis focused on vehicle performance. Nevertheless, there are others that seek to enhance the efficiency of the system itself (e.g., P2 in Table 7). To model such improvements, it may be required to have a full representation of the operational network with a detailed analysis of origin-destination routes. Moreover, infrastructure enhancements have not been considered. It has been assumed throughout that demand is unconstrained such that supply will always meet any increase in demand. However, airport capacities pose a threat to the future growth of commercial aviation. An analysis of system capacity, its relation to delay propagation, and how this ultimately ties back to system fuel burn could be a possible avenue for future development.

This thesis only focused on two system metrics: fuel burn and CO_2 emissions. The expansion of the methodological framework to encompass additional metrics such as noise or safety could be an option in order to obtain a more complete assessment of the system. Fuel consumption and CO_2 emissions are directly related and therefore, no trade-offs were required. Modeling the interplay between different, possibly competing metrics can also be a topic of future research.

As for the assumptions, they were inevitable in order to scope the work and reduce the problem into a manageable one. The major assumptions discussed in section 4.3.1 can be tackled in future works. Including cargo aircraft would require the formulation of a new system-level metric that accounts for the transport of both seats and tonnage. Similarly, an extension from partial to general equilibrium may require a multimodal analysis to be conducted in order to investigate the interaction between aviation and other modes of transportation.

Furthermore, several assumptions within the model can be the subject of future research. Several system factors have been assumed constant within the framework. Parameters such as pass-through and price elasticity are strongly linked to the system economics and if a more detailed system representation is embedded, those parameters

may be computed rather than fixed. Similarly, for fleet growth, it was assumed that all vehicle classes grow proportionally. Bottom-up economic representation of airline fleet planning may be utilized to account for disproportionate fleet growth.

The work presented in this thesis addressed a crucial research gap and identified important opportunities for the performance enhancement of aviation systems. Yet, many challenges remain to be tackled. As shown above, ample opportunity exists for future works to build on this thesis and address several of these challenges.

APPENDIX A

JUSTIFICATION OF ASSUMPTIONS

Eqs. 28 and 36 rely on two primary assumptions: 1) fleet growth occurs proportionally across all vehicle classes, and 2) relative operating costs can be approximated using an expression that relates them to fuel fraction and system fuel efficiency. Those two assumptions are justified using aerospace forecasts and historical system performance.

A.1 Fleet Growth

The baseline fleet composition is subject to change in the future depending on market demand trends and airline acquisition strategies. Yet, vehicle class proportions were assumed constant in this thesis for two reasons. First, the FAA 2016–2036 aerospace forecast does not predict a future fleet composition that is considerably different from the current one. The forecast categorizes passenger jet aircraft in the combined US fleet of mainline and regional air carriers into three classes: regional, narrowbody and widebody. As shown in Figure 63, the vehicle classes retain their respective shares throughout the forecast period to a great extent.

Second, in order to distort the baseline fleet composition, an algorithmic logic is required to allow vehicle classes to grow at different rates, and to allow aircraft from different vehicle classes to replace one another upon retirement. This logic would not only introduce additional sources of uncertainty (which is unnecessary since forecasts predict minimal variations in fleet composition, as explained above), but more importantly would add computational complexity. As illustrated in Algorithm 1, for every scenario or Monte Carlo run, the fleet turnover model is run multiple times within the system equilibrium procedure until convergence is achieved. Replacing aircraft

on a vehicle class basis provides the advantage of simplifying such model allowing for rapid evaluations that minimize computational run time. The implementation of an additional algorithmic logic would increase computational cost significantly.

A.2 Operating Costs

Airline operating costs consist of both fuel and non-fuel costs. Eq. 36 approximates relative operating costs primarily based on the progression of fuel costs, without much analysis of non-fuel costs. However, this approximation proved to work very well when compared with historical data derived from different BTS databases. Using the P1.2, P5.2 and T2 databases, fuel costs, total operating costs and fuel efficiency in terms of ASM/Gallon can be determined, respectively [19, 114]. By accounting for inflation, and using Eq. 36, effective fuel fraction and relative operating costs were examined for the years 2005–2015. The fuel fraction in 2005 of 0.225 was used as a baseline. Actual and predicted values are listed in Table 16 and plotted in Figure 64.

It is clear from Figure 64 that there is a very close agreement between actual and predicted values. This is especially significant since multiple events took place during the 2005–2015 time period. This period included a major economic depression in 2008 and huge fluctuations in jet fuel price. It also included the introduction of the first more electric aircraft the Boeing 787 in 2011, which offered savings of 20–30% in fuel burn and CO_2 emissions relative to the vehicles it replaced (also, the Boeing 787 fleet was grounded for three months in 2013 resulting in huge costs to both Boeing and airline operators). In addition, other aircraft of enhanced efficiency were introduced during the same time period such as the CRJ-1000 (RJ), A-350-XWB (LTA) and the A-380 (VLA). The fact that Eq. 36 closely matched real cost data during this time period in which both big economic and technological changes have occurred, gives confidence that such approximation can be representative (or can provide a close enough estimate) of future changes in operating costs.

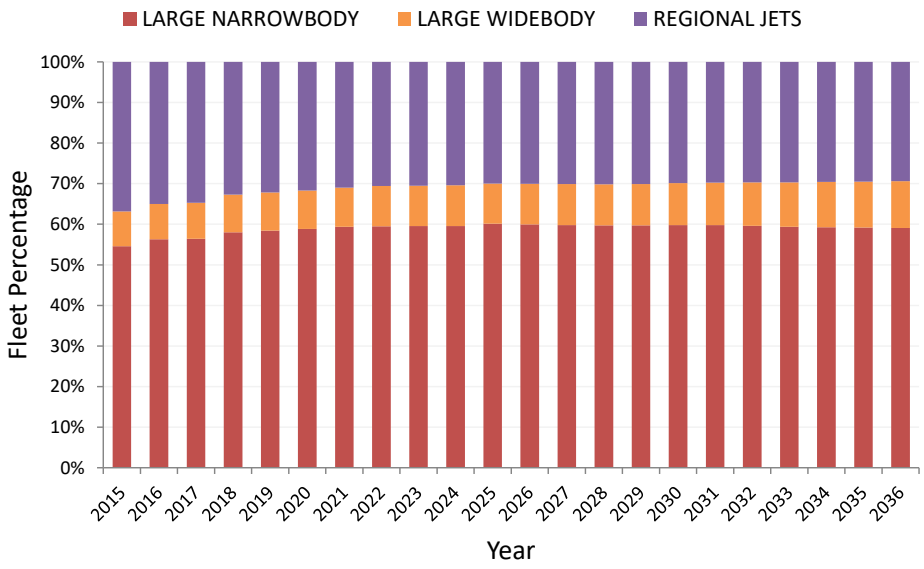

Figure 63: Forecast growth in passenger jet aircraft proportions of US mainline and regional air carriers [4]

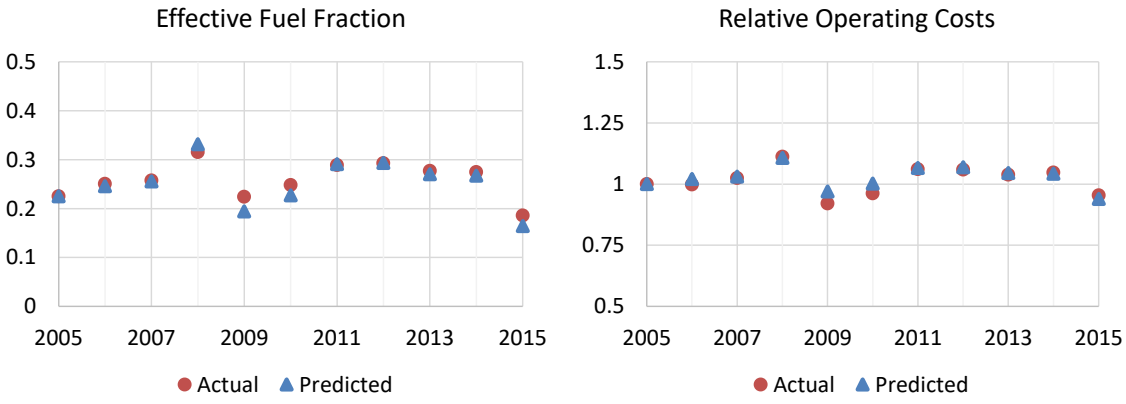

Figure 64: Actual and predicted values of effective fuel fraction and relative operating costs

Table 16: Actual and predicted values of effective fuel fraction and relative operating costs [19, 114]

Year	Actual rel. η (T2)	Actual FF (P1.2/5.2)	Predicted eff. FF	Actual rel. OC (P5.2)	Predicted rel. OC
2005	1	0.224939	0.224939	1	1
2006	1.016562	0.250457	0.245867	0.997935	1.020928
2007	1.033677	0.257528	0.255281	1.024660	1.030342
2008	1.057209	0.315450	0.331747	1.111826	1.106808
2009	1.061446	0.223951	0.194213	0.920497	0.969274
2010	1.050916	0.247902	0.227013	0.962362	1.002074
2011	1.054610	0.289026	0.290780	1.061010	1.065841
2012	1.056119	0.292589	0.293390	1.059010	1.068451
2013	1.064779	0.277223	0.270329	1.038299	1.045390
2014	1.077072	0.274598	0.267103	1.047675	1.042164
2015	1.078014	0.185788	0.164455	0.954231	0.939516

APPENDIX B

IMPACT OF BIOFUELS

The parameter κ_b varies not only by biofuel type, but also based on the process from which the biofuel is produced. Stratton et al. published a comprehensive report on the life cycle emissions of both conventional and unconventional fuels [97]. Figure 65 summarizes their findings. As shown in the figure, life cycle emissions resulting from the production of different fuels through different processes vary from zero to eight times that of conventional jet fuel. The assumption that $\kappa_b = 0.25 \cdot \kappa_c$ is according to estimates for the Fischer-Tropsch (F-T) fuel being produced from switchgrass/biomass (highlighted in green in Figure 65). This assumption was also utilized by the FAA in a recent study [15]. It is to be noted that κ as defined by Eq. 38, takes into account other fuel properties such as heating value and density. For F-T fuel, Stratton et al. show that these properties are almost equal to that of conventional jet fuel [97].

Figure 66 demonstrates the impact biofuels had on system CO_2 emissions for the Monte Carlo simulations, which was calculated using Eq. 31 as:

$$\begin{aligned} \delta_{\text{Bio}} &= (\kappa_c - \kappa_b) \cdot \text{FBB} \\ &= 0.75 \cdot \kappa_c \cdot \text{FBB} \end{aligned} \tag{45}$$

where FBB is biofuel quantity. Despite the high magnitude of CO_2 reductions, mainly due to the assumption that $\kappa_b = 0.25 \cdot \kappa_c$, the impact of ϕ_{ABF} was associated with large $\pm|\Delta CO_2|$ bounds due to the uncertainty in biofuel availability. Similar to operational improvements, biofuels had a prompt impact on the system as a whole. Their impact continued to grow into the future as availability increased. Figure 66 shows that in both simulations, ϕ_{ABF} had a strong impact on system CO_2 emissions with decreased reductions, on average, for the second simulation, in which availability was lower.

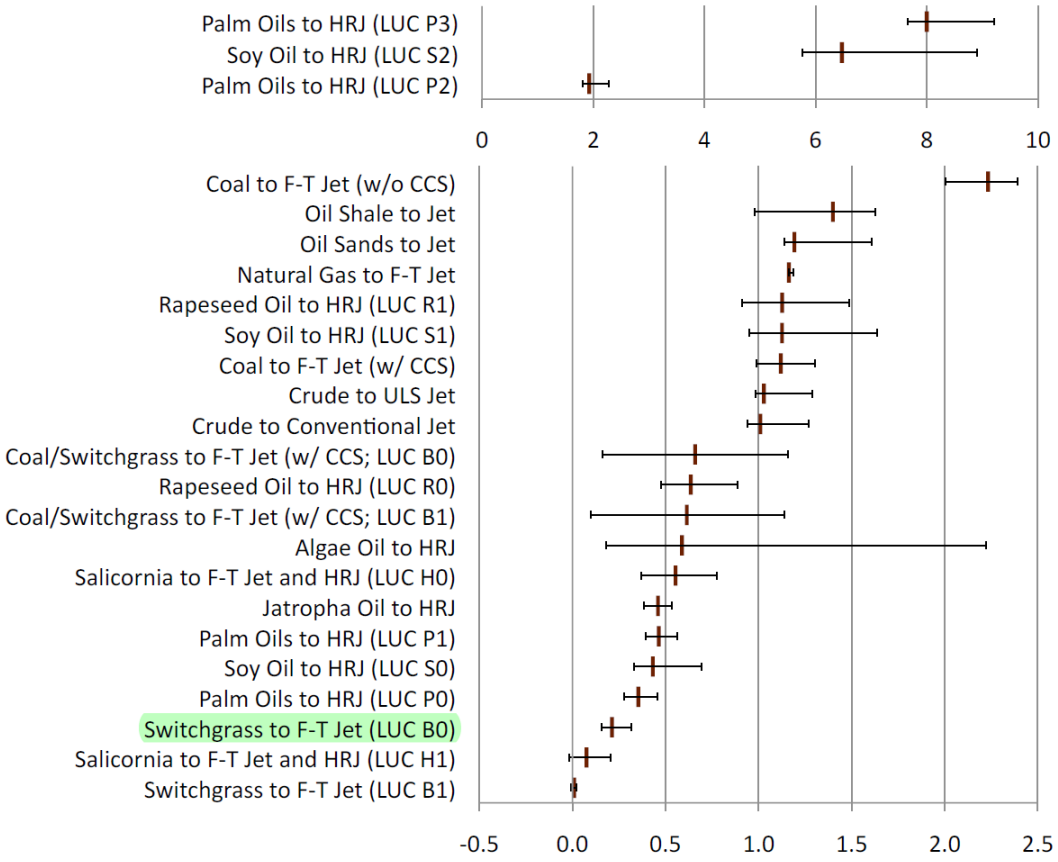

Figure 65: Life cycle emissions normalized by conventional jet fuel [97]

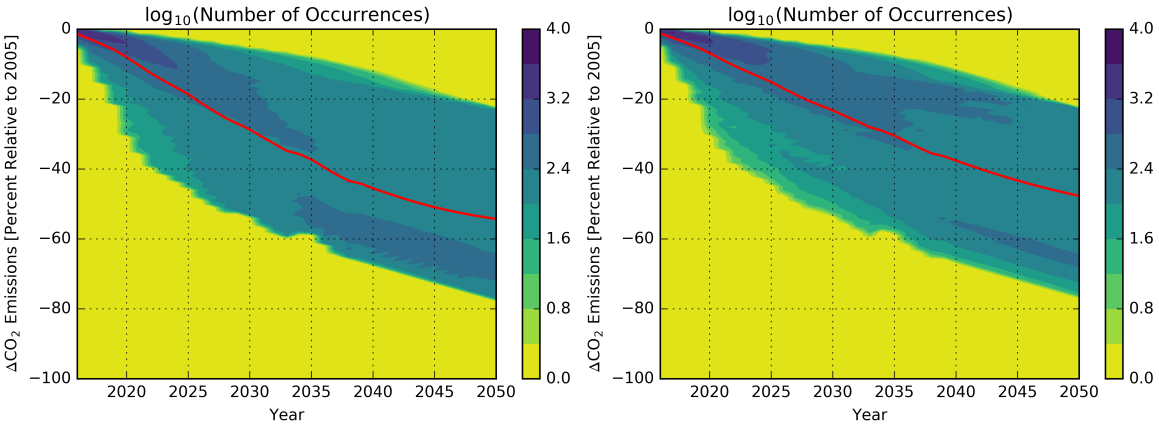

Figure 66: Contour plots of system CO_2 emissions reduction due to ϕ_{ABF} for two Monte Carlo simulations (left: uniform sampling of all variables; right: uniform sampling of efficiency variables and triangular sampling of scaling variables; mean trends overlaid in red)

APPENDIX C

SURROGATE MODEL VALIDATION

Surrogate models developed for system fuel burn (Chapter 5) and system fuel burn reduction due to α, β interaction (Chapter 6) were checked for adequacy using four main measures: coefficient of determination (R^2), Root Mean Square Error (RMSE), actual versus predicted plots, and residual versus predicted plots (Tables 17 and 18; Figures 67–74). R^2 and RMSE are calculated as:

$$R^2 = 1 - \frac{\sum_{i=1}(y_i - \hat{y}_i)^2}{\sum_{i=1}(y_i - \bar{y})^2} \qquad \text{RMSE} = \sqrt{\frac{\sum_{i=1}(y_i - \hat{y}_i)^2}{n - p}} \tag{46}$$

where y_i is the actual value, $\hat{y}_i$ is the predicted value, $\bar{y}$ is the mean of actual values, n is the number of observations, and p is the number of degrees of freedom. A good fit is characterized by: an R^2 value close to unity, a small RMSE value, an actual versus predicted plot that follows the $y = x$ trend, and residual values close to zero.

Table 17: Measures of goodness of surrogate models for system fuel burn in 2030, 2040 and 2050

	RSM			ANN		
	2030	2040	2050	2030	2040	2050
R^2	0.996084	0.997238	0.994928	0.996520	0.999695	0.999996
RMSE	1.105049	1.327095	2.391111	1.044357	0.439520	0.069225

Table 18: Measures of goodness of surrogate models for system fuel burn reduction due to α, β interaction in 2030, 2040 and 2050

	RSM			ANN		
	2030	2040	2050	2030	2040	2050
R^2	0.849584	0.963725	0.986760	0.855366	0.971908	0.995798
RMSE	0.036044	0.076214	0.119235	0.034992	0.066918	0.066802

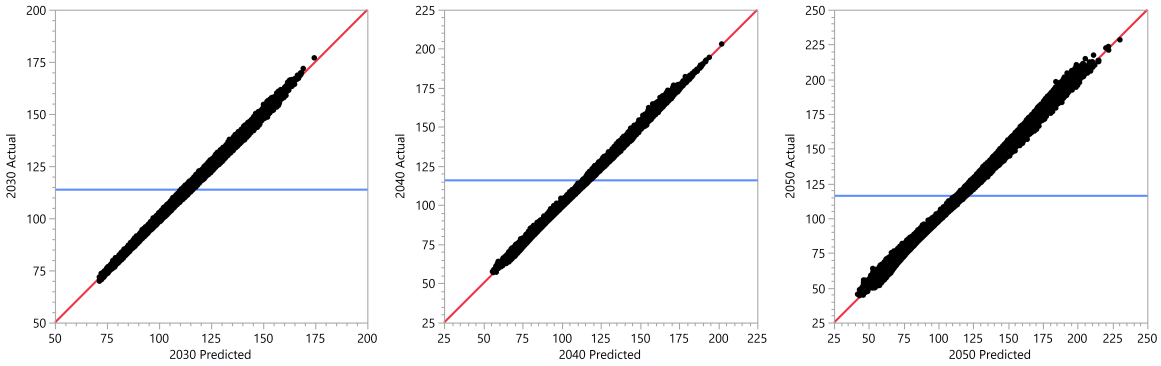

Figure 67: Actual versus predicted plots of RSM models for system fuel burn in 2030, 2040 and 2050

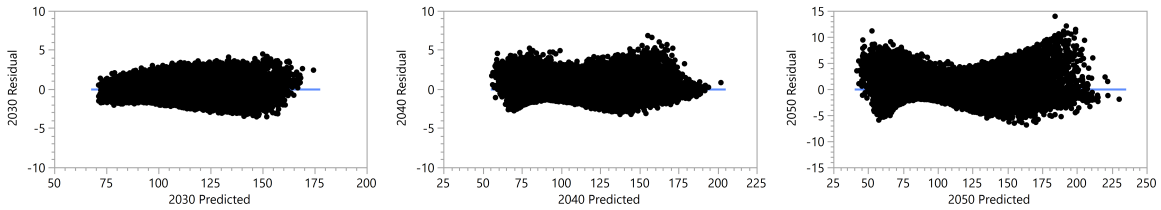

Figure 68: Residual versus predicted plots of RSM models for system fuel burn in 2030, 2040 and 2050

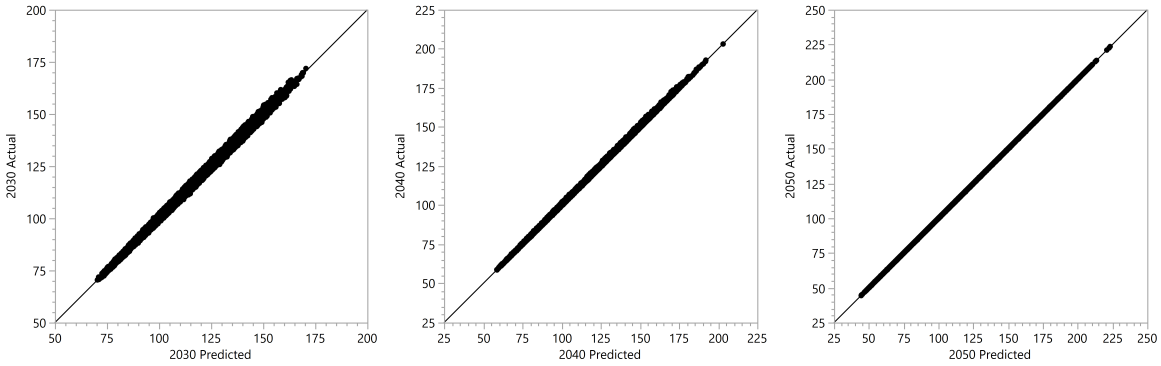

Figure 69: Actual versus predicted plots of ANN models for system fuel burn in 2030, 2040 and 2050

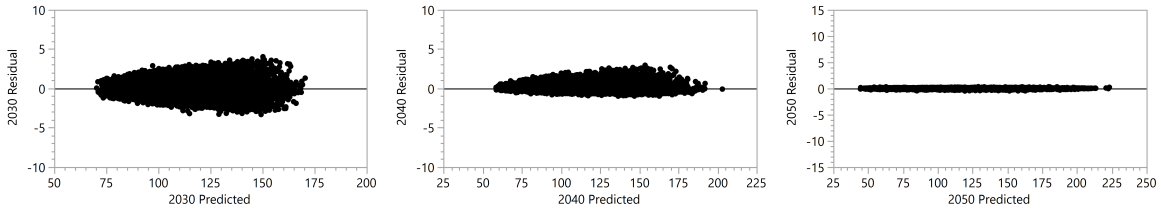

Figure 70: Residual versus predicted plots of ANN models for system fuel burn in 2030, 2040 and 2050

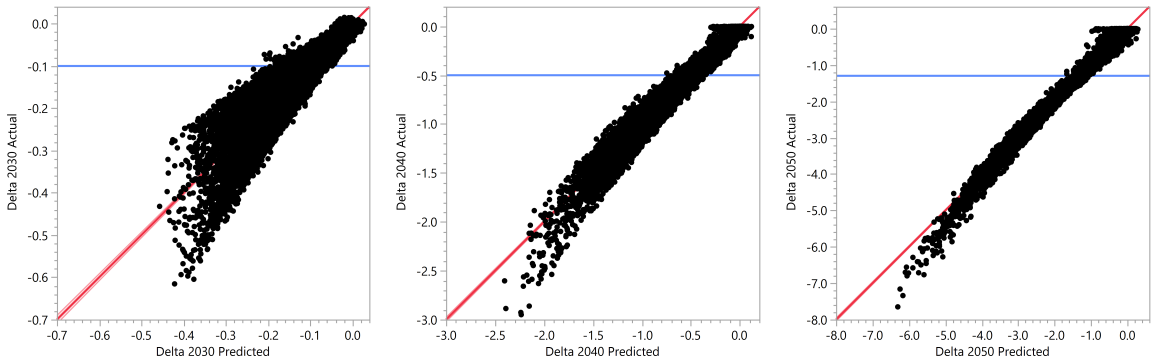

Figure 71: Actual versus predicted plots of RSM models for system fuel burn reduction due to α, β interaction in 2030, 2040 and 2050

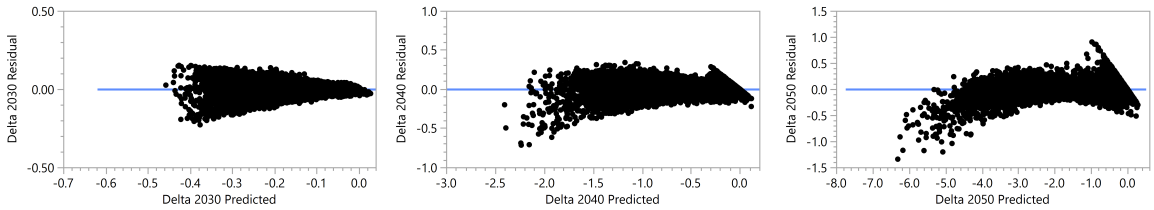

Figure 72: Residual versus predicted plots of RSM models for system fuel burn reduction due to α, β interaction in 2030, 2040 and 2050

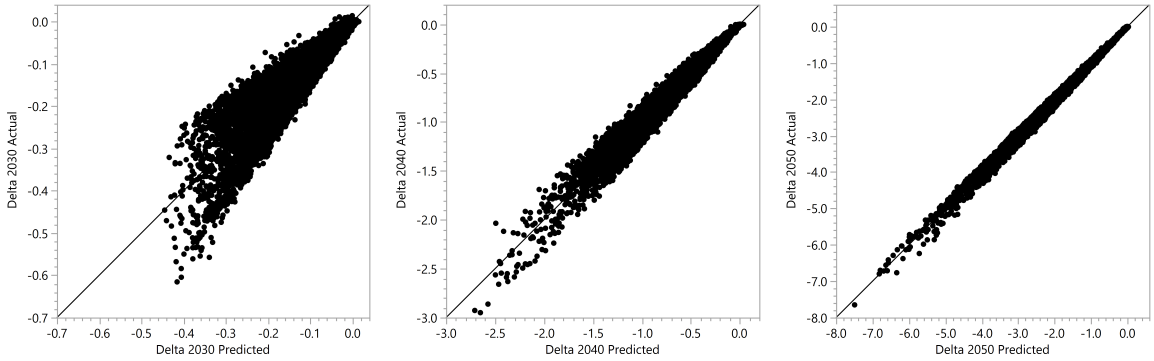

Figure 73: Actual versus predicted plots of ANN models for system fuel burn reduction due to α, β interaction in 2030, 2040 and 2050

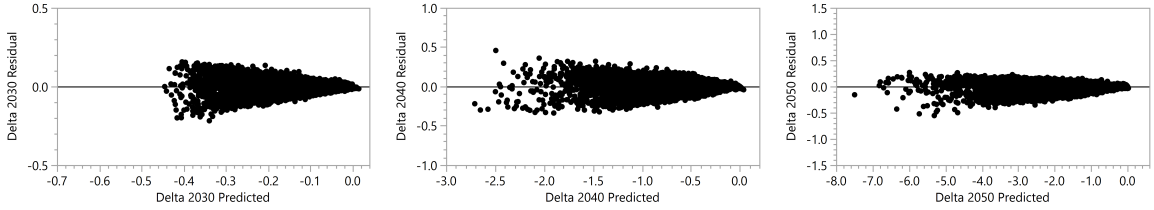

Figure 74: Residual versus predicted plots of ANN models for system fuel burn reduction due to α, β interaction in 2030, 2040 and 2050

REFERENCES

[1] International Civil Aviation Organization, "Annual Report of the ICAO Council." 2015, http://www.icao.int/annual-report-2015/Documents/Appendix_1_en.pdf [accessed 01 May 2017].

[2] Boeing, "Current Market Outlook 2016–2035." 2016, http://www.boeing.com/boeing/commercial/cmo/ [accessed 01 May 2017].

[3] Airbus, "Global Market Forecast 2016–2035." 2016, http://www.airbus.com/company/market/global-market-forecast-2016-2035/ [accessed 01 May 2017].

[4] Federal Aviation Administration, "FAA Aerospace Forecast FY 2016-2036." 2016, http://www.faa.gov/data_research/aviation/aerospace_forecasts/ [accessed 01 May 2017].

[5] National Aeronautics and Space Administration, "Green Aviation: A Better Way to Treat the Planet." 2013, http://www.hq.nasa.gov/office/aero/pdf/green_aviation_fact_sheet_web.pdf [accessed 01 May 2017].

[6] United States Department of Transportation. *Budget and Performance Documents*, https://www.transportation.gov/mission/budget/dot-budget-and-performance-documents [accessed 01 May 2017].

[7] Federal Aviation Administration, "The Future of the NAS." June 2016, https://www.faa.gov/nextgen/media/futureOfTheNAS.pdf [accessed 01 May 2017].

[8] Collier, F. and Wahls, R., "NASA Aeronautics Strategic Implementation Plan: Strategic Thrust 3A Roadmap Overview." June 2016, http://nari.arc.nasa.gov/sites/default/files/attachments/Thrust%203a_1june2016-web.pdf [accessed 01 May 2017].

[9] National Aeronautics and Space Administration. *Budget Documents, Strategic Plans and Performance Reports*, http://www.nasa.gov/news/budget/index.html [accessed 01 May 2017].

[10] National Aeronautics and Space Administration, "NASA Aeronautics: Strategic Implementation Plan." 2015, http://www.hq.nasa.gov/office/aero/pdf/armd-strategic-implementation-plan.pdf [accessed 01 May 2017].

[11] Air Transport Action Group, "The Right Flightpath to Reduce Aviation Emissions." United Nations Framework Convention on Climate Change, Cancun Climate Change Conference, November 2010, http://www.atag.org/component/downloads/downloads/72.html [accessed 01 May 2017].

[12] International Civil Aviation Organization, "Resolution A37-19: Consolidated statement of continuing ICAO policies and practices related to environmental protection – Climate change." 2010, http://www.icao.int/environmental-protection/37thAssembly/A37_Res19_en.pdf [accessed 01 May 2017].

[13] International Air Transport Association, "IATA Technology Roadmap." 2013, http://www.iata.org/whatwedo/environment/Documents/technology-roadmap-2013.pdf [accessed 01 May 2017].

[14] Bureau of Transportation Statistics. *Air Carrier Statistics (Form 41 Traffic)- U.S. Carriers*, http://www.transtats.bts.gov/ [accessed 01 May 2017].

[15] United States Government, "United States Aviation Greenhouse Gas Emissions Reduction Plan." June 2015, http://www.icao.int/environmental-protection/Lists/ActionPlan/Attachments/30/UnitedStates_Action_Plan-2015.pdf [accessed 01 May 2017].

[16] National Research Council, *A Review of the Next Generation Air Transportation System: Implications and Importance of System Architecture*. The National Academies Press, 2015.

[17] Scovel III., C. L., "FAA's Progress and Challenges in Advancing the Next Generation Air Transportation System." July 2013, https://www.oig.dot.gov/sites/default/files/FAA%20Progress%20and%20Challenges%20Advancing%20NextGen%5E7-16-13.pdf [accessed 01 May 2017].

[18] Scovel III., C. L., "Status of FAA's Efforts to Operate and Modernize the National Airspace System." Nov. 2014, https://www.oig.dot.gov/sites/default/files/Master%20Statement%2011-17-14_final_508.pdf [accessed 01 May 2017].

[19] Bureau of Transportation Statistics. *Air Carrier Summary Data (Form 41 and 298C Summary Data)*, http://www.transtats.bts.gov/ [accessed 01 May 2017].

[20] Statement on Signing the Vision 100 – Century of Aviation Reauthorization Act, *Weekly Compilation of Presidential Documents*, 39-WCPD-1795, Office of the Federal Register – National Archives and Records Administration, vol. 39, no. 51, pp. 1795–1797, 22 Dec. 2003.

[21] O'Leary, J. and Srivastava, A., "Development of Controller Pilot Automatic Data Communication (DataComm) System." Federal Aviation Administration, 2012, http://www.cister.isep.ipp.pt/ae2012/presentations_pdf/wednesday/ua/srivastava.pdf [accessed 01 May 2017].

[22] Federal Aviation Administration, "NextGen Implementation Plan 2013." June 2013, https://www.faa.gov/nextgen/library/media/nextgen_implementation_plan_2013.pdf [accessed 01 May 2017].

[23] Pearce, R. A., "The NextGen JPDO Model of Interagency Planning," in *9th AIAA Aviation Technology, Integration, and Operations Conference*, Sept. 2009.

[24] Executive Order 13419 – National Aeronautics Research and Development, *Federal Register*, 71-FR-77565, Office of the Federal Register – National Archives and Records Administration, vol. 71, no. 247, pp. 77565–77567, 26 Dec. 2006.

[25] National Science and Technology Council, "National Plan for Aeronautics Research and Development and Related Infrastructure," Dec. 2007.

[26] Gawdiak, Y., "JPDO Portfolio Analysis of NextGen," in *9th AIAA Aviation Technology, Integration, and Operations Conference*, Sept. 2009.

[27] Smith, J. C. and Neitzke, K. W., "Metrics for the NASA Airspace Systems Program," tech. rep., National Aeronautics and Space Administration, SP-2009-6115, Dec. 2009.

[28] United States Environmental Protection Agency, "Inventory of U.S. Greenhouse Gas Emissions and Sinks." EPA-430-R-16-002, Apr. 2016, https://www.epa.gov/sites/production/files/2016-04/documents/us-ghg-inventory-2016-main-text.pdf [accessed 01 May 2017].

[29] Schrage, D. P. and Mavris, D. N., "Integrated Design and Manufacturing for the High Speed Civil Transport," in *AIAA Aircraft Design, Systems and Operations Meeting*, Aug. 1993.

[30] Bahill, T. A. and Gissing, B., "Re-evaluating Systems Engineering Concepts Using Systems Thinking," *IEEE Transactions on Systems, Man, and Cybernetics – Part C: Applications and Reviews*, vol. 28, Nov. 1998.

[31] Committee on Aviation Environmental Protection, "Economic Analysis of NOx Emissions Stringency Options." International Civil Aviation Organization, CAEP/6-IP/13, Feb. 2004.

[32] International Civil Aviation Organization, "Global Air Navigation Plan." 2007, http://www.icao.int/publications/Documents/9750_3ed_en.pdf [accessed 01 May 2017].

[33] Palopo, K., Windhorst, R., Musaffar, B., and Refai, M., "Economic and Safety Impacts of Flight Routing in the National Airspace System," in *7th AIAA Aviation Technology, Integration, and Operations Conference*, Sept. 2007.

[34] Hollingsworth, P., Pfaender, H., and Jimenez, H., "A Method for Assessing the Environmental Benefit of Future Aviation Technologies," in *26th International Congress of the Aeronautical Sciences*, Sept. 2008.

[35] Graham, M., Augustine, S., Ermatinger, C., DiFelici, J., Thompson, T. R., Marcolini, M. A., and Creedon, J. F., "Evaluating the Environmental Performance of the U.S. Air Transportation System, Quantitative Estimation of Noise, Air Quality, and Fuel-Efficiency Performance," in *8th USA/Europe Air Traffic Management Research and Development Seminar*, June 2009.

[36] Kar, R., Bonnefoy, P. A., Hansman, R. J., and Sgouridis, S., "Dynamics of Implementation of Mitigating Measures to Reduce Commercial Aviations Environmental Impacts," in *9th AIAA Aviation Technology, Integration and Operations Conference*, Sept. 2009.

[37] Marais, K. B., Reynolds, T. G., Uday, P., Muller, D., Lovegren, J., Dumont, J., and Hansman, R. J., "Evaluation of Potential Near-Term Operational Changes to Mitigate Environmental Impacts of Aviation," *Proceedings of the Institution of Mechanical Engineers, Part G: Journal of Aerospace Engineering*, vol. 227, no. 8, pp. 1277–1299, 2012.

[38] Jimenez, H., Pfaender, H., and Mavris, D. N., "Fuel Burn and CO_2 System-Wide Assessment of Environmentally Responsible Aviation Technologies," *Journal of Aircraft*, vol. 49, Dec. 2012.

[39] Anderson, Jr., J. D., *Aircraft Performance and Design*, ch. 5. McGraw-Hill, 1999.

[40] Zeinali, M. and Rutherford, D., "Trends in Aircraft Efficiency and Design Parameters." The International Council on Clean Transportation, Mar. 2010, `http://www.theicct.org/sites/default/files/publications/aircraft_efficiency_trends.pdf` [accessed 01 May 2017].

[41] Scheelhaase, J. D., Dahlmann, K., Jung, M., Keimel, H., Niesse, H., Sausen, R., Schaefer, M., and Wolters, F., "How to Best Address Aviations Full Climate Impact from an Economic Policy Point of View? – Main Results from AviClim Research Project," *Transportation Research Part D: Transport and Environment*, vol. 45, pp. 112–125, June 2016.

[42] Roberts, E. B., "Exploratory and Normative Technological Forecasting: A Critical Appraisal," *Technological Forecasting*, vol. 1, no. 2, pp. 113–127, 1969.

[43] Jantsch, E., *Technological Forecasting in Perspective*. Organisation for Economic Cooperation and Development, 1967.

[44] McCullers, L. A., "Aircraft Configuration Optimization Including Optimized Flight Profiles," 1984.

[45] Claus, R. W., Evans, A. L., Lylte, J. K., and Nichols, L. D., "Numerical Propulsion System Simulation," *Computing Systems in Engineering*, vol. 2, no. 4, pp. 357–364, 1991.

[46] Tong, M. T. and Naylor, B. A., "An Object-Oriented Computer Code for Aircraft Engine Weight Estimation," in *ASME Turbo Expo 2008: Power for Land, Sea, and Air*, 2008.

[47] Nickol, C. L. and Haller, W. J., "Assessment of the Performance Potential of Advanced Subsonic Transport Concepts for NASAs Environmentally Responsible Aviation Project," in *54th AIAA Aerospace Sciences Meeting*, Jan. 2016.

[48] Berton, J. J. and Guynn, M. D., "Multi-Objective Optimization of a Turbofan for an Advanced, Single-Aisle Transport," *Journal of Aircraft*, vol. 48, no. 5, pp. 1795–1805, 2011.

[49] Nickol, C. L., "Technologies and Concepts for Reducing the Fuel Burn of Subsonic Transport Aircraft," in *NATO AVT-209 Workshop on Energy Efficient Technologies*, Oct. 2012.

[50] Green, J. E. and Jupp, J. A., "CAEP/9-Agreed Certification Requirement for the Aeroplane CO_2 Emissions Standard: A Comment on ICAO Cir 337," *The Aeronautical Journal*, vol. 120, pp. 693–723, Apr. 2016.

[51] Hileman, J. I., Blanco, E. D., Bonnefoy, P. A., and Carter, N. A., "The Carbon Dioxide Challenge Facing Aviation," *Progress in Aerospace Sciences*, vol. 63, Nov. 2013.

[52] Kharina, A. and Rutherford, D., "Fuel Efficiency Trends for New Commercial Jet Aircraft: 1960 to 2014." The International Council on Clean Transportation, Aug. 2015, `http://www.theicct.org/sites/default/files/publications/ICCT_Aircraft-FE-Trends_20150902.pdf` [accessed 01 May 2017].

[53] Mattingly, J. D., Heiser, W. H., and Pratt, D. T., *Aircraft Engine Design*, ch. 2. AIAA Education Series, 2002.

[54] National Aeronautics and Space Administration, "Technology Readiness Level." 2012, `https://www.nasa.gov/directorates/heo/scan/engineering/technology/txt_accordion1.html` [accessed 01 May 2017].

[55] National Aeronautics and Space Administration, "Technology Readiness Level Definitions." `https://www.nasa.gov/pdf/458490main_TRL_Definitions.pdf` [accessed 01 May 2017].

[56] Jimenez, H., Burdette, G., Schutte, J., and Mavris, D. N., "Probabilistic Technology Assessment for NASA Environmentally Responsible Aviation (ERA) Vehicle Concepts," in *11th AIAA Aviation, Technology, Integration, and Operations Conference*, Sept. 2011.

[57] Penner, J. E., Lister, D. H., Griggs, D. J., Dokken, D. J., and McFarland, M., *Aviation and the Global Atmosphere: A Special Report of the Intergovernmental Panel on Climate Change*. Cambridge University Press, 1999.

[58] Mattingly, J. D., Heiser, W. H., and Pratt, D. T., *Aircraft Engine Design*, ch. 3. AIAA Education Series, 2002.

[59] Goetz, A. R. and Sutton, C. J., "The Geography of Deregulation in the U.S. Airline Industry," *Annals of the Association of American Geographers*, vol. 87, pp. 238–263, June 1997.

[60] Belobaba, P., Odoni, A., and Barnhart, C., *The Global Airline Industry*, ch. 3 and 6. John Wiley & Sons, Inc., 2009.

[61] Gillen, D. and Morrison, W. G., "Regulation, Competition and Network Evolution in Aviation," *Journal of Air Transport Management*, vol. 11, pp. 161–174, May 2005.

[62] Franke, M., "Competition Between Network Carriers and Low Cost Carriers – Retreat Battle or Breakthrough to a New Level of Efficiency?," *Journal of Air Transport Management*, vol. 10, pp. 15–21, Jan. 2004.

[63] Airlines for America. *Annual Results: U.S. Passenger Airlines*, `http://airlines.org/dataset/annual-results-u-s-passenger-airlines/` [accessed 01 May 2017].

[64] Huang, A. S. and Graham, M., "Fleet Substitution Algorithm and Fleet Evolution Process Comparison Using Future Demand Scenarios," in *AIAA Modeling and Simulation Technologies Conference*, Aug. 2009.

[65] International Civil Aviation Organization, "ICAO Environmental Report 2007." 2007, `http://www.icao.int/environmental-protection/documents/env_report_07.pdf` [accessed 01 May 2017].

[66] Jiang, H., "Key Findings on Airplane Economic Life." 2013, `http://www.boeing.com/assets/pdf/commercial/aircraft_economic_life_whitepaper.pdf` [accessed 01 May 2017].

[67] National Research Council, *Maintaining U.S. Leadership in Aeronautics: Scenario-Based Strategic Planning for NASA's Aeronautics Enterprise*. The National Academies Press, 1997.

[68] Schoemaker, P. J. H., "Scenario Planning: A Tool for Strategic Thinking," *Sloan Management Review*, vol. 36, no. 2, pp. 25–40, 1995.

[69] Peterson, G. D., Cumming, G. S., and Carpenter, S. R., "Scenario Planning: A Tool for Conservation in an Uncertain World," *Conservation Biology*, vol. 17, pp. 358–366, Apr. 2003.

[70] Eppinger, S. D., "Model-based approaches to managing concurrent engineering," *Journal of Engineering Design*, vol. 2, no. 4, pp. 283–290, 1991.

[71] Kroo, I., Altus, S., Braun, R., Gage, P., and Sobieski, I., "Multidisciplinary Optimization Methods for Aircraft Preliminary Design," in *5th Symposium on Multidisciplinary Analysis and Optimization*, Sept. 1994.

[72] Gamble, R. E., *Decoupling, Complexity and Importance in the Design and Analysis of Complex Transport Systems* . PhD thesis, Department of Mechanical Engineering, University of California, Berkeley, 2002.

[73] Sim, S. K. and Duffy, A. H. B., "Towards an Ontology of Generic Engineering Design Activities," *Research in Engineering Design*, vol. 14, no. 4, pp. 200–223, 2003.

[74] Mavris, D. N. and Schutte, J., "Application of Deterministic and Probabilistic System Design Methods and Enhancements of Conceptual Design Tools for ERA Project," tech. rep., National Aeronautics and Space Administration, CR2016-219201, May 2016.

[75] Mavris, D. N., Tai, J., and Perullo, C., "Systems Analysis and Enhancement of Conceptual Design Tools for the Advanced Air Transportation Technologies Project." unpublished, expected 2017.

[76] Antoine, N. E. and Kroo, I. M., "Framework for Aircraft Conceptual Design and Environmental Performance Studies," *AIAA Journal*, vol. 43, pp. 2100–2109, Oct. 2005.

[77] Kirby, M. R. and Mavris, D. N., "The Environmental Design Space," in *26th International Congress of the Aeronautical Sciences*, Sept. 2008.

[78] Converse, G. L. and Giffin, R. G., "Extended Parametric Representation of Compressor Fans and Turbines – Volume 1," tech. rep., National Aeronautics and Space Administration, CR-174645, Mar. 1984.

[79] Zorumski, W. E., "Aircraft Noise Prediction Program Theoretical Manual," tech. rep., National Aeronautics and Space Administration, TM-83199, Feb. 1982.

[80] Barros, P. A., Kirby, M. R., and Mavris, D. N., "An Approach For Verification And Validation Of The Environmental Design Space," in *26th International Congress of the Aeronautical Sciences*, Sept. 2008.

[81] Schutte, J., Jimenez, H., and Mavris, D. N., "Technology Assessment of NASA Environmentally Responsible Aviation Advanced Vehicle Concepts," in *49th AIAA Aerospace Sciences Meeting*, Jan. 2011.

[82] Schutte, J., Kestner, B., Tai, J., and Mavris, D. N., "Updates and Modeling Enhancements to the Assessment of NASA Environmentally Responsible Aviation Technologies and Vehicle Concepts," in *50th AIAA Aerospace Sciences Meeting*, Jan. 2012.

[83] Pfaender, H., Jimenez, H., Schutte, J., Garcia, E., and Mavris, D. N., "Enhanced System-wide Fuel Estimates for N+ 2 Aircraft Technologies and Concepts towards Carbon Neutral Growth," in *AIAA/3AF Aircraft Noise and Emissions Reduction Symposium*, June 2014.

[84] Kroo, I. and Takai, M., "A Quasi-Procedural, Knowledge-Based System for Aircraft Design," in *Aircraft Design, Systems and Operations Conference*, Sept. 1988.

[85] Kroo, I., "An Interactive System for Aircraft Design and Optimization," in *Aerospace Design Conference*, Feb. 1992.

[86] Kroo, I., "PASS: Program for Aircraft Synthesis Studies." Software Package, Desktop Aeronautics, Inc., Palo Alto, CA, 2011.

[87] Antoine, N. E. and Kroo, I. M., "Multiobjective AAircraft Design Optimization for Low Noise and Emissions," in *24th International Congress of the Aeronautical Sciences*, Sept. 2004.

[88] Wintzer, M., Kroo, I., Aftosmis, M., and Nemec, M., "Conceptual Design of Low Sonic Boom Aircraft Using Adjoint-Based CFD," in *7th International Conference on Computational Fluid Dynamics*, July 2012.

[89] Greitzer, E. M. *et al.*., "N+3 Aircraft Concept Designs and Trade Studies, Final Report – Volume 1," tech. rep., National Aeronautics and Space Administration, CR-2010-216794/VOL1, Dec. 2010.

[90] Greitzer, E. M. *et al.*., "N+3 Aircraft Concept Designs and Trade Studies, Final Report – Volume 2: Appendices," tech. rep., National Aeronautics and Space Administration, CR-2010-216794/VOL2, Dec. 2010.

[91] Drela, M., "Simultaneous Optimization of the Airframe, Powerplant, and Operation of Transport Aircraft," 2010.

[92] Pantalone, G., Blanco, E. D., and Willcox, K., "TASOPT Engine Model Development." Partnership for Air Transportation Noise and Emissions Reduction, 2016, `http://partner.mit.edu/sites/partner.mit.edu/files/report/file/tasopt-eng-mod-dev-proj48.pdf` [accessed 01 May 2017].

[93] Wakayama, S., *Lifting Surface Design Using Multidisciplinary Optimization*. PhD thesis, Department of Aeronautics and Astronautics, Stanford University, 1994.

[94] Wakayama, S., "Blended-Wing-Body Optimization Problem Setup," in *8th Symposium on Multidisciplinary Analysis and Optimization*, Sept. 2000.

[95] Willcox, K. and Wakayama, S., "Simultaneous Optimization of a Multiple-Aircraft Family," *Journal of Aircraft*, vol. 40, no. 4, pp. 616–622, 2003.

[96] Drela, M., "Development of the D8 Transport Configuration," in *29th AIAA Applied Aerodynamic Conference*, June 2011.

[97] Stratton, R. W., Wong, H. M., and Hileman, J. I., "Life Cycle Greenhouse Gas Emissions from Alternative Jet Fuels." Partnership for Air Transportation Noise and Emissions Reduction, 2010, `http://web.mit.edu/aeroastro/partner/reports/proj28/partner-proj28-2010-001.pdf` [accessed 01 May 2017].

[98] Argonne National Laboratory, "GREET Life-Cycle Model." 2014, `https://greet.es.anl.gov/` [accessed 01 May 2017].

[99] Hassan, M., Payan, A., O'Sullivan, S., Pfaender, H., and Mavris, D., "Parametric Assessment of Aviation Environmental Goals: Implications on R&D Decision Making," in *15th AIAA Aviation Technology, Integration, and Operations Conference*, June 2015.

[100] Hofer, C., Dresner, M. E., and Windle, R. J., "The Environmental Effects of Airline Carbon Emissions Taxation in the US," *Transportation Research Part D: Transport and Environment*, vol. 15, 2010.

[101] Winchester, N., Wollersheim, C., Clewlow, R., Jost, N. C., Paltsev, S., Reilly, J. M., and Waitz, I. A., "The Impact of Climate Policy on US Aviation," *Journal of Transport Economics and Policy*, vol. 47, no. 1, 2013.

[102] Krammer, P., Dray, L., and Köhler, M. O., "Climate-Neutrality versus Carbon-Neutrality for Aviation Biofuel Policy," *Transportation Research Part D: Transport and Environment*, vol. 23, Aug. 2013.

[103] Hassan, M., Pfaender, H., and Mavris, D., "Probabilistic Assessment of Aviation CO_2 Emission Targets." unpublished, expected 2017.

[104] Gegg, P., Budd, L., and Ison, S., "The Market Development of Aviation Biofuel: Drivers and Constraints," *Journal of Air Transport Management*, vol. 39, July 2014.

[105] Hassan, M. and Mavris, D. N., "A Methodology for the Prediction of Air Transportation Network Growth Dynamics," in *15th AIAA/ISSMO Multidisciplinary Analysis and Optimization Conference*, June 2014.

[106] Hassan, M., Payan, A., Pfaender, H., Garcia, E., Schutte, J., and Mavris, D., "Framework Development for Performance Evaluation of the Future National Airspace System," in *15th AIAA Aviation Technology, Integration, and Operations Conference*, June 2015.

[107] Gillen, D. W., Morrison, W. G., and Stewart, C., "Air Travel Demand Elasticities: Concepts, Issues and Measurement." Department of Finance, Government of Canada, Jan. 2003, http://www.fin.gc.ca/consultresp/Airtravel/airtravStdy_-eng.asp [accessed 01 May 2017].

[108] Ferjan, K., "Another Successful Year." Airline Cost Conference, Aug. 2016, http://www.iata.org/whatwedo/workgroups/Documents/ACC-2016-GVA/Another_Successful_ACMG_Year_Klemen_Ferjan.pdf [accessed 01 May 2017].

[109] Gillen, D. W., "International Air Transport in the Future," in *18th International Transport Research Symposium*, Nov. 2009.

[110] Vivid Economics, "A Study to Estimate Ticket Price Changes for Aviation in the EU ETS." UK Department for Environment, Food and Rural Affairs, Nov. 2007, http://www.vivideconomics.com/wp-content/uploads/2015/03/Vivid_Econ_Aviation_Tickets.pdf [accessed 01 May 2017].

[111] Bureau of Transportation Statistics. *American Travel Survey (ATS) 1995*, http://www.transtats.bts.gov/ [accessed 01 May 2017].

[112] Pfaender, H. and Mavris, D., "Effect of Fuel Price on Aviation Technology and Environmental Outcomes," in *12th Aviation Technology, Integration and Operations Conference*, Sept. 2012.

[113] Allen, T. D. *et al.*, "Framework and Guidance for Estimating Greenhouse Gas Footprints of Aviation Fuels," tech. rep., Air Force Research Laboratory, AFRL-RZ-WP-TR-2009-2206, Apr. 2009.

[114] Bureau of Transportation Statistics. *Air Carrier Financial Reports (Form 41 Financial Data)*, http://www.transtats.bts.gov/ [accessed 01 May 2017].

[115] United States Department of Energy, "2016 Billion-Ton Report: Advancing Domestic Resources for a Thriving Bioeconomy, Volume 1: Economic Availability of Feedstocks." Langholtz, M. H., Stokes, B. J. and Eaton, L. M. (Leads), ORNL/TM-2016/160, Oak Ridge National Laboratory, Oak Ridge, TN, 448p, July 2016.

[116] Energy Information Administration, "Annual Energy Outlook 2016." 2016, http://www.eia.gov/forecasts/aeo/pdf/0383(2016).pdf [accessed 01 May 2017].

[117] Continuum Analytics, "Anaconda." https://www.continuum.io/anaconda-overview [accessed 01 May 2017].

[118] Kraft, D., "A Software Package for Sequential Quadratic Programming," Tech. Rep. DFVLR-FB 88-28, DLR German Aerospace Center – Institute for Flight Mechanics, 1988.

[119] Perez, R. E., Jansen, P. W., and Martins, J. R. R. A., "pyOpt: A Python-Based Object-Oriented Framework for Nonlinear Constrained Optimization," *Structures and Multidisciplinary Optimization*, vol. 45, no. 1, 2012.

[120] Myers, R. H., Douglas, C. M., and Anderson-Cook, C. M., *Response Surface Methodology: Process and Product Optimization Using Designed Experiments*, vol. 705. John Wiley & Sons, Inc., 3rd ed., 2009.

[121] Dayhoff, J. E. and DeLeo, J. M., "Artificial Neural Networks: Opening the Black Box," *Cancer*, vol. 91, pp. 1615–1635, 2001.

VITA

Mohammed Hassan is from Cairo, Egypt. He received his Bachelor of Science degree in Mechanical Engineering from the American University of Sharjah in 2010 and his Master of Science degree in Mechanical Engineering from King Abdullah University of Science and Technology in 2011. He then joined the Georgia Institute of Technology and earned his Master of Science degree in Aerospace Engineering in 2014 and his Doctor of Philosophy degree in 2017.